Interpretation of Exploration Geochemical Data for the Mount Katmai Quadrangle and Adjacent Parts of the Afognak and Naknek Quadrangles, Alaska

U.S. GEOLOGICAL SURVEY BULLETIN 2020

Interpretation of Exploration Geochemical Data for the Mount Katmai Quadrangle and Adjacent Parts of the Afognak and Naknek Quadrangles, Alaska

By S.E. Church, J.R. Riehle, *and* R.J. Goldfarb

U.S. GEOLOGICAL SURVEY BULLETIN 2020

Descriptive and interpretive supporting data for the mineral resource assessment of this Alaska Mineral Resource Assessment Program (AMRAP) study area

UNITED STATES GOVERNMENT PRINTING OFFICE, WASHINGTON : 1994

U.S. DEPARTMENT OF THE INTERIOR
BRUCE BABBITT, Secretary

U.S. GEOLOGICAL SURVEY
Gordon P. Eaton, Director

For Sale by U.S. Geological Survey, Map Distribution
Box 25286, MS 306, Federal Center
Denver, CO 80225

Library of Congress Cataloging-in-Publication Data

Church, S.E.
Interpretation of exploration geochemical data for the Mount Katmai quadrangle and adjacent parts of the Afognak and Naknek quadrangles, Alaska / by S.E. Church, J.R. Riehle, and R.J. Goldfarb.
p. cm. — (U.S. Geological Survey bulletin ; 2020)
Includes bibliographical references.
Supt. of Docs. no. : I19.3 : 2020
1. Mines and mineral resources—Alaska. 2. Mining geology—Alaska. 3. Geochemical prospecting—Alaska. I. Riehle, J.R. II. Goldfarb, R.J. III. Title. IV. Series.
QE75.B9 no. 2020
[TN24.A4]
557.3 s—dc20 93–2012
[553'.09798] CIP

CONTENTS

PLATES

[Plates are in pocket]

FIGURES

TABLES

Interpretation of Exploration Geochemical Data for the Mount Katmai Quadrangle and Adjacent Parts of the Afognak and Naknek Quadrangles, Alaska

By S.E. Church, J.R. Riehle, *and* R.J. Goldfarb

ABSTRACT

Analysis of the geologic and geochemical data collected during this study of the Mount Katmai, western Afognak, and eastern Naknek quadrangles, Alaska, defines areas favorable for undiscovered porphyry Cu, porphyry Cu-Mo, porphyry Cu-Au, and porphyry Mo deposits, and for base- and precious-metal-bearing polymetallic and epithermal quartz-vein deposits. Factor analysis of stream-sediment geochemical data defines one element suite that delimits areas prospective for undiscovered porphyry and polymetallic-vein deposits. Factor analysis of aqua-regia-leachate data from stream sediments not only delimits these same areas, but also identifies geochemical signatures of hydromorphic phases that may reflect secondary weathering and transport of metals important in defining concealed mineral deposits. Factor analysis of the nonmagnetic heavy-mineral concentrates from stream sediments refines and expands the boundaries of these areas and delimits areas prospective for precious-metal-bearing epithermal quartz-vein deposits.

Mineral occurrences in the Katmai study area are spatially associated with plutonic rocks of Tertiary age. We describe one occurrence in the Margot Creek drainage basin in the Buttress Range that has both the geochemical and geologic attributes of a porphyry Cu-Mo deposit. Polymetallic veins have been identified in the Kulik Lake area, the Fourpeaked Mountain area, the Barrier Range area, and the Ikagluik Creek area. Pyritic, gold-bearing quartz veins have been identified at Dakavak Lake, Hagelbargers Pass, and in the Kulik Lake area. Many of these same areas also have potential for additional porphyry-type mineral deposits, as well as polymetallic and epithermal quartz-vein deposits. The presence of epithermal veins deposited by hot springs is suggested by anomalous concentrations of gold and mercury found along Martin Creek near Mount Mageik.

The geologic and geochemical data do not support occurrence of several other types of mineral deposits found in the same lithologic units elsewhere in southwestern Alaska. Our geologic and geochemical data do not indicate areas favorable for undiscovered Kuroko-type massive sulfide deposits in the rocks of the Talkeetna Formation. Because of the paucity of exposed carbonate host rocks, such as the Upper Triassic Kamishak Formation, we found only scant evidence for copper-rich iron-skarns in the Katmai study area. Skarn mineral assemblages occur locally where calcareous rocks of the Herendeen Formation have been intruded by middle Tertiary plutons. Finally, evidence for undiscovered skarn or polymetallic-vein deposits associated with the Jurassic intrusive rocks of the Alaska–Aleutian Range batholith has been found in only one drainage basin just north of Becharof Lake.

INTRODUCTION

The U.S. Geological Survey is required by the Alaska National Interest Lands Conservation Act (ANILCA, Public Law 96–487) to survey Federal lands in Alaska to determine their mineral resource endowment. As a part of the Alaska Mineral Resource Assessment Program (AMRAP), a study of the geology and geochemistry of the Mount Katmai quadrangle and adjoining parts of the Afognak and Naknek quadrangles was undertaken during the summer field seasons 1983–87. We refer to this area as the "Katmai study area," or simply the "study area."

The Katmai AMRAP study consisted mainly of geologic mapping at 1:250,000 scale and reconnaissance sampling of both bedrock and stream sediments for geochemical analysis. An interpretation of aeromagnetic data from the Naknek quadrangle (Andreasen and others, 1963) is included in Church and others (1992); no new aeromagnetic data were acquired in the present study; thus no aeromagnetic data are available for the Mount Katmai and western Afognak quadrangles. Geochemical analyses of rock, stream-sediment, and heavy-mineral-concentrate samples were utilized to define localities having abnormally high metal concentrations. As time permitted, some of the areas for which groups of samples had multiple-element anomalies were selected for followup examination and additional sampling during the last two field seasons. The geochemical data were previously released in four reports: semiquantitative emission spectrographic data from stream sediments and nonmagnetic heavy-mineral concentrates panned from stream sediments (Bailey and others, 1986); inductively coupled plasma (ICP) atomic-emission spectrometric analysis of aqua-regia leachates of the stream sediments (Erlich and others, 1988); semiquantitative emission spectrographic and atomic-absorption analyses of the rock samples (Riehle and others, 1989), and mineralogy of the nonmagnetic heavy-mineral concentrates panned from stream sediments (Bennett and Church, 1987).

In this report, we present an interpretation of the geologic and geochemical data collected during the Katmai AMRAP study. Extensive reference is made to the interpretative geochemical maps (Church, Bailey, and Riehle, 1989; Church and Arbogast, 1989; and Church and Motooka, 1989) and to mineralogical maps of nonmagnetic heavy-mineral concentrates (NMHMC) panned from stream sediments (Church and Bennett, 1989), which we will refer to collectively in this text as the reconnaissance geochemical data base. Geochemical sampling methods used and geochemical results obtained during the study are summarized and plots of the geochemical data from rock samples presented (pls. 1–3). Element associations, identified by factor analysis of the geochemical data from the stream-sediment and nonmagnetic heavy-mineral concentrates, are also discussed. Factor analyses confirmed the geochemical suites we chose to use in our geochemical interpretations. The geochemical data are interpreted in the context of geologic processes, known mineral occurrences in the region, and inferred mineral deposit models. Areas having permissive geologic attributes and favorable geochemical expressions of mineral deposit types are defined, and the geology of each area is briefly summarized.

GEOLOGIC SETTING

The Katmai study area is on the Alaska Peninsula between 58° and 59° north latitude (fig. 1). The eastern and western boundaries of the study area are at the coast and incorporate parts of the Afognak and Naknek quadrangles, respectively. Little geochemical sampling was done in the western part of the Naknek quadrangle, where much of the study area is overlain by glacial deposits. That part of Cape Douglas that extends into the southern part of the Iliamna quadrangle was also included in the geochemical sampling but is not included in this report because no geochemical anomalies were found (Bailey and others, 1986).

The study area comprises two physiographic provinces: the Nushagak–Bristol Bay Lowland province along the coast of Bristol Bay and the Aleutian Range province (Wahraftig, 1965). The Nushagak–Bristol Bay Lowland province is characterized by broad coastal plains, low topographic relief, numerous bogs and small lakes, and low-gradient, meandering streams. Few samples were collected in this province. In contrast, the Aleutian Range province is mountainous, has undergone alpine glaciation, and contains streams having steep gradients and occupying youthful valleys. The Aleutian Range is a continuation of the large mountain range extending from the Mount McKinley (Denali) area southwest to the Alaska Peninsula, where it crosses the Katmai study area west of the Bruin Bay fault (fig. 1). Plutonic rocks of the Alaska–Aleutian Range batholith crop out in a belt that crosses the Katmai study area west of the Bruin Bay fault.

High mountain peaks in the Katmai study area are capped by upper Tertiary and Quaternary volcanic flows and deposits that partly cover Mesozoic and Tertiary sedimentary and igneous rocks. Elevations exceed 2,000 m at several of the Quaternary volcanoes, namely Mount Katmai, Mount Mageik, Mount Griggs (Knife Peak), Snowy Mountain, Mount Denison, Fourpeaked Mountain, and Mount Douglas. Glaciers are present on the large peaks, and both Hallo Glacier and Fourpeaked Glacier extend nearly to sea level on the east coast of the study area. The Valley of Ten Thousand Smokes is filled with pumice and volcanic ash from the 1912 eruption of Novarupta dome. Cenozoic volcanic rocks of the Aleutian volcanic arc were emplaced roughly parallel to the Pacific coast, but the Mesozoic sedimentary rocks that underlie them extend offshore beneath Shelikof Strait (Burk, 1965; Detterman and others, 1987; von Huene and others, 1985). The Aleutian Trench lies about 300 km southeast of the study area, southeast of Kodiak Island (Jacob and others, 1977; von Huene and others, 1985).

Acknowledgments.—We thank the U.S. National Park Service and the U.S. Fish and Wildlife Service for permission to conduct these scientific studies in the Katmai National Park and Preserve and the Becharof National Wildlife Refuge. We also thank S.J. Sutley and Ted Botinelly for the X-ray diffraction and direct-current-arc emission spectrographic work reported here on the samples from the Hagelbargers Pass prospect. Finally, we thank our colleagues who have worked with us during the sampling and analytical phases of our work in the Katmai study area; their work is referenced extensively throughout the text. Without their diligent efforts, this study could not have been completed.

GEOLOGY OF THE KATMAI STUDY AREA

The geologic setting of the Katmai study area is that of a convergent plate margin. The Cenozoic Aleutian volcanic

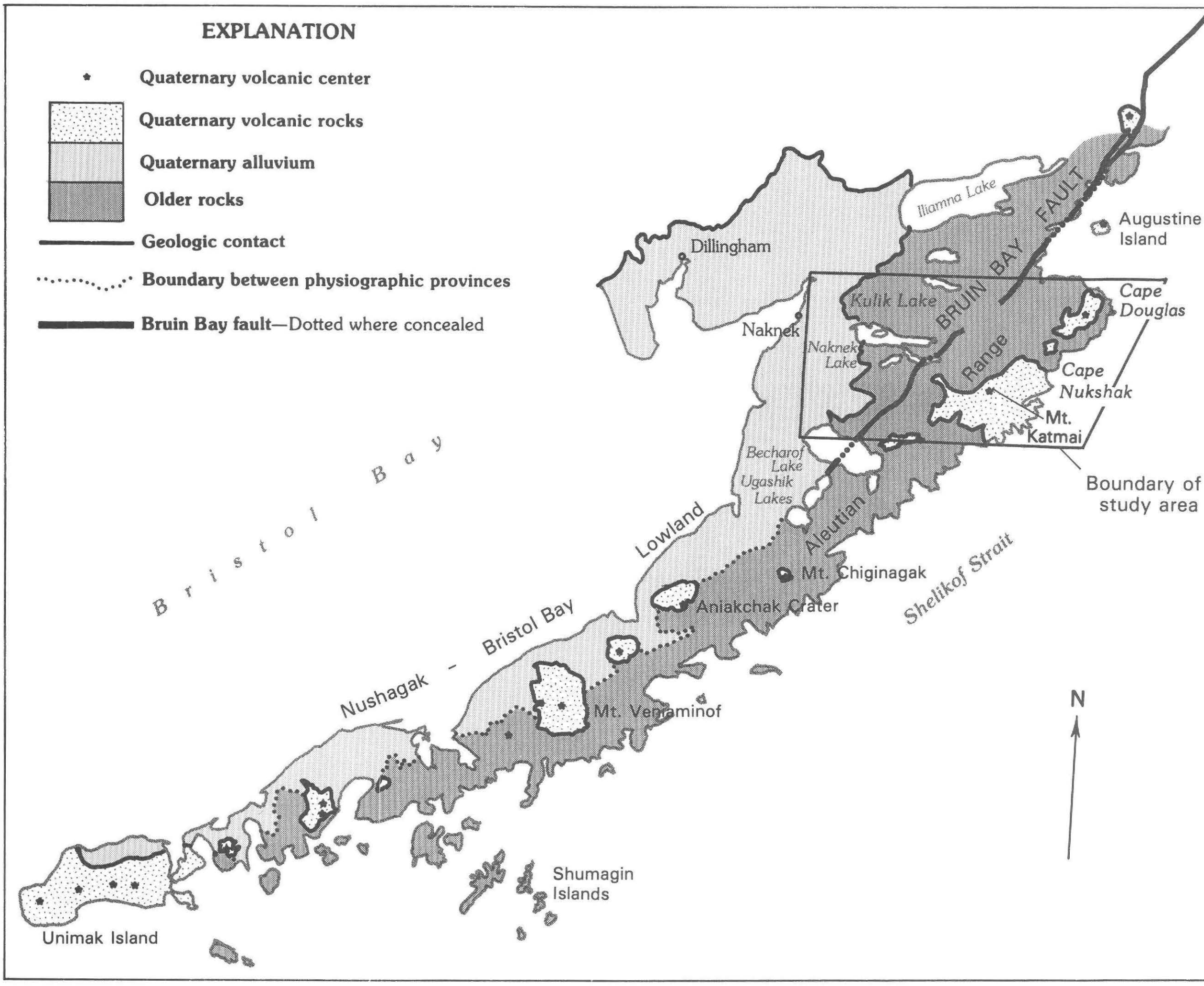

Figure 1. Index map of the Alaska Peninsula showing the location of the Katmai study area comprising the Mount Katmai, eastern Naknek, and western Afognak 1:250,000 quadrangles, Alaska. The Iliamna 1:250,000 quadrangle is immediately north of the study area, and the Ugashik and Karluk quadrangles are immediately south of the study area. Physiographic provinces, major rock units and faults, Quaternary volcanoes, and several major geographic features of the Alaska Peninsula are shown for reference; scale 1:5,000,000.

arc is superimposed on a Mesozoic continental-margin sequence of marine and nonmarine sedimentary rocks. These Mesozoic sedimentary rocks were derived chiefly from the erosion of a Jurassic calc-alkaline batholith and volcanic arc. Systematic geologic mapping by Keller and Reiser (1959 and citations therein) summarizes the early work done in the Katmai study area. Additional geologic studies have concentrated on either the 1912 eruption of Novarupta volcano and its associated ash-flow deposit in the Valley of Ten Thousand Smokes (for example, Fenner, 1920), or paleontology and stratigraphy along Shelikof Strait (see citations in Riehle and others, in press). Here, we describe briefly the geology of the Katmai study area in order to provide a geologic framework for the interpretation of the geochemical results. Stratigraphic relations and correlations among map units on the 1:1,000,000-scale map figures that follow are simplified from the 1:250,000 geologic base map used for the accompanying plates. Descriptions of the sedimentary rocks are based largely on Detterman and others (in press).

PALEOZOIC(?) AND EARLY MESOZOIC ROCKS

The oldest rocks in the Katmai study area are schist, quartzite, amphibolite, gneiss, and migmatite assigned to the Kakhonak Complex, defined by Detterman and Reed (1980) in the Iliamna quadrangle to the north. These metamorphic rocks crop out in a northeast-trending belt as roof pendants in the Alaska–Aleutian Range batholith. Most of the rocks consist of plagioclase-epidote-chlorite-actinolite mineral

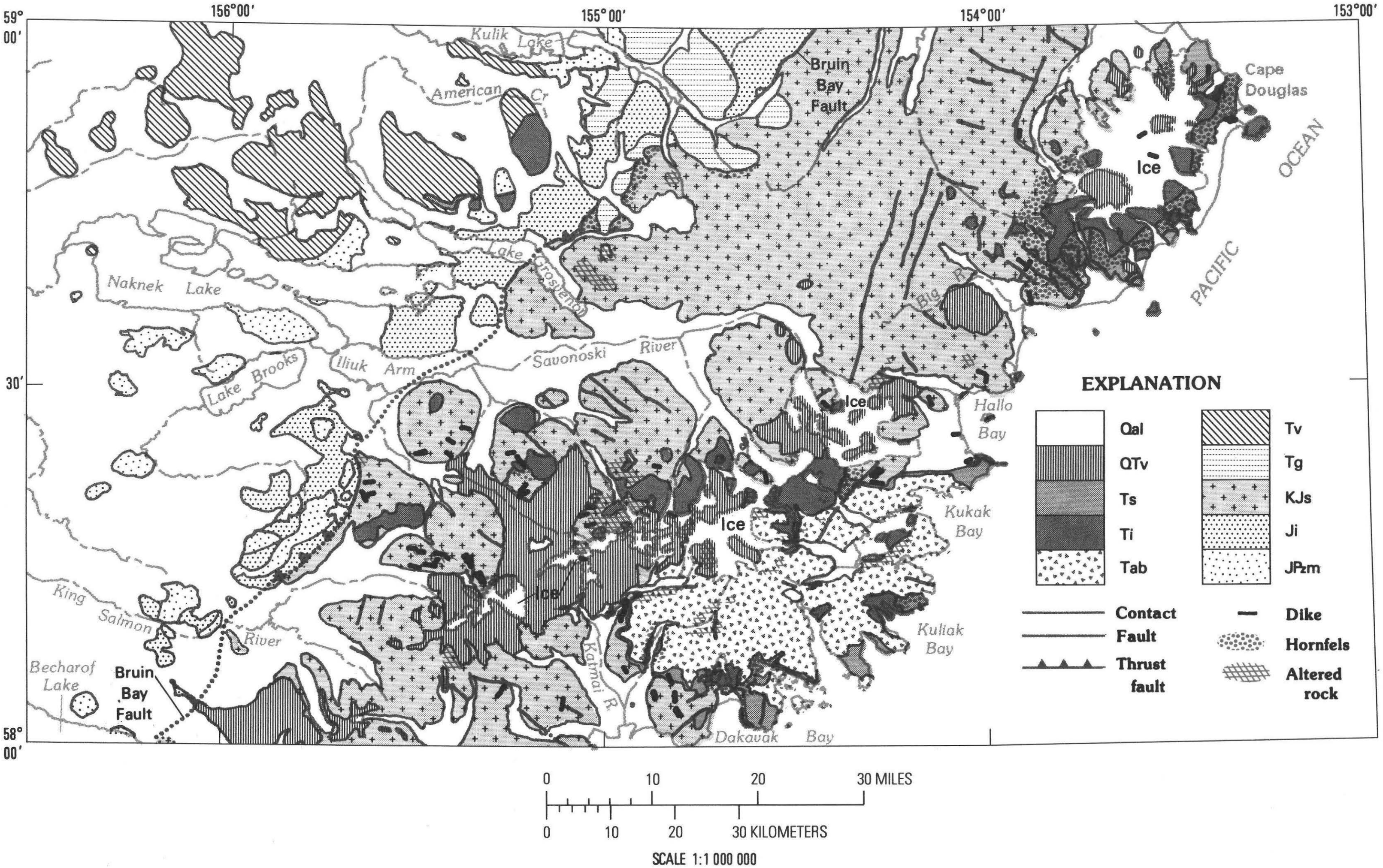

Figure 2. Generalized geologic map of the Mount Katmai, western Afognak, and eastern Naknek quadrangles, Alaska. Geologic units: Qal, Quaternary alluvium; QTv, Quaternary and latest Tertiary volcanic rocks of Aleutian volcanic arc; Ts, Tertiary sedimentary rocks (includes Hemlock Conglomerate and Copper Lake Formation); Ti, Tertiary intrusive rocks (includes plutons mapped as units Ti, Tiu, and Td from western side of Aleutian volcanic arc as shown on pl. 1); Tab, Tertiary volcanic rocks of Barrier Range (late Tertiary volcanic rocks of Aleutian arc); Tv, Tertiary volcanic rocks north of Naknek Lake (early Tertiary volcanic rocks of Aleutian volcanic arc); Tg, Tertiary granitic to gabbroic intrusive and hypabyssal rocks (includes units Tgb, Tqd, and Tgd as shown on pl. 1); KJs, Cretaceous and Jurassic sedimentary rocks (includes sedimentary rocks of Kaguyak, Pedmar, Herendeen, Staniukovich, and Naknek Formations); Ji, Jurassic granitic to gabbroic intrusive rocks of Alaska–Aleutian Range batholith (includes units Jgr, Jgd, Jqd, and Jgb as shown on pl. 1); JPzm, Jurassic to Paleozoic(?) pre-batholithic rocks (includes Jurassic Talkeetna and Triassic Kamishak Formations, Triassic Cottonwood Bay Greenstone, and metamorphic rocks of Paleozoic(?) to Jurassic Kakhonak Complex as shown on pl. 1). Faults are dotted where approximately located; sawteeth on upper plate of thrust faults.

assemblages indicative of greenschist facies, but, locally, rocks having andesine-hornblende assemblages probably reflect higher grade contact-metamorphic aureoles around Jurassic plutons. Protoliths presumably consist of units older than Middle Jurassic that have been mapped in the Katmai study area, as well as unnamed sandstone and argillite units.

MESOZOIC ROCKS

The oldest rocks of relatively certain age (as determined by fauna in the overlying limestone) in the Katmai study area are submarine basalt flows and diabase sills of the Cottonwood Bay Greenstone, which were recrystallized to fine-grained assemblages suggestive of greenschist(?) facies but which retain primary igneous textures. This unit was defined in the adjacent Iliamna quadrangle (Detterman and Reed, 1980), where it is inferred to be of Late Triassic age. In the Katmai region, this unit crops out only as roof pendants in the Alaska–Aleutian Range batholith near the south margin of the study area, and the unit is projected beneath the glacial cover in the Naknek quadrangle on the basis of an interpretation of aeromagnetic data (Church and others, 1992). Marine limestone and locally interbedded basalt flows overlie the Cottonwood Bay Greenstone. This limestone was originally reported to be Paleozoic in age (Detterman and others, 1979) but is now assigned (Detterman and others, in press) to the Upper Triassic Kamishak Formation (Detterman and Reed, 1980).

The Lower Jurassic Talkeetna Formation, composed mainly of volcanic rocks and interbedded volcaniclastic or marine sedimentary rocks, is part of a volcanic arc (Reed and Lanphere, 1973) that crops out as far as 500 km to the northeast in the Talkeetna Mountains (Martin, 1926). In the Katmai study area the unit consists mostly of sandstone and siltstone, which are interbedded with volcanic tuff and lahar deposits, volcaniclastic conglomerate and lava flows, and breccia.

The plutonic rocks of the Alaska–Aleutian Range batholith intrude the Talkeetna Formation and older rocks in the Katmai study area. These intrusive rocks are mainly tonalite, granodiorite, and quartz diorite, but also include diorite, granite, and gabbro (classified on the basis of modal quartz-plagioclase-alkali feldspar ratios after the method of Streckeisen, 1973). Reed and Lanphere (1969, 1972) found Jurassic, Late Cretaceous to early Tertiary, and middle Tertiary age groupings of plutons in the Alaska–Aleutian Range batholith north of the study area. Potassium-argon ages determined from 11 samples of Mesozoic plutonic rocks from the Katmai study area range from about 153±4.6 to 173±5.2 Ma (Reed and Lanphere, 1972; Shew and Lanphere, 1992), that is, from late Early to Late Jurassic. The potassium-argon data acquired during this study support the earlier age groupings of plutons in the Alaska–Aleutian Range batholith (Reed and Lanphere, 1969). There are no new potassium-argon data indicating that Late Cretaceous to early Tertiary intrusive rocks are present in the Katmai study area.

The Naknek Formation, the most extensive rock unit of the Alaska Peninsula, was deposited in Late Jurassic time and is composed of debris eroded from the Alaska–Aleutian Range batholith and its roof rocks (Egbert and Magoon, 1981) during uplift northwest of the Bruin Bay fault. In the Katmai study area, this unit averages 1,900 m in thickness and is subdivided into five members (Detterman and others, in press). The lowermost member, the Chisik Conglomerate Member, consists of conglomerate and fluvial sandstone; the conglomerate clasts are mostly metamorphic and plutonic rock fragments. The overlying member, the Northeast Creek Sandstone Member, consists of mixed marine and nonmarine sandstone and siltstone. The sandstone units contain magnetite-rich laminae; the interbedded siltstone units contain plant debris and are locally bioturbated. The next overlying member, the Snug Harbor Siltstone Member, is marine siltstone consisting of thin limestone beds and containing abundant limestone concretions. The next overlying member, the Indecision Creek Sandstone Member, is a marine sandstone and silty sandstone that also contains plant debris. The uppermost member, the Katolinat Conglomerate Member, occurs nearly exclusively within the Katmai study area and consists of interbedded marine sandstone and conglomerate. Sandstone units in the lower part of the Naknek Formation south of Becharof Lake are arkose or feldspathic wacke (Mullen, 1987) that are sufficiently rich in magnetite to yield aeromagnetic anomalies (Case and others, 1988).

There were four cycles of emergence followed by submergence and marine deposition during and at the end of the Cretaceous in the Katmai region. These cycles of marine deposition are represented by the Staniukovich, Herendeen, Pedmar, and Kaguyak Formations: each is bounded by unconformities. However, farther south on the Alaska Peninsula rocks of the Naknek, Staniukovich, and Herendeen Formations are conformable and represent continuous sedimentary deposition (Detterman and others, in press). The Staniukovich Formation consists of feldspathic marine sandstone and siltstone. In the Katmai region the Herendeen Formation is a calcareous sandstone that is interbedded with an equal volume of siltstone. Erosional remnants of the unit are widespread on the Alaska Peninsula, but it apparently has been removed in most places by erosion. The upper contact of the Herendeen is a major regional unconformity (Detterman and others, in press). Carbonaceous sandstone and siltstone of the Pedmar Formation disconformably overlie the Herendeen Formation in the Katmai study area and are the only well-documented occurrence of Albian rocks on the Alaska Peninsula (Detterman and others, in press). The Upper Cretaceous Kaguyak Formation unconformably overlies all older strata in the Katmai study area. This unit consists of interbedded marine sandstone and siltstone which, in its lower part, contains thin limestone beds. The upper part of the unit contains rip-up clasts, flame structures, and load casts indicative of turbidite deposition in a marine basin (Keller and Reiser, 1959; Detterman and Miller, 1985).

TERTIARY ROCKS

About 6,000 m of marine and continental Tertiary strata are preserved on the southern Alaska Peninsula (Detterman and others, in press), and at least 7,800 m of continental Tertiary strata are present in the subsurface in the Cook Inlet region (Calderwood and Fackler, 1972). Tertiary strata are absent or thin, however, from Becharof Lake north to Cape Douglas (fig. 1), indicating the presence of a structural high (Fisher and others, 1981; Detterman and others, 1987). A maximum of 1,025 m of the lower Tertiary Copper Lake Formation is preserved near Cape Douglas, and 558 m of the upper Oligocene Hemlock Conglomerate is exposed near Cape Nukshak in the Katmai study area. The Copper Lake Formation consists of well-indurated, polymictic conglomerate and fluvial sandstone and siltstone; it contains altered volcanic clasts that were probably derived from the Talkeetna Formation. The Hemlock Conglomerate consists of poorly indurated fluvial conglomerate, tuffaceous sandstone, siltstone, shale, coal, and tuff.

Sedimentary rocks of Tertiary age crop out west of the crest of the Aleutian volcanic arc in the Katmai study area, but their maximum thickness is only about 300 m. The strata are poorly indurated to moderately well indurated and comprise fluvial sandstone, siltstone, conglomerate, and tuffaceous sandstone and siltstone. Some of these rocks are probably laterally equivalent to the Copper Lake Formation, but their localized occurrence suggests that they may have been deposited in small scattered basins having no necessary temporal relation to one another.

Early to middle Tertiary lava flows, domes, and dikes crop out in the western part of the Katmai study area, in the Nushagak–Bristol Bay Lowland. The flows are mainly andesitic in composition, whereas the dikes and domes are basaltic. These volcanic rocks typically contain incipient secondary chlorite, but they show little other evidence of alteration. A single nearly aphyric quartz-bearing dome, now silicified and altered, and the pumiceous tuff, occurring as boulders in till, indicate the presence of rocks more siliceous than andesite. Five potassium-argon radiometric ages determined from samples of the western lava flows range from about 34.3±0.7 to 44.3±0.8 Ma, and two dikes are 36.8±0.3 and 25.0±1.6 Ma (Shew and Lanphere, 1992).

Late Tertiary lava flows, dikes, sills, and small plutons east of the crest of the Aleutian Range are a part of the Aleutian volcanic arc that has been active since Miocene time. Extrusive rocks are mostly andesitic or dacitic lava flows that overlie, and locally deform, upper Oligocene sedimentary rocks of the Hemlock Conglomerate. The contact between magmatic and sedimentary rocks is locally gradational due to intrusion of sills in the uppermost part of the sedimentary section. Both volcanic and sedimentary rocks have been intruded by small tonalitic or granodioritic plugs or plutons. Contact-metamorphic aureoles surround these plutons, and the rocks within the aureoles, as well as in the plutons themselves, in many cases have propylitic alteration zones. Weathering of these alteration zones has yielded reddish-brown color anomalies, probably formed by the oxidization of pyrite. Two lava flows of the eastern volcanic rock group are each about 13.9 Ma, and several of the intrusive rocks range in age from about 2.5 to 8 Ma (Shew and Lanphere, 1992).

Sills, dikes, and plutons of tonalite or quartz diorite crop out between Yori Pass and Rainbow River, northwest of the Aleutian Range crest in the central part of the study area. These shallow intrusive rocks are commonly associated with reddish-brown color anomalies developed both in the intrusive rocks and in their sedimentary wallrocks. Widespread deuteric(?) alteration of the intrusive rocks has precluded age determination using potassium-argon methods. The plutons have intruded sedimentary rocks as young as Late Cretaceous in age; hence, a Tertiary age for these sedimentary rocks is inferred on the basis of geologic relationships (Riehle and others, in press).

Tertiary plutons northwest of the Bruin Bay fault, in the Alaska–Aleutian Range batholith, are mostly granodiorite and quartz monzodiorite, but also include tonalite, quartz diorite, and gabbro. Potassium-argon ages of nine samples range from about 26.0±0.81 to 37.6±1.1 Ma (Reed and Lanphere, 1972; Shew and Lanphere, 1992). Two of these middle Tertiary plutons intrude the Bruin Bay fault near Kulik Lake. Contact-alteration effects (primarily induration by silicification and possibly recrystallization), anastomosing quartz veins, and color anomalies are locally prominent near the Tertiary plutons where they have intruded both Jurassic plutons and Mesozoic sedimentary rocks east of the Bruin Bay fault. Altered zones surrounding the middle Tertiary plutons within the Alaska–Aleutian Range batholith are not as pervasive as those around the hypabyssal rocks between Yori Pass and the Rainbow River.

QUATERNARY ROCKS AND DEPOSITS

Quaternary deposits in the Katmai study area are primarily glacial deposits (Riehle and Detterman, 1993), or volcanic rocks and deposits of the active Aleutian volcanic arc. Although the entire Katmai study area was extensively glaciated several times, thick deposits of drift are extensive only west of the Aleutian Range in the Nushagak–Bristol Bay Lowland province.

Quaternary volcanic deposits of the Aleutian volcanic arc are confined mainly to the large stratovolcanoes along the crest of the Aleutian Range. The lava flows are mainly andesite or dacite, whereas the domes range from dacite to rhyolite. Ash-flow tuffs, chiefly dacite to rhyolite, are present along the southern margin of the Katmai study area, in the Valley of Ten Thousand Smokes (formed during the 1912 Novarupta eruption; Fenner, 1920; Curtis, 1968; Hildreth, 1983, 1987), and at Kaguyak Crater. Pumice deposited during the 1912 Novarupta eruption is more than 1 m thick in the area extending from the head of the Valley of Ten Thousand Smokes east to Shelikof Strait (J.E. Fierstein, written commun., 1990).

STRUCTURAL GEOLOGY

The major structural feature in the Katmai region is the Bruin Bay fault, a high-angle reverse fault that extends from 400 km north of the study area in upper Cook Inlet (Detterman and others, 1976) to Becharof Lake, where it is concealed beneath thick Quaternary deposits (fig. 1). Movement is clearly up on the west side of the fault in the Katmai study area, although one strand of the fault several kilometers in length near the center of the Katmai study area is a high-angle normal fault. Because the fault in the Katmai study area juxtaposes only Jurassic intrusive rocks on the northwest against the Naknek Formation, there is no unambiguous evidence of the amount of stratigraphic throw or possible horizontal displacement. To the north, in the Iliamna quadrangle, as much as 3 km of stratigraphic throw can be demonstrated and there is a suggestion of as much as 65 km of left-lateral offset (Detterman and Reed, 1980, p. 69). On the basis of crosscutting plutons dated by potassium-argon methods (Shew and Lanphere, 1992), the last movement on the Bruin Bay fault took place no later than middle Tertiary time (Riehle and others, in press).

The style of folding changes at the Bruin Bay fault. Folds in isolated roof pendants of rocks older than Upper Jurassic northwest of the fault are tight and possibly overturned, whereas those in Upper Jurassic, Cretaceous, and Tertiary strata southeast of the fault are open. The trend of fold axes in both areas is generally northeast, parallel to the structural grain of the Alaska Peninsula elsewhere (Burk, 1965). Fold axes in Tertiary strata along Shelikof Strait, however, locally deviate from the average northeasterly trend. In some places, this deviation from the regional structural trend is clearly due to deformation during intrusion by adjacent plugs and domes; other local deviations in structure may likewise be the result of unexposed plutons. Southeast of the Bruin Bay fault, both sedimentary and volcanic rocks are also commonly fractured or are broken by minor faults, quartz veins, or dikes that have a general northwesterly trend.

At least two main periods of regional deformation can be demonstrated in the Katmai study area (Riehle and others, in press). Northwest of the Bruin Bay fault, the rocks of the Lower Jurassic Talkeetna Formation dip homoclinally, but are not folded. However, underlying Triassic rocks as well as the rocks of the Kakhonak Complex are folded about northeast-trending axes. As shown by Detterman and Reed (1980) in the adjacent Iliamna quadrangle, deformation also probably accompanied emplacement of plutons in Middle Jurassic time. Southeast of the Bruin Bay fault, rocks of the Hemlock Conglomerate of late Oligocene age (Riehle and others, in press) and overlying early Miocene volcanic rocks are folded on a regional scale.

MINERAL EXPLORATION

Exploration by early prospectors began on the Alaska Peninsula about the turn of the century (Atwood, 1911). In 1918, most of the Katmai study area was declared a National Monument, and thus these Federal lands were withdrawn from mineral exploration; the monument was enlarged to establish Katmai National Park and Preserve in 1980. As a result, there has been only limited exploration for minerals in much of the Katmai study area. Atwood (1911) reported no known mineral prospects in the Katmai study area through 1908. Martin (1920) reported mineral exploration activity near Kukak Bay. A few placer gold claims and lode-copper prospects had been previously reported (see summary by MacKevett and Holloway, 1977). The mineral-occurrence data and the mineral resource assessment of the Katmai study area are summarized in Church and others (1992). Detailed descriptions of newly defined mineral occurrences within the Katmai study area are summarized below.

KNOWN MINERAL OCCURRENCES ON THE ALASKA PENINSULA AND IN THE AREA NORTH OF THE KATMAI STUDY AREA

Mineral occurrences on the Alaska Peninsula can be classified by their age and geologic association. In evaluating the Katmai study area, we have effectively narrowed the search for mineral deposits by the use of restrictive geologic criteria for specific types of mineral deposits (see Cox and Singer, 1986). Thus, within the Katmai study area, massive sulfide deposits associated with the pre-Jurassic volcanic rocks would be found only west of the Bruin Bay fault where submarine volcanic rocks crop out (fig. 2). Skarn and polymetallic-vein deposits associated with middle Tertiary plutons would be expected only in the north-central part of the Katmai study area. Porphyry Cu and porphyry Cu-Mo deposits and related skarns, and polymetallic and epithermal quartz-vein deposits might be expected within and adjacent to Tertiary and Quaternary plutonic rocks of the Aleutian volcanic arc. For the most part, areas favorable for these types of mineral deposits are east of the Bruin Bay fault. The notable exception is the area underlain by lower to middle Tertiary volcanic rocks north of Naknek Lake.

Descriptions of mineral occurrences found elsewhere on the Alaska Peninsula, briefly summarized below, serve as examples of the types of mineral deposits that might be expected within the Katmai study area. The mineral deposit models, summarized largely from Cox and Singer (1986), serve as a classification and nomenclature scheme as well as being an effective method to compare geologic attributes of other mineral deposits and field observations from the Katmai study area.

MINERAL OCCURRENCES ASSOCIATED WITH PRE-JURASSIC ROCKS AND PRE-BATHOLITHIC ROCKS

The Johnson River prospect (Steefel, 1987), in the Lower Jurassic Talkeetna Formation about 120 km north of the Katmai study area, is a quartz-sulfide stockwork in a series of subaqueous tuffs and debris flows of dacitic composition. Anhydrite is abundant, occurring as spherical nodules enclosed in magnesian chlorite containing disseminated pyrite. Later-stage veins of quartz and anhydrite are found in an iron-rich chloritic matrix. Disseminated, massive, and vein pyrite, chalcopyrite, sphalerite, galena, and minor gold also are present in the iron-rich chloritic matrix. Adjacent dacitic hypabyssal plugs may have served as the source of the tuffs as well as the heat needed to form the Johnson River deposit. Steefel (1987) has interpreted the Johnson River deposit, on the basis of its geologic setting, geochemistry, and morphology, to be a Kuroko-type massive sulfide deposit. Similar occurrences have also been investigated in the Talkeetna Formation farther north in the Talkeetna Mountains (Newberry, 1986; Newberry and others, 1986). Results of stream-sediment or rock exploration surveys around the Johnson River deposit have not been reported. However, the reported data on Kuroko-type massive sulfide deposits elsewhere indicate that rock samples would contain anomalous concentrations of Zn, Cu, Pb, Ba, Ag, and Au. Stream-sediment samples would likewise contain anomalous concentrations of these same elements (Singer, 1986a).

Reed and Detterman (1965) described two occurrences of magmatic magnetite associated with the rocks of the Alaska–Aleutian Range batholith in the Iliamna quadrangle. At Frying Pan Lake, there is a magnetite-rich breccia body at the margin of a Jurassic pluton about 100 km north of the study area. The breccia, which is composed almost entirely of magnetite-bearing pyroxenite fragments, was formed during a Late Jurassic intrusive event (Reed and Detterman, 1965). A second magnetite occurrence, the Pile Bay locality at the north end of Iliamna Lake, is a magnetite-rich hornblendite. Here, magnetite is present primarily as disseminated grains comprising from 15 to 20 percent of the rock (Reed and Detterman, 1965). Both the rocks and the stream sediments from this area contained anomalous concentrations of iron, titanium, and vanadium that are directly related to high concentrations of magnetite (Reed, 1967). The magmatic magnetite occurrences at Frying Pan Lake and Pile Bay have characteristics of the Bushveld Fe-Ti-V mineral deposit model (Page, 1986). These are the only mineral occurrences associated with the Jurassic batholith in the Iliamna quadrangle (Detterman and Reed, 1980). Because gabbro is found only in scattered outcrops in the Katmai study area (Riehle and others, in press), sites where this type of mineral deposit might be present are very limited.

MINERAL OCCURRENCES ASSOCIATED WITH LATE CRETACEOUS TO MIDDLE TERTIARY PLUTONIC ROCKS OF THE ALASKA–ALEUTIAN RANGE BATHOLITH

A variety of claims and lode prospects, largely for the commodities gold, silver, and copper, have been filed in the Iliamna quadrangle. These claims and occurrences are generally in contact-metamorphic zones in limestone of the Triassic Kamishak Formation, where skarns have developed adjacent to Late Cretaceous and Tertiary plutons. Where these skarns are found adjacent to the greenstones of the Talkeetna Formation, they are primarily quartz veins that contain pyrite, some of which is auriferous; commonly, they also contain chalcopyrite, or magnetite and hematite (Martin and Katz, 1912; Detterman and Reed, 1980, p. 76). Reed (1967) discussed several sites in the Iliamna quadrangle, as well as the Kasna Creek area in the Lake Clark quadrangle, where exploration reconnaissance studies indicate areas favorable for undiscovered copper-rich iron-skarn deposits. The Kasna Creek area, 135 km north of the Katmai study area, and the Crevice Creek prospect (McNeil claims), 12 km north of the Katmai study area, are the largest and best described; both have features characteristic of a copper-rich iron-skarn mineral deposit model (Cox, 1986a).

The Crevice Creek prospect is in a large tactite body that was formed along the contact between the Kamishak Formation and the greenstones of the Talkeetna Formation. It contains both disseminated and lode pyrite and chalcopyrite. Nearby, on Sargent Creek, quartz-magnetite lodes are found within epidote-garnet tactite formed in the upper chert-rich member of the Kamishak Formation. Both areas are cut by numerous quartz-feldspar porphyry dikes. Additional magnetite-rich lenses of tactite are exposed on Pilot

Knob just north of Crevice Creek at the contact with the granodiorite of Pilot Knob (Richter and Herreid, 1965). Geologic characteristics similar to those reported for Sargent Creek are also described for the Dutton claim, 85 km north of the Katmai study area (Martin and Katz, 1912), as well as for sites elsewhere along the strike of the Kamishak Formation in the Iliamna quadrangle (Detterman and Reed, 1980, fig. 6, p. 74). In all descriptions of these skarns, mineralized rock is said to be localized along the contact between the Kamishak and the Talkeetna Formations and largely confined to the limestone exposures.

The Kasna Creek prospect is a large, low-grade Cu-Fe deposit consisting mostly of disseminated to massive hematite and magnetite, which is pseudomorphous after hematite, and lesser amounts of pyrite, chalcopyrite, and minor sphalerite in a tactite developed at the contact with a Tertiary intrusion (Warfield and Rutledge, 1951; Nelson and others, 1985). Pyrite and chalcopyrite are generally restricted to contact-metasomatic zones within the Kamishak Formation.

Reconnaissance exploration geochemical studies of the area around these copper-rich iron-skarn prospects indicate that stream sediments have anomalous concentrations of Fe, Cu, Mo, As, Zn, and Pb, and nonmagnetic-heavy-mineral-concentrate (NMHMC) samples contained anomalous concentrations of Au, Ag, Pb, and Bi. Rock samples of skarn likewise contained anomalous concentrations of Fe, Cu, Co, Zn, Ag, and Au (Reed, 1967; Richter and Herreid, 1965; King and others, 1985).

Anomalous concentrations of lead, silver, and zinc are found in galena- and sphalerite-bearing veins in brecciated limestone at the Duryea prospect 2 km northeast of the Dutton prospect. Martin and Katz (1912) described small galena-sphalerite lodes along fissures in limestone cut by numerous small dikes. Galena, sphalerite, and minor amounts of pyrite are also disseminated in the limestone. Weathering of these lodes has resulted in manganiferous gossans that carry elevated levels of silver. The Duryea prospect best fits the description of a Zn-Pb skarn mineral deposit model (Cox, 1986b).

MINERAL OCCURRENCES ASSOCIATED WITH TERTIARY AND QUATERNARY VOLCANIC ARC ROCKS

Wilson and Cox (1983) described porphyry Cu mineral occurrences in the southern part of the Alaska Peninsula (fig. 1) that are associated with early Tertiary to Quaternary intrusive rocks of intermediate composition that intrude earlier volcanic rocks and marine and nonmarine sedimentary clastic rocks. Studies of the Ugashik and Karluk quadrangles, immediately south of the Katmai study area, outlined several areas favorable for undiscovered porphyry Cu deposits (Church, Detterman, and Wilson, 1989; Church, Frisken, and Wilson, 1989) of Tertiary age (Wilson and Shew, 1988). The porphyry Cu occurrences of the Alaska Peninsula are characterized by drainage basins in which stream sediments are anomalous in both copper and molybdenum and that also commonly contain anomalous concentrations of tungsten and tin. In many cases, stream-sediment samples from drainage basins peripheral to these central geochemical anomalies are anomalous in one or more of the following elements: Pb, Zn, Bi, As, Ag, and Au. These zoned geochemical patterns, which are evident when shown at the 1:250,000 scale, are indicative of the relatively large size of undiscovered porphyry Cu deposits. Rocks in the central part of the porphyry Cu anomaly pattern typically contain potassic or phyllic alteration mineral assemblages. Sulfide minerals are found in quartz-vein stockworks; pyrite, molybdenite, and chalcopyrite are also disseminated in the host rocks. Altered rock samples commonly contained anomalous concentrations of Cu, Mo, and Co, and, less commonly, Sn and W. Surrounding these central anomalies are zones of argillic and propylitic altered rock containing both disseminated and vein pyrite and pyrrhotite, and lesser amounts of galena, sphalerite, arsenopyrite, precious metals, barite, and tourmaline. Altered and mineralized rock samples commonly contained anomalous concentrations of Pb, Zn, Cd, Ag, and Ba, and, less commonly, of As, Bi, or B. Anomalous concentrations of gold are associated with some porphyry deposits, and placer gold may be found in streams surrounding porphyry Cu-Au deposits (Cox, 1986d; Church, Frisken, and Wilson, 1989). Weathering and oxidation of sulfide minerals commonly produce characteristic yellow-brown and reddish-brown color anomalies in the bedrock. Hollister (1978, p. 68–76) summarized the geologic and geochemical characteristics of a number of porphyry occurrences on the Alaska Peninsula. The most common porphyry-type occurrences on the Alaska Peninsula have characteristics of the porphyry Cu, porphyry Cu-Mo, and porphyry Cu-Au mineral deposit models (Cox, 1986c,d,e).

Precious-metal-bearing epithermal quartz-vein deposits, exemplified by the quartz veins at the Apollo Mine and Shumagin prospect on Unga Island, are also found on the Alaska Peninsula. The Apollo Mine, 470 km southwest of the Katmai study area, has produced 3,469 kg of gold (Green and others, 1989). This deposit is in reticulate, nearly vertical quartz veins hosted by Oligocene lava flows and domes, mainly of andesitic composition (Atwood, 1911; Wilson and others, 1988). The mineralized zone ranges in width from about 2 to 5 m and extends for more than 250 m. Quartz veins contain pyrite, chalcopyrite, sphalerite, galena, and free gold. Stream sediments in the area of the Apollo Mine have anomalous concentrations of Au, Ag, B, Cu, Mo, Pb, Sn, and Zn (Frisken and Arbogast, 1992).

The Shumagin prospect, also located on Unga Island, has similar mineralogy and geologic features. White and Queen (1989) reported results from a drilling program indicating reserves of 270,000 tonnes of gold ore at 16.8 g/tonne gold from a quartz vein ranging in width from 1 to 15 m over a length of 370 m. The ore zone is a pyrite-bearing quartz vein that contains Au, Ag, Te, Pb, Zn, and Mn at anomalous concentrations. Anomalous concentrations of arsenic and copper in altered rock are detected in some places in the ore zone; mercury forms a 75-m-wide halo surrounding the deposit. Late-stage vuggy quartz veins, which parallel the ore veins, and crosscutting carbonate veins are generally barren of gold. Both the Apollo Mine and the Shumagin prospect, as well as some other prospects on Unga Island, are on or near through-going regional shear zones that have localized quartz veins in silicified volcanic rocks (White and Queen, 1989). W.H. White (oral commun., 1990) classified the Apollo and Shumagin deposits as adularia-sericite type, gold-bearing epithermal quartz veins (Heald and others, 1987).

Base-metal anomalies in stream sediments from drainage basins peripheral to porphyry Cu occurrences are described in both the Ugashik and Karluk (Church, Frisken, and Wilson, 1989; Church, Detterman, and Wilson, 1989) and the Chignik and Sutwik Island quadrangles (Cox and others, 1981). Similar geochemical anomaly suites are present in numerous drainage basins within the Katmai study area. Many of these anomalies are interpreted to reflect polymetallic veins (mineral deposit model 22c; Cox, 1986f). Three previously described polymetallic veins from elsewhere on the Alaska Peninsula are outlined below as examples of the types of polymetallic veins that might be expected in the Katmai study area.

The Braided Creek occurrence (Cox and others, 1981), 165 km south of the Katmai study area, is described as a quartz-vein system that strikes N. 20°–45° and dips 70° W., cutting the Naknek Formation and Tertiary intrusive rocks. It contains only a small tonnage and the ore is of low grade (0.1 percent Cu, 0.2 percent Zn, 0.15 percent Pb, and 0.5 percent As; table 2, Cox and others, 1981). The quartz veins contain pyrrhotite, arsenopyrite, sphalerite, pyrite, chalcopyrite, and galena.

Immediately south of the Katmai study area (15 km) on Cape Kubugakli, quartz stringers in late Tertiary hypabyssal dikes (Detterman and others, 1987) contain stibnite, molybdenite, galena, and tetrahedrite (Smith, 1925; Church, Detterman, and Wilson, 1989). Placer gold (5 kg) was produced from one stream draining the area (Smith, 1925). Wilson and O'Leary (1986, 1987) reported anomalous concentrations of copper, silver, gold, zinc, and molybdenum in samples of the quartz vein from this locality. Church, Detterman, and Wilson (1989) interpreted the geologic and geochemical data from this deposit to be characteristic of a polymetallic-vein mineral deposit model (Cox, 1986f).

A less well studied Au-Ag-Cu-bearing polymetallic quartz vein is exposed near Battle Lake, 13 km north of the Katmai study area. Detterman and Reed (1980) reported that this quartz vein, which varies in thickness from a few centimeters to as much as 2 m along a discontinuous outcrop of about 300 m, cuts Tertiary volcanic rocks. Free gold, chalcopyrite, pyrite, and an unidentified sulfosalt mineral are present sporadically throughout the vein, which is pervasively stained with malachite. Anomalous concentrations of Cu, Au, Ag, Mn, Pb, and Zn are present in samples of the quartz vein material (Detterman and Reed, 1980; S.E. Church, unpub. data, 1990).

EXPLORATION GEOCHEMISTRY

SAMPLE AND DATA COLLECTION

Stream-sediment samples and heavy-mineral-concentrate samples from stream sediments were collected from active stream channels in drainage basins ranging in area from 5 to 25 square kilometers. A total of 1,198 stream-sediment samples and 1,038 heavy-mineral-concentrate samples were collected during the reconnaissance geochemical sampling program during the summer field seasons of 1983–86. Both sample media were collected by wet sieving through a 9-mesh (2-mm) stainless-steel screen. One 35-cm gold pan full of sediment was collected and about 0.5 kg was retained as the stream-sediment sample. The remaining material was panned at the site to produce the heavy-mineral-concentrate sample (Bailey and others, 1986).

The minus-2-mm stream sediments were air-dried and sieved through an 80-mesh screen. The minus-80-mesh fraction was ground to minus-150 mesh using ceramic plates and chemically analyzed. The heavy-mineral concentrates were air-dried and sieved to minus-20-mesh. Following removal of the light-mineral fraction by flotation in bromoform (specific gravity about 2.8), the heavy-mineral fraction was separated into three magnetic splits with a Frantz Isodynamic Magnetic Separator. The most magnetic fraction contained magnetite and rock fragments including large amounts of magnetite. The second fraction was of intermediate magnetic susceptibility and consisted of rock fragments as well as most of the more magnetic, mafic rock-forming silicate minerals. The nonmagnetic fraction contained the high-specific-gravity rock-forming minerals, such as apatite, zircon, rutile, and sphene, as well as minerals that might be indicative of mineralized areas, such as epidote, tourmaline, fluorite, barite, scheelite, wulfenite, cassiterite, gold, and the sulfide minerals. The nonmagnetic fraction was split if adequate sample was recovered, and one portion was used for mineral identification (1,033 of 1,038 in this study; Bennett and Church, 1987). A second portion was ground for spectrographic analysis (Bailey and others, 1986). For brevity, the stream-sediment samples and the nonmagnetic heavy-mineral-concentrate samples from stream sediments will be referred to as the "SS samples" and the "NMHMC samples," respectively, in this report.

During the collection of the reconnaissance stream sediments, we also examined rocks along the streams and sampled material that contained either veins or disseminated sulfides or that appeared to be hydrothermally altered. These samples will be referred to as "float samples" in subsequent discussions. Rock samples for geochemical analysis were also taken from outcrop both during the geologic mapping and during our followup work. These samples were crushed, split, and a representative fraction ground to minus-150-mesh with ceramic plates.

Stream-sediment, rock, float, and NMHMC samples were analyzed by a six-step, semiquantitative, direct-current-arc emission spectrographic method (Grimes and Marranzino, 1968). For selected rock samples (about 10 percent of those collected), the concentrations of As, Ag, Bi, Cd, Sb, and Zn were determined by atomic absorption after digestion in nitric acid. Mercury was determined by cold-vapor atomic absorption and gold was determined by atomic absorption after digestion in hydrobromic acid and separation into methyl-isobutyl ketone (MIBK) (see O'Leary and Meier, 1986). The geochemical data resulting from analysis of the SS and NMHMC were reported in Bailey and others (1986). Geochemical results from analyses of the float and rock samples were reported in Riehle and others (1989).

The SS samples were also analyzed by an ICP-aqua-regia digestion procedure (Church and others, 1987). This digestion, which was done on 0.5–1.0 g of sample, affords a more representative sample than the 0.010 g of sample used in the semiquantitative emission spectrographic analysis. Analytical reproduciblity is much better than that given by semiquantitative emission spectrographic analysis (Church and others, 1983; 1987). Geochemical data determined from the aqua-regia leachates of the SS samples were reported in Erlich and others (1988).

DISCUSSION OF THE RECONNAISSANCE GEOCHEMICAL DATA

A map showing the distribution of SS samples containing anomalous concentrations of selected elements was presented in Church, Bailey, and Riehle (1989). A brief statistical summary of the SS data is given in table 1, and the elemental distributions of the SS data (fig. 3) are shown by the boxplot method of Tukey (1977). Threshold values were determined by examination of the histograms and percentiles (table 1) of each of the elements plotted.

Maps showing the distribution of SS samples containing anomalous concentrations of selected elements detected in the aqua-regia leachates were presented in Church and Motooka (1989). The ICP analytical procedure was used to provide data on metals, for example phosphorous, arsenic, and zinc, which can be more readily determined at crustal abundance levels by ICP analytical methods than by semiquantitative emission spectrography. The aqua-regia-leachate data supplement the geochemical results for the SS samples and were used to enhance the interpretation of the SS geochemical data. A brief statistical summary of the aqua-regia-leachate data is given in table 2. Thresholds were determined by examination of histograms and percentiles (table 2), and by evaluation of cumulative frequency distributions of the elements plotted (Sinclair, 1976).

The aqua-regia-digestion procedure is a partial leach (Church and others, 1983); the procedure yields elemental values that represent only partial recoveries from the sample. Studies of geochemical data from hand-picked mineral separates show that the aqua-regia-leach procedure significantly enhances metal anomalies important in exploration geochemistry. Many oxide, carbonate, and sulfide minerals are more readily dissolved in aqua regia than are silicate minerals (Church and others, 1987). However, this digestion does not leach significantly most metals bound in silicate minerals. The clay minerals are the only silicates that provide a significant contribution to the geochemical background. Thus, interpretation of the data must take into account the geochemical contrast achieved by the analytical method. A detailed comparison of the results from the ICP-aqua-regia-leach and the semiquantitative emission procedure can best be made by visual inspection of the maps of the geochemical anomalies defined by the data determined using the two methods. The results from both methods are similar for many elements, and clusters of elements having anomalous concentrations were determined for the same localities with both analytical methods. However, the ICP-aqua-regia-leach data define somewhat broader geochemical anomaly patterns and they also provide information on the distribution of arsenic and zinc at crustal-abundance levels without additional chemical digestion of the samples. This method, therefore, is a superior geochemical technique for this study area.

Maps showing the distribution of NMHMC samples containing anomalous concentrations of selected elements were presented in Church and Arbogast (1989). These data are from samples collected and processed to detect trace-element suites associated with sulfide mineralization, and, as such, they represent a highly biased sampling technique. The NMHMC data are used in this report to refine and further define geochemical anomalies outlined by the two SS data bases. A brief statistical summary of the NMHMC data is given in table 3. Threshold values were determined by examination of histograms and percentiles of the data (table 3).

Of the six types of mineral deposits described earlier, the geologic mapping and geochemical data suggest that the Katmai study area is generally favorable for undiscovered deposits of only three: porphyry Cu (Cox, 1986c),

Table 1. Summary of emission spectrographic data for stream-sediment samples from the Katmai study area, Alaska.[1]

[Analysis by semiquantative emission spectrography; all values reported in parts per million except for Mg, Ca, Fe, and Ti, which are reported in percent. Geometric mean determined from the log-transformed data. Dashes (---), no data or insufficient data]

Element	DR[2]	Observed range	Median	Geometric mean	Percentiles 90th	Percentiles 95th	Percentiles 98th	Threshold value[3]
Mg	1.000	0.2–5.0	1.5	1.41	2.0	2.0	3.0	---
Ca	1.000	.05–10.0	1.0	1.10	2.0	2.0	2.0	---
Fe	1.000	1.0–20.0	5.0	5.14	10.0	10.0	15.0	15.0
Ti	0.976	.1–1.0	0.5	0.51	1.0	1.0	>1.0	---
B	.859	10–1,500	70	14	50	100	175	100
Be	.081	1–2	---	---	---	1	1	---
Sr	.988	100–700	200	241	500	500	500	---
Ba	1.000	50–1,500	300	333	500	700	700	700
La	.035	20–150	---	---	---	---	30	---
Y	.999	10–150	20	25	50	50	50	---
Zr	.997	20–1,000	100	98	200	200	500	---
Sc	1.000	5–70	20	22	30	50	50	---
Mn	.996	50–5,000	1,000	964	1,500	2,000	2,000	2,000
V	1.000	10–1,500	150	197	500	700	1,000	---
Cr	.997	10–500	70	64	150	150	200	---
Ni	.992	5–100	20	17	30	30	50	50
Co	.997	5–150	20	25	70	70	100	70
Cu	.997	5–1,500	20	23	50	70	200	100
Mo	.055	5–30	---	---	---	5	10	7
Pb	.681	10–200	10	10	20	30	50	30
Ag	.027	.5–50	---	---	---	0.5	0.7	0.7
Au	.001	200	---	---	---	---	---	10
Zn	.119	200–1,500	---	---	200	200	500	300
As	.003	200	---	---	---	---	200	200
Sb	.002	100–500	---	---	---	---	100	100
W	.001	50	---	---	---	---	---	50

[1]Data from Church, Bailey and Riehle (1989); analytical determinations made on 1,198 samples.

[2]Detection ratio (DR) is the number of uncensored values divided by the total number of samples analyzed for a given element.

[3]Threshold values determined from the statistical distribution of the data and from histograms of the distribution of each of the elements (Church, Bailey and Riehle, 1989).

polymetallic veins (Cox, 1986f), and epithermal quartz veins (Berger, 1986; Mosier and others, 1986; Heald and others, 1987). On plates 1–3, we outline areas of drainage basins that contain anomalous concentrations of elements, as shown by the reconnaissance geochemical data base, that are indicative of possible porphyry Cu, polymetallic-vein, and precious-metal-bearing, epithermal quartz-vein mineral deposits. Scattered, single-element anomalies shown by the reconnaissance geochemical data were not considered in drawing area outlines unless the samples were taken from within, or adjacent to, drainage basins containing multi-element anomalies. For the evaluation of the porphyry Cu and related types of mineral deposits, drainage basins that contain anomalous concentrations of copper and molybdenum, with or without tin or tungsten, are shown on plate 1. Occurrences of scheelite identified in the NMHMC samples are shown on plate 1, but were not used to draw the boundaries in this geochemical interpretation because of the uncertainty associated with the identification of scheelite in NMHMC samples. The outline of

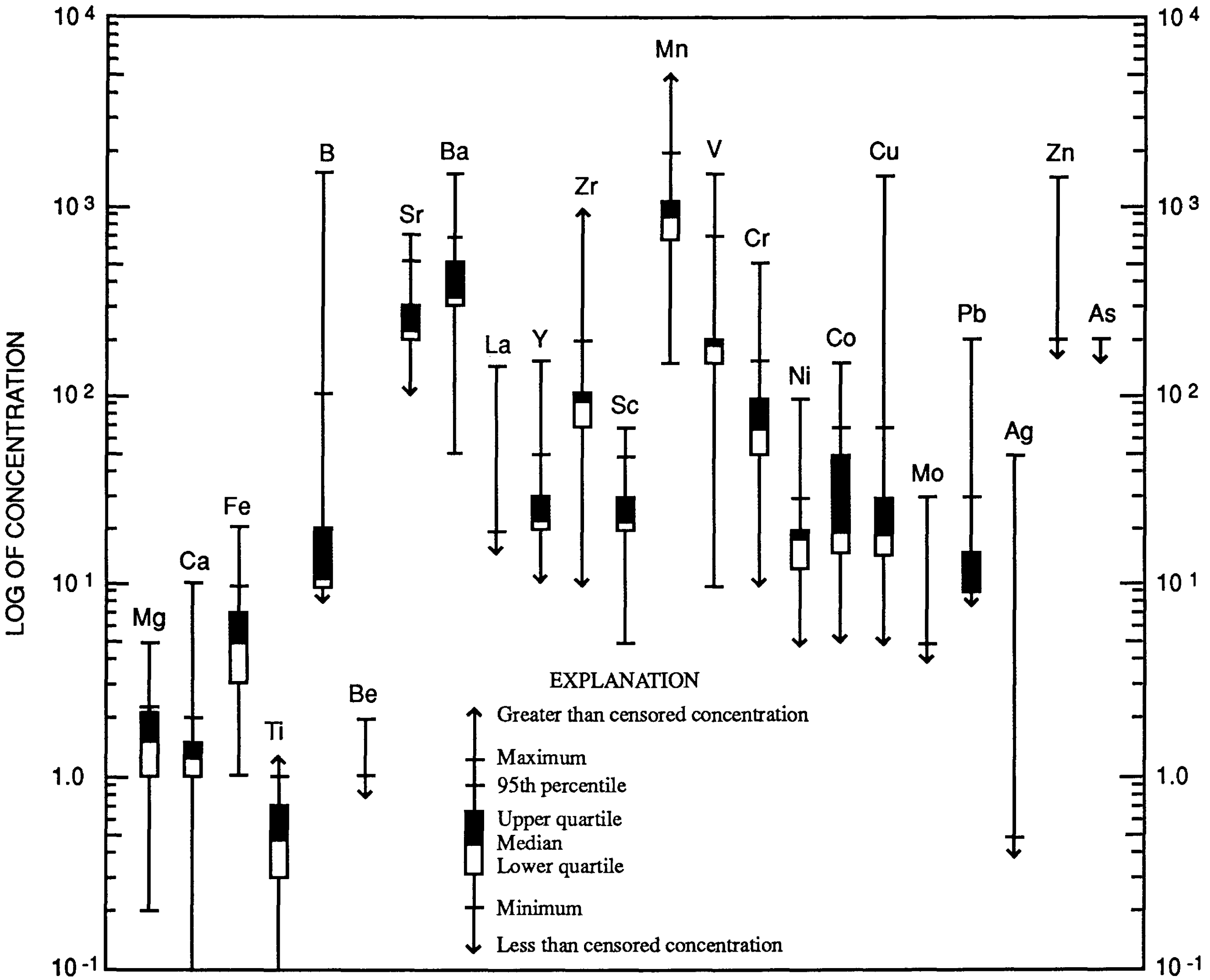

Figure 3. Boxplot of geochemical data for stream-sediment samples from the Katmai study area, Alaska. Analyses by semiquantitative emission spectrography; concentrations of Mg, Ca, Fe, and Ti are expressed in weight percent, all others expressed in parts per million (see table 1 for values plotted).

drainage basins having a geochemical signature indicative of polymetallic veins is also included on plate 1 and should be compared with the geochemical signature of the porphyry Cu deposits because these are related deposit types that are commonly peripheral to porphyry Cu deposits (Cox, 1986c,f). Drainage basins that contain anomalous concentrations of several base metals (Cu, Pb, and (or) Zn, with or without As, Mo, Ag, Cd, or Bi) are shown on plate 2. Finally, the geochemical signature of precious-metal-bearing, polymetallic-vein and epithermal quartz-vein types of mineral deposits are restricted to drainage basins that contain anomalous concentrations of As, Sb, Au, and Ag, with or without Hg or Mn (pl. 3). Drainage basin sites where the mineral gold was observed in the NMHMC samples are also shown on plate 3.

DISCUSSION OF THE ROCK GEOCHEMICAL DATA

Geochemical data for rock and float samples have been interpreted and the results presented in a manner similar to the reconnaissance geochemical data. Elemental groupings, based on the geochemical attributes of the types of mineral deposits defined above, are shown on plates 1–3 by star diagrams. The rock samples were placed into seven lithologic groups for statistical analysis of the geochemical data. The results are summarized in table 4, where we report the geometric means and the 95th and 98th percentiles determined for each lithologic group. Entries for elements whose distributions are

Table 2. Summary of aqua-regia-leachate data for stream-sediment samples, Katmai study area, Alaska.[1]

[Analysis by inductively coupled plasma–atomic emission spectroscopy (ICP–AES); all values reported in parts per million. Geometric mean determined from the log-transformed data. Dashes (---), no data or insufficient data]

Element	DR[2]	Observed range	Median	Geometric mean	Percentiles			Threshold value[3]
					90th	95th	98th	
Mg	1.000	320–33,000	3,200	3,276	7,500	9,000	10,500	---
Ca	1.000	370–75,000	3,900	3,885	7,350	8,500	11,000	---
Fe	1.000	4,500–340,000	29,000	30,740	76,000	95,000	120,000	95,000
Al	1.000	1,600–71,000	9,100	8,520	15,000	17,000	21,000	---
Ti	0.958	7.1–9,800	1,000	753	3,000	4,100	5,500	---
P	.947	15–1,500	260	197	410	460	545	---
B	.041	27–80	---	---	---	---	52	---
Be	.149	0.2–10	---	---	0.3	0.5	1.0	---
Sr	.959	3.2–410	24	20	55	65	76	---
Ba	1.000	1.8–290	34	30	87	100	130	100
La	.972	.9–11	2.6	2.6	4.8	5.6	6.6	---
Ce	.669	.9–18	2.4	1.8	6.6	8.2	10	---
Y	.424	.04–12	---	---	3.2	4.2	5.5	---
Mn	1.000	47–20,000	320	329	635	845	1,300	1,000
V	.959	15–530	88	76	200	250	300	---
Cr	.841	3.6–150	24	17	38	45	58	55
Ni	.958	1.0–330	7.4	6.9	15	17	22	17
Co	.967	2.0–43	8.4	8.4	17	21	25	20
Cu	.988	.50–910	12	11	27	36	74	50
Mo	.144	.4–30	---	---	0.6	1.2	2.2	1.5
Pb	.157	3.6–81	---	---	8.3	12	19	12
Ag	.005	.35–1.0	---	---	---	---	---	0.5
Bi	.003	16–33	---	---	---	---	---	25
Zn	.984	8–31,000	40	39	80	97	130	100
Cd	.010	.4–11	---	---	---	---	---	10
Sn	.004	2–13	---	---	---	---	---	10
As	.111	5–190	---	---	7	12	24	20
Sb	.003	14–19	---	---	---	---	---	14

[1]Data from Church and Motooka (1989); analytical determinations made on 1,185 samples. Erlich and others (1988) reported values for tungsten in 31 stream-sediment samples; however, these samples have subsequently been analyzed by the method developed by Welch (1983) and none of the reported values was confirmed. This is, undoubtedly, due to the uncertainty associated with the interference correction for iron on the tungsten line at 239.7 nm (Church, 1981).

[2]Detection ratio (DR) is the number of uncensored values divided by the total number of samples analyzed for a given element.

[3]Threshold values determined from the statistical distribution of the data and from histograms of the distribution of each of the elements (Church and Motooka, 1989).

censored[1] were calculated and reported where that portion of the distribution was determinate. Comparison of the geometric means and the 95th percentiles for the bedrock samples with those for the SS samples is presented in figure 4. Some elements show little variation in the mean among lithologic groups (for example, Fe, Zr and Co), whereas the means of other elements vary widely (for example, B, Cr, Zn, and Ni). The data in table 4, grouped on the basis of lithology, were used to define anomalous concentrations of each element. Threshold values (generally selected at the 98th percentile) used to define the anomalous concentrations for the rock data are given in table 4. Threshold values were increased one spectrographic interval above the 98th percentile for rock samples from the Naknek Formation for chromium (to 300 ppm, or parts per million) and nickel (to 100 ppm) because chip samples taken through the

[1]Censored distributions are those distributions of elements that could not be determined in their entirety because of a lack of instrumental sensitivity or calibration.

Table 3. Summary of emission spectrographic data for nonmagnetic-heavy-mineral concentrates from stream sediments, Katmai study area, Alaska.[1]

[Analysis by semiquantative emission spectrography; all values reported in parts per milion except for Mg, Ca, Fe, and Ti, which are reported in percent. Geometric mean determined from the log-transformed data. Dashes (---), no data or insufficient data; >, concentration is greater than reported value]

Element	DR[2]	Observed range	Median	Geometric mean	Percentiles			Threshold value[3]
					90th	95th	98th	
Mg	0.983	0.05–10.0	0.3	0.39	2.0	3.0	5.0	---
Ca	1.000	.1–20.0	2.0	2.38	5.0	7.0	10.0	---
Fe	.997	.1–50.0	2.0	2.39	15.0	20.0	30.0	20.0
Ti	.673	.02–2.0	1.5	1.47	>2.0	>2.0	>2.0	---
B	.910	20–5,000	70	105	1,000	5,000	>5,000	5,000
Be	.014	2.0–7.0	---	---	---	---	2	---
Sr	.564	200–10,000	200	224	1,000	1,000	2,000	2,000
Ba	.885	50–10,000	700	839	10,000	>10,000	>10,000	>10,000
La	.506	50–2,000	50	41	200	300	500	---
Y	.999	20–2,000	200	255	1,000	1,500	2,000	---
Zr	.132	20–2,000	>2,000	>2,000	>2,000	>2,000	>2,000	---
Sc	.855	10–200	30	27	70	100	100	---
Mn	1.000	50–5,000	500	592	1,500	2,000	2,000	3,000
V	.992	20–3,000	100	113	200	300	500	---
Cr	.650	20–1,000	20	28	150	200	300	---
Ni	.377	10–500	---	---	100	150	300	200
Co	.609	10–1,500	10	13	70	100	300	200
Cu	.805	10–3,000	20	25	200	300	1,000	300
Mo	.160	10–2,000	---	---	20	50	200	50
Pb	.478	20–20,000	---	---	200	700	3,000	1,000
Bi	.041	20–1,000	---	---	---	---	70	20
Ag	.161	1.0–2,000	---	---	5	20	200	30
Au	.048	20–1,000	---	---	---	30	700	20
Zn	.102	500–20,000	---	---	500	1,000	3,000	2,000
Cd	.025	50–500	---	---	---	---	50	50
As	.061	500–20,000	---	---	---	500	1,500	500
Sb	.001	500	---	---	---	---	500	---
W	.048	100–5,000	---	---	---	100	200	100
Sn	.120	20–1,500	---	---	20	30	50	30

[1]Data from Church and Arbogast (1989); analytical determinations made on 1,038 samples.

[2]Detection ratio (DR) is the number of uncensored values divided by the total number of samples analyzed for a given element.

[3]Threshold values determined from the statistical distribution of the data and from histograms of the distribution of each of the elements (Church and Arbogast, 1989).

siltstone facies of the Naknek Formation, which showed no evidence of alteration (Riehle and others, 1989), would have been classified as anomalous if the 98th percentile had been used as the threshold. Since many of the mineralized areas are underlain by rocks of the Naknek Formation, the lower threshold values for chromium and nickel used on plate 1 may reflect a lithologic component (that is, at the 95th percentile). The thresholds established for the SS samples (table 1) were used to pick appropriate threshold values for the rocks that were collected from altered areas and for the float samples (Riehle and others, 1989).

FACTOR ANALYSIS OF THE RECONNAISSANCE GEOCHEMICAL DATA

Factor analysis of the reconnaissance geochemical data for the SS and NMHMC samples was used to define geochemical suites that might indicate areas of mineralized

Table 4. Summary of geometric means and the 95th and 98th percentiles of individual element distributions for seven lithologic groups in the Katmai study area, Alaska.

[Mg, Ca, Fe, and Ti are reported in weight percent, all other elements are reported in parts per million. Analysis by semiquantitative emission spectrography except where noted by an asterisk (*), which indicates data determined by atomic absorption; mercury (Hg*) determined by cold-vapor atomic absorption. Dashes (---), no data; the geometric means or the various percentiles cannot be calculated where the distribution of a given element is censored. No values given for percentiles where data not determinate; >, concentration is greater than reported value. Data summarized from Riehle and others, 1989]

Element	Geometric mean	95th percentile	98th percentile
[1]Unit 1			
Mg	1.45	5	7
Ca	1.46	7	15
Fe	4.51	10	15
Ti	0.36	0.7	1.0
B	24	100	300
Sr	262	700	1,000
Ba	386	1,500	2,000
Y	24	70	70
Zr	75	200	200
Sc	20	50	50
Mn	952	3,000	>5,000
V	137	300	500
Cr	30	300	500
Ni	13	70	100
Co	20	70	100
Cu	20	150	200
Mo	---	---	7
Pb	---	50	50
Ag	---	.5	1
Au*	---	---	---
Zn*	36	100	210
Cd*	---	.15	0.50
As*	---	25	30
Sb*	---	---	2
Hg*	---	.19	.28
[1]Unit 2			
Mg	1.54	3	3
Ca	1.46	10	15
Fe	4.37	10	15
Ti	.34	.5	.7
B	26	100	150
Sr	261	700	1,000
Ba	498	1,500	2000
Y	24	50	70
Zr	89	200	200
Sc	19	30	50
Mn	778	2,000	3,000
V	158	300	500
Cr	75	200	200
Ni	28	70	70
Co	21	50	50
Cu	30	100	200
Mo	---	---	5
Pb	9.7	50	50
Ag	---	---	.5
Au*	---	.05	.08
Zn*	60	130	155

Table 4. Summary of geometric means and the 95th and 98th percentiles of individual element distributions for seven lithologic groups in the Katmai study area, Alaska—Continued.

Element	Geometric mean	95th percentile	98th percentile
[1]Unit 2—Continued			
Cd*	---	.2	.3
As*	---	20	30
Sb*	---	2	3
Hg*	---	.24	.50
[1]Unit 3			
Mg	1.08	2	3
Ca	.56	3	5
Fe	3.77	10	15
Ti	.32	.7	.7
B	48	500	700
Sr	201	700	1,000
Ba	514	1,500	2,000
Y	21	50	70
Zr	96	200	200
Sc	17	30	30
Mn	636	2,000	3,000
V	143	200	300
Cr	53	200	200
Ni	28	70	70
Co	20	50	50
Cu	20	100	200
Mo	---	---	7
Pb	12	50	70
Ag	---	---	.5
Au*	---	---	.05
Zn*	63	190	335
Cd*	---	.6	.9
As*	---	30	100
Sb*	---	3	4
Hg*	---	.06	.20
[1]Unit 4			
Mg	1.29	3	5
Ca	1.60	3	5
Fe	3.54	10	10
Ti	.27	.5	.5
B	13	50	100
Sr	277	700	1,000
Ba	431	1,500	2,000
Y	22	50	70
Zr	73	200	200
Sc	16	50	50
Mn	739	1,500	2,000
V	100	300	300
Cr	19	150	200
Ni	11	50	50
Co	17	70	100
Cu	23	150	500
Mo	---	---	---
Pb	---	30	50
Ag	---	---	---
Au*	---	---	---
Zn*	27	60	140
Cd*	---	.2	.25
As*	---	10	15
Sb*	---	---	---
Hg*	---	.09	.16

Table 4. Summary of geometric means and the 95th and 98th percentiles of individual element distributions for seven lithologic groups in the Katmai study area, Alaska—Continued.

	[1]Unit 5		
Mg	1.60	3	5
Ca	1.29	3	5
Fe	4.5	10	15
Ti	.44	.5	.7
B	17	50	70
Sr	410	1,000	1,500
Ba	481	2,000	2,000
Y	22	50	70
Zr	98	150	200
Sc	21	30	50
Mn	770	1,500	2,000
V	162	300	500
Cr	36	200	200
Ni	19	70	100
Co	24	50	50
Cu	27	100	150
Mo	---	10	15
Pb	7.4	50	70
Ag	---	.7	3
Au*	---	.08	.10
Zn*	43	90	100
Cd*	---	.15	.30
As*	---	10	15
Sb*	---	---	6
Hg*	---	1.1	1.15

	[1]Unit 6		
Mg	1.46	5	5
Ca	1.29	5	5
Fe	3.78	10	10
Ti	.36	.7	.7
B	12	100	150
Sr	326	1,000	1,000
Ba	267	1,000	1,500
Y	25	70	70
Zr	96	200	200
Sc	19	50	50
Mn	623	1,500	2,000
V	143	300	300
Cr	39	200	300
Ni	20	100	100
Co	19	50	70
Cu	26	150	700
Mo	---	7	25
Pb	8.4	50	70
Ag	--	.5	2
Au*	---	.1	.4
Zn*	38	90	170
Cd*	---	.2	.6
As*	---	30	70
Sb*	---	2	2
Hg*	---	.13	.20

Table 4. Summary of geometric means and the 95th and 98th percentiles of individual element distributions for seven lithologic groups in the Katmai study area, Alaska—Continued.

	[1]Unit 7		
Mg	1.56	3	5
Ca	1.65	3	5
Fe	4.17	7	10
Ti	.35	.5	.7
B	12	50	70
Sr	346	700	1,000
Ba	362	1,000	1,500
Y	28	70	100
Zr	96	200	200
Sc	22	30	50
Mn	852	1,500	1,500
V	132	200	300
Cr	20	150	200
Ni	14	50	50
Co	23	50	50
Cu	25	100	100
Mo	---	5	7
Pb	---	30	50
Ag	---	---	---
Au*	---	---	---
Zn*	23	60	80
Cd*	---	---	.1
As*	---	---	10
Sb*	---	---	---
Hg*	---	.08	.14

[1]Lithologic units:

1, Metamorphosed rocks northwest of Bruin Bay fault (Kakhonak Complex, Cottonwood Bay Greenstone, Kamishak Formation, Talkeetna Formation) and, locally, southwest of Bruin Bay fault, hornfelsed rocks adjacent to plutons; 94 samples were analyzed for most elements.

2, Mesozoic sedimentary rocks (Naknek, Staniukovich, Herendeen, Pedmar, and Kaguyak Formations); 357 samples were analyzed for most elements.

3, Tertiary sedimentary rocks (Copper Lake Formation, Hemlock Conglomerate, and undifferentiated Tertiary rocks); 90 samples were analyzed for most elements.

4, Jurassic and Tertiary plutonic rocks of the Alaska–Aleutian Range batholith (gabbro, diorite, quartz diorite, tonalite, granodiorite, and granite) and Tertiary hypabyssal plutons and sills occurring throughout the Katmai study area; 86 samples were analyzed for most elements.

5, Tertiary dikes (primarily middle to late Tertiary); 28 samples were analyzed for most elements.

6, Tertiary volcanic rocks (informally named "volcanic rocks of the Barrier Range" and "volcanic rocks north of Naknek Lake"); 474 samples were analyzed for most elements.

7, Quaternary volcanic rocks (chiefly lava flows and domes at or near the crest of the Aleutian Range); 73 samples were analyzed for most elements.

rock. We emphasize those areas where mineralized ground is indicated by clusters of samples having anomalous geochemical values and microscopically visible sulfide minerals. Special attention was given to areas where hydrothermal alteration was observed during our field studies. Geochemical data for the several media were compared to evaluate the spatial distribution of geochemical anomalies in relation to the geologic setting.

Factor analysis is a mathematical technique that can be used to group elements that behave similarly within a data set into a smaller number of variables (Johnston, 1980, p. 127–128). These factors are derived from the correlation matrix to group together elements that show geochemically coherent behavior. The factors define the mathematical structure within the data set and may be interpretable in

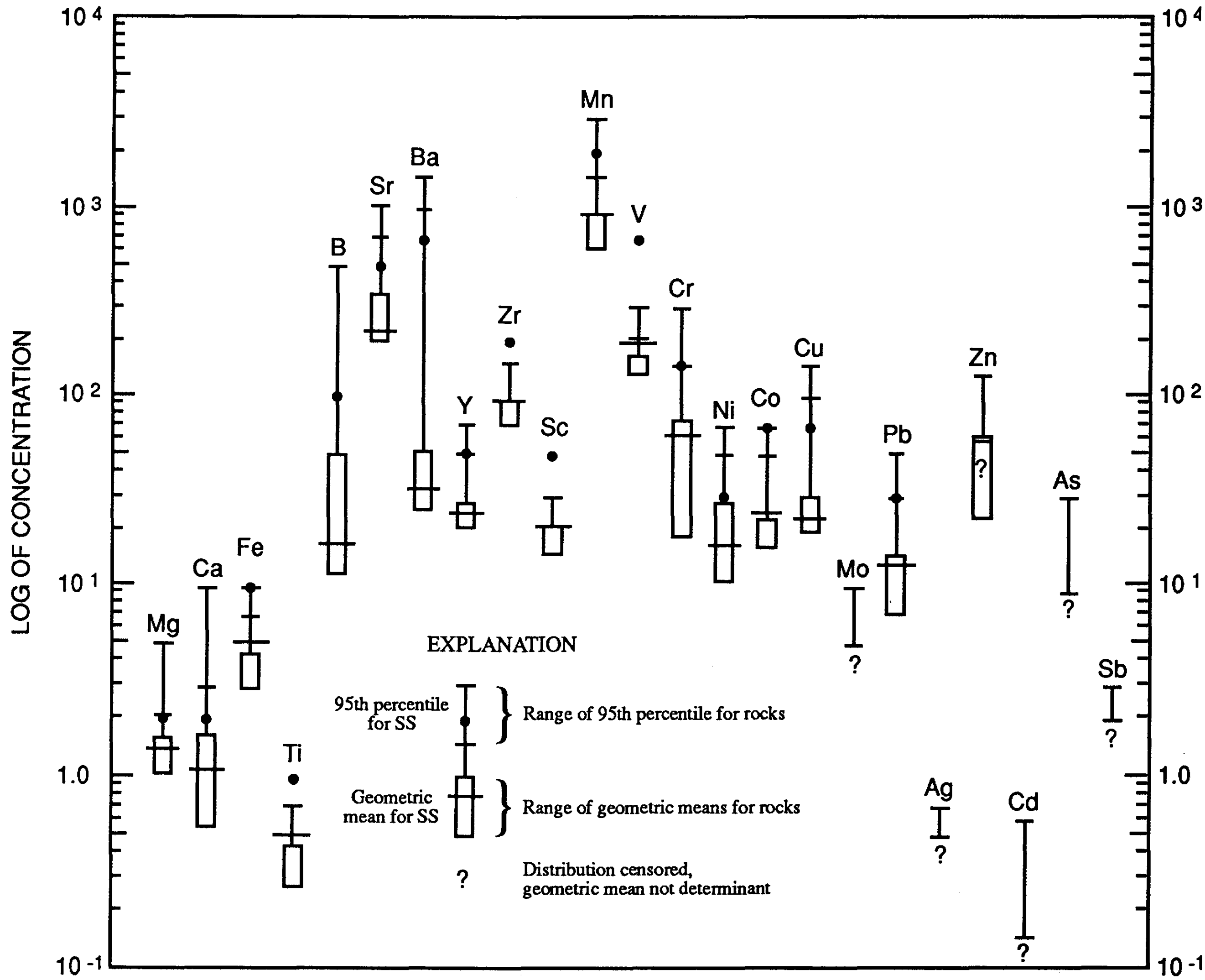

Figure 4. Log plot of range in concentration of geometric means and 95th percentiles of elements in selected lithologic groups (see table 4) from the Katmai study area, Alaska. These same parameters are also plotted for the stream-sediment data (SS, see table 1) for comparison with variation within different lithologic groups. Concentrations of Mg, Ca, Fe, and Ti are expressed in weight percent, whereas concentrations of all other elements are expressed in parts per million.

terms of geochemical processes or suites of lithologically related minerals. The reader is referred to Davis (1973, p. 473–536) or Johnston (1980, p. 127–182) for further discussion of factor analysis.

We used the R-mode factor analysis program available from the U.S. Geological Survey's STATPAC library (Van Trump and Miesch, 1977) for the analysis of the geochemical data for the SS and NMHMC samples. For the semiquantitative emission spectrographic data for the SS samples, a varimax solution was obtained from log-transformed data for 16 elements for which detection ratios were greater than 0.86; lead, which has a detection ratio of 0.68 (table 1), was also included in this solution. The program first determines the principal components from the correlation coefficient matrix. The number of factors was determined from the discontinuity criterion described by Rummel (1970, p. 364). There was a significant break in the eigenvalue curve between factor 5 (1.11) and factor 6 (0.90), so a five-factor model was selected. The five factors were rotated using Kaiser's orthogonal varimax criteria; the factor loadings (SSFT 1–5) are given in table 5. Seventy-three percent of the total variance of the data is explained by the five factors.

Zinc, beryllium, and molybdenum, which may also be useful in defining areas of mineralized ground, were highly censored and have detection ratios of 0.119, 0.081, and 0.055, respectively. Correlation analysis was performed for each of these elements using subsets of element pairs where the concentrations of each were determinate. Statistically meaningful values of r, the correlation coefficient, were

Table 5. Factor loadings for the first five factors after varimax rotation of the stream-sediment data, Katmai study area, Alaska.

[The five stream-sediment factors (SSFT 1–5) explain 73 percent of the total variance of the data set. Factor loadings less than 0.30 are indicated by dashes (---); loadings between 0.3 and 0.4 are enclosed in parentheses]

Element	SSFT–1	SSFT–2	SSFT–3	SSFT–4	SSFT–5
Mg	0.63	---	(0.33)	(0.35)	---
Ca	---	---	---	.86	---
Fe	.88	---	---	---	---
Ti	.85	---	---	---	---
Mn	.47	---	---	.63	---
B	---	0.60	---	---	---
Ba	---	.49	---	---	0.45
Co	.87	---	---	---	---
Cr	.44	---	.78	---	---
Cu	---	.73	---	---	---
Ni	---	---	.86	---	---
Pb	---	.85	---	---	---
Sc	.84	---	---	---	---
Sr	---	---	---	.58	(0.32)
V	.89	---	---	---	---
Y	.58	---	---	---	.56
Zr	---	---	---	---	.81
Percent of total variance explained by each factor					
	34	16	10	7	6

Table 6. Factor loadings for the first four factors after varimax rotation of the data for aqua-regia leachates from stream sediments, Katmai study area, Alaska.

[The four factors determined from the aqua-regia-leachate data for the stream sediments (SSFP 1-4) explain 75 percent of the total variance of the data set. Factor loadings less than 0.40 are indicated by dashes (---); loadings between 0.3 and 0.4 are enclosed in parentheses]

Element	SSFP–1	SSFP–2	SSFP–3	SSFP–4
Mg	0.62	---	---	0.63
Ca	.71	---	---	---
Fe	---	---	0.86	---
Al	.85	---	---	---
Ti	---	0.93	---	---
P	---	.86	---	---
Sr	.42	.85	---	---
Ba	.82	---	---	---
La	.82	---	---	---
Ce	.75	---	---	---
Mn	(0.36)	---	.74	---
V	---	.95	---	---
Cr	---	---	---	.67
Co	---	---	.82	---
Ni	---	.80	---	.41
Cu	---	---	---	.82
Zn	---	.46	.54	---
Percent of total variance explained by each factor				
	31	20	16	8

chosen from the tables published by Fisher (1970, p. 211); the degrees of freedom were 2 fewer than the number of samples, and the 5 percent level-of-significance value was used. In this manner, possible geochemical associations for those elements whose distributions were highly censored and that have detection ratios greater than 0.05 can be inferred (Church, Frisken, and Wilson, 1989). Molybdenum and zinc correlate with lead and copper, whereas beryllium has no significant correlations. These correlations suggest that molybdenum and zinc are members of SSFT–2 (table 5); however, no statistical significance can be attached to these geochemical associations. These elements, when included in the elemental suite for a given factor, are always enclosed in brackets, for example, SSFT–2: Pb, Cu, B, Ba, [Mo], and [Zn]. Because lead was the most highly censored of the group of elements used for the final factor analysis solution, we also evaluated the correlation of lead with other metals to verify that lead correlated independently with SSFT–2 when excluded from the factor analysis model. Lead was found to correlate with copper, boron, and barium as indicated in table 5. Inclusion of the more highly censored lead population in the factor analysis of the data from the SS samples did not change the factor loading significantly. A similar approach was used for other factor analysis solutions in this study in which elements whose populations were more than 20 percent censored were included.

A second varimax solution was calculated from the aqua-regia-leachate data from SS (table 2) following log transformation. These data yield information on the acid-soluble portion of the SS sample and enhance metal anomalies detected in the hydromorphic oxide and the sulfide mineral components of the SS sample. Seventeen elements from this data set had detection ratios greater than 0.67. There was a significant break in the eigenvalue curve between factor 4 (1.44) and factor 5 (0.79), so a four-factor model was selected; the factor loadings (SSFP 1–4) are given in table 6. Seventy-five percent of the total variance of the data is explained by the four factors.

In the aqua-regia-leachate data set, the elements lead, molybdenum, and arsenic, which may be indicative of areas of mineralized ground, have detection ratios of 0.157, 0.144, and 0.111, respectively. Correlation analysis was performed for each of these elements using subsets of element pairs where the concentrations of each were determinate following the procedure described above. The following geochemical associations are inferred for these elements: Pb correlates with Cu, Zn, and Co; Mo correlates with Cu, Fe, Co, and Zn; and As correlates with Cu, Pb, Zn, Co, and Mo. These correlations suggest that lead, molybdenum, and arsenic behave in a way similar to the elements cobalt and zinc, which are members of factor SSFP–3 (table 6). However, lead, molybdenum, and arsenic also strongly correlate with copper, which is a member of factor SSFP–4. These elements, when included in the elemental suite for a given factor, are always enclosed in brackets.

A different type of factor analysis solution was derived for the geochemical data for the NMHMC samples. The log-transformed data for 16 elements that had detection ratios greater than 0.48 were used. After derivation of the principal components, the principal-component vectors were rotated to oblique positions representing the extreme variables. The extreme-variable solution was chosen because it has the best correlation with the observed mineralogical suites found in the NMHMC samples (Church and Bennett, 1989). There was a significant break in the eigenvalue curve between factor 4 (1.53) and factor 5 (0.82), so a four-factor model was chosen. Seventy percent of the variance in the data is explained by the four-factor model. The factor loadings (PCF 1–4) are given in table 7.

The elements Ni, Ag, Mo, Sn, Zn, As, W, Au, Bi, and Cd, which may be indicative of sulfide mineralization, have detection ratios of 0.377, 0.161, 0.160, 0.120, 0.102, 0.061, 0.048, 0.048, 0.041, and 0.025, respectively. Because the distributions for these elements were highly censored, they were not included in the factor analysis solution as were other elements listed in table 3 that have lower detection ratios. Correlation analysis was performed for each of these elements, as described above, to determine their possible geochemical associations. The following geochemical associations are inferred for these elements: Ni correlates with Cu and Co; Ag correlates with Au; Mo correlates with Cu, Pb, Sn, and Zn; Sn correlates with Ca, Fe, and Cu; As correlates with Co, Ca, Ti, and Cd; W correlates with Ca; and Bi correlates with Au. All of these elements, except W, are inferred to be members of PCF–1, although the associations for Ag, Au, Bi, and Cd are weak. These ten elements, when included in the elemental suite for a given factor, are always enclosed in brackets.

Table 7. Factor loadings for the first four factors from the nonmagnetic heavy-mineral-concentrate data using an extreme variable solution, Katmai study area, Alaska.

[The four factors derived from the data for the nonmagmetic fraction of the panned concentrates from stream sediments (PCF 1–4) explain 70 percent of the total variance of the data set. Factor loadings less than 0.40 are indicated by dashes; (---) loadings between 0.3 and 0.4 are enclosed in parentheses]

Element	PCF-1 (Cu)	PCF-2 (La)	PCF-3 (Mg)	PCF-4 (Sr)
Mg	---	---	1.0	---
Ca	---	0.73	---	0.82
Fe	0.91	---	---	---
Ti	(0.34)	.96	---	---
Mn	---	.61	0.88	---
B	---	.74	---	---
Ba	.55	---	---	.53
Co	.98	---	---	---
Cr	---	---	.88	---
Cu	1.0	---	---	---
La	---	1.0	---	---
Pb	.81	---	---	---
Sc	---	.54	.56	---
Sr	---	---	---	1.0
V	.44	.85	.52	---
Y	---	.86	---	---
Percent of total variance explained by each factor				
	25	23	12	10

GEOLOGIC EVALUATION OF THE FACTOR-ANALYSIS SOLUTIONS

The factor analysis solutions obtained from the reconnaissance geochemical data were interpreted to help evaluate areas within the Katmai study area that might have potential for mineralized rock. The solutions were evaluated by comparing areas that have multi-element anomalies for rock samples and favorable geologic attributes for mineralized ground with areas that have high factor sample-scores determined for the reconnaissance geochemical samples. Several of the factor sample-score plots, which aid in evaluating areas of mineralized and altered rock, are presented in figures 5–9. High factor sample-scores from the spectrographic data for the SS samples (SSFT) are interpreted to represent primarily rock compositions, whereas high factor sample-scores for the ICP-aqua-regia-leachate data from SS samples (SSFP) are interpreted to represent distribution of acid-soluble metals in carbonates, hydromorphic Fe-Mn oxides, and sulfide minerals. In contrast, high factor sample-scores obtained from the NMHMC samples (table 7) are interpreted to represent the distribution of metals in sulfide minerals. For the purpose of outlining areas most favorable for sulfide mineralization, PCF–1 proved to be the most useful.

Most SSFT factors reflect the predominant geochemical signature of the underlying bedrock. The map area defined by SS samples having high SSFT–1 factor sample-scores (SSFT–1: V, Fe, Co, Ti, Sc, Mg, Y, Mn, and Cr) and by NMHMC samples having high PCF–3 factor sample-scores (PCF–3: Mg, Mn, Cr, Sc, and V) is largely underlain by volcanic rocks of intermediate to mafic composition (units Tab and QTv; see fig. 2) and, to a lesser extent, by plutonic rocks of intermediate composition. This geochemical signature is interpreted to reflect the geochemical behavior (or presence) of these elements in the Fe-Ti oxide minerals, pyroxene, or amphibole.

Samples that have high SSFT–5 factor sample-scores (SSFT–5: Zr, Y, Ba, and Sr), and high SSFP–1 and SSFP–2 factor sample-scores (SSFP–1: Al, Ba, La, Ce, Ca, Mg, Sr, and Mn; SSFP–2: V, Ti, P, Sr, Ni, and Zn) from the partial leaches are interpreted as having been derived from Mesozoic sedimentary rocks (KJs; see fig. 2). Samples that have high PCF–2 factor sample-scores (PCF–2: La, Ti, Y, V, B, Ca, Sc, and Mn) appear to represent resistent detrital minerals from the Naknek Formation. However, some samples having high PCF–2 factor sample-scores also are present in the area underlain by volcanic rocks of the Barrier Range (Tab; see fig. 2).

Samples having high SSFT–3 factor sample-scores (SSFT–3: Ni, Cr, and Mg) are interpreted as containing a high concentration of mafic minerals, and their localities plot in areas underlain by the Naknek Formation (KJs; see fig. 2) and Tertiary volcanic rocks of the Barrier Range (Tab). The Naknek Formation, although largely composed of feldspar and quartz, which were not detected by this analysis because sodium, potassium, aluminum, and silicon were not determined, contains lenses of resistant detrital minerals that erode into the active drainage basins. Thus, they appear to be a source of resistant heavy minerals detected by this analytical technique.

Samples having high SSFT–4 factor sample-scores (SSFT–4: Ca, Mn, Sr, and Mg) are interpreted to reflect carbonate minerals in the Mesozoic sedimentary rocks (KJs; see fig. 2). The distribution of sedimentary barite is shown by the distribution of sample localities having high PCF–4 factor sample-scores (PCF–4: Sr, Ca, and Ba; fig. 5) associated with the Mesozoic sedimentary rocks. Barium also is a member of the mineralization factor (PCF–1), reflecting areas where there are multi-element base- and precious-metal anomalies. The separation of the two types of barite is possible in factor analysis because the association of barite with sulfide minerals provides a correlation matrix that is different from that of the association of barite with carbonate minerals in the sedimentary environment. The distinction between hydrothermal barite and sedimentary barite is apparent in comparing the distribution of NMHMC samples that contained abundant barite with those sample localities that have high PCF–4 factor sample-scores (fig. 5). High PCF–4 factor sample-scores for the zone of altered rock surrounding Ikagluik Creek area may also reflect hydrothermal circulation within the Naknek Formation in the vicinity of inferred, unexposed small plutons in the area.

The remaining factors are interpreted to reflect the presence of mineralized or altered rock within the Katmai study area. Factor SSFP–4 is interpreted to represent propylitic mineral assemblages surrounding Tertiary intrusive centers (Ti, Tg; fig. 6). Factor SSFT–2, the mineralization factor in the SS reconnaissance data, appears to be the most useful for outlining areas where mineralized rock occur (fig. 7). Factor PCF–1 is interpreted to represent sulfide minerals in the NMHMC samples (fig. 8). Factor SSFP–3 is interpreted to represent the acid-soluble sulfides and the hydromorphic oxide and carbonate minerals that result from weathering of mineral deposits (fig. 9).

Samples having high SSFP–4 factor sample-scores (SSFP–4: Cu, Cr, Mg, and Ni) are from the outcrop area of the volcanic rocks of the Barrier Range (Tab, fig. 6), from the area around Fourpeaked Mountain on Cape Douglas, and from an area surrounding the Tertiary plutons (Tg, fig. 6) on either side of Kulik Lake. Samples having high SSFP–4 factor sample-scores (fig. 6) are interpreted to contain abundant chlorite derived from zones of propylitic altered rock (Church and others, 1987). Samples having high SSFP–4 factor sample-scores are from drainage basins containing anomalous concentrations of metals in the Cape Douglas area, where Tertiary plutons (Ti, fig. 6) intrude Mesozoic (KJs, fig. 6) and Tertiary sedimentary rocks (Ts, fig. 6). The rock geochemical data are indicative of undiscovered porphyry Cu deposits and polymetallic veins (pls. 1 and 2). Samples having high SSFP–4 factor sample-scores also are from localities in the area around Kulik Lake, where middle Tertiary granitic rocks (Tg, fig. 6) intrude the Jurassic batholith (Ji, fig. 2) and older metamorphic rocks (JРm, fig. 2), as well as the Mesozoic sedimentary rocks (KJs). The rock geochemical data from this area are indicative of either undiscovered porphyry Cu deposits or polymetallic veins (pls. 1 and 2). Although not readily apparent from the mapped areas of alteration (fig. 6), the hornfels and plutons at Kulik Lake and on Cape Douglas show the strongest propylitic alteration signature in the rock geochemical data. These areas are indicated by the presence of anomalous concentrations of cobalt, nickel, chromium, and boron (pl. 1).

Samples having high SSFT–2 factor sample-scores (SSFT–2: Pb, Cu, B, Ba, [Mo], and [Zn]) indicate areas favorable for porphyry Cu and porphyry Cu-Mo deposits, and for polymetallic veins associated with Tertiary (Tg, Ti; fig. 7) and Tertiary and Quaternary (QTv) intrusive centers (fig. 2). Four prominent areas of geochemical anomalies were defined on the basis of anomalous concentrations of Cu, Mo, Ag, Pb, Zn, and B in the SS data (Church, Bailey, and Riehle, 1989). High factor sample-scores for SSFT–2 also show these areas to be anomalous. The Kulik Lake area, intruded by the middle Tertiary granites (Tg, fig. 7), is geochemically anomalous. A suite of samples having high SSFT–2 factor sample-scores are also from localities that define the area where middle Tertiary intrusive rocks (Tg, fig. 7) crop out near Kulik Lake. A prominent cluster of multi-element geochemical anomalies in the SS data (Church, Bailey, and Riehle, 1989) is evident in the western Buttress Range, where Tertiary plutons (Ti, fig. 7) intrude Mesozoic sedimentary rocks (KJs, fig. 2), in the Naknek Formation at Mount Katolinat, and in the area near Mount Griggs (Knife Peak), where widespread base-metal anomalies are associated with polymetallic veins in the Naknek Formation (KJs, in part; fig. 2). Samples having high SSFT–2 factor sample-scores indicate and somewhat extend the area of these geochemical anomalies. Geochemical anomalies in SS data also are evident on the south side of Cape Douglas (Church, Bailey, and Riehle, 1989). Samples having high SSFT–2 factor sample-scores are from an area underlain by altered and contact-metamorphosed sedimentary rocks (units Ts and KJs, fig. 2) and intrusive (Ti, fig. 7) rocks northeast of Big River on the south and east sides of Fourpeaked Mountain. A small cluster of sample localities having high SSFT–2 factor sample-scores also correlates with a small group of base-metal geochemical anomalies on the north side of Ninagiak River where Tertiary plutons intrude the Mesozoic sedimentary rocks (KJs, fig. 2). One sample collected near the head of Dakavak Bay has a high SSFT–2 factor sample-score. There are scattered geochemical anomalies in the Kejulik Mountains where late Tertiary and early Quaternary volcanic rocks (QTv, fig. 2) intrude

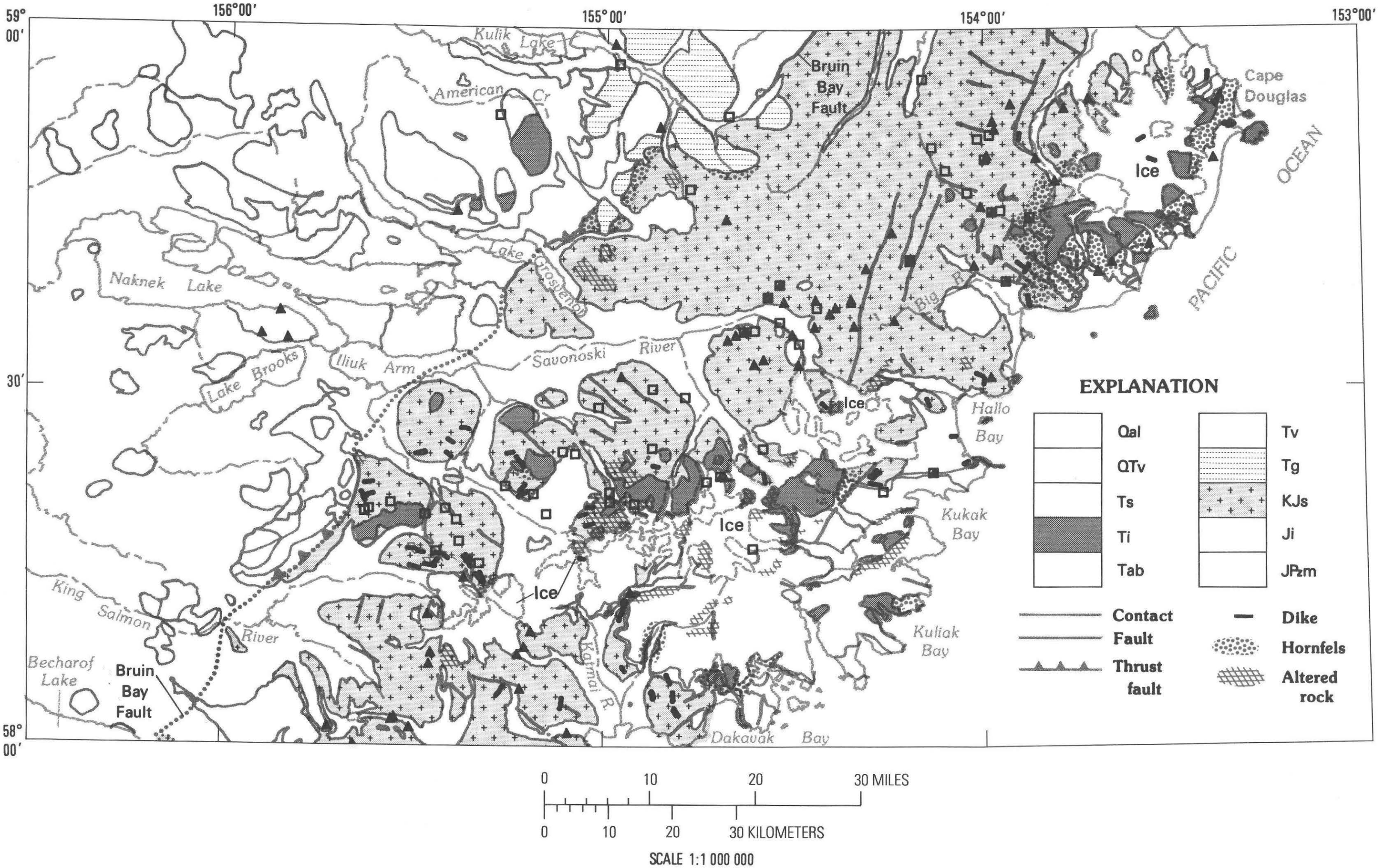

Figure 5. Map of the Katmai study area, Alaska, showing distribution of sedimentary barite and its correlation with Jurassic and Cretaceous rocks. Heavy-mineral-concentrate factor 4 (PCF–4: Sr, Ca, and Ba), which is interpreted to indicate sedimentary barite, is shown as a point plot of high factor sample-scores (95th percentile shown as an open square). Also shown is distribution of localities for all nonmagnetic heavy-mineral-concentrate (NMHMC) samples that contained more than 5 percent barite (filled triangle); a similar pattern is also obtained by plotting all NMHMC samples that contained more than 10,000 ppm Ba. See figure 2 for explanation of other geologic map symbols.

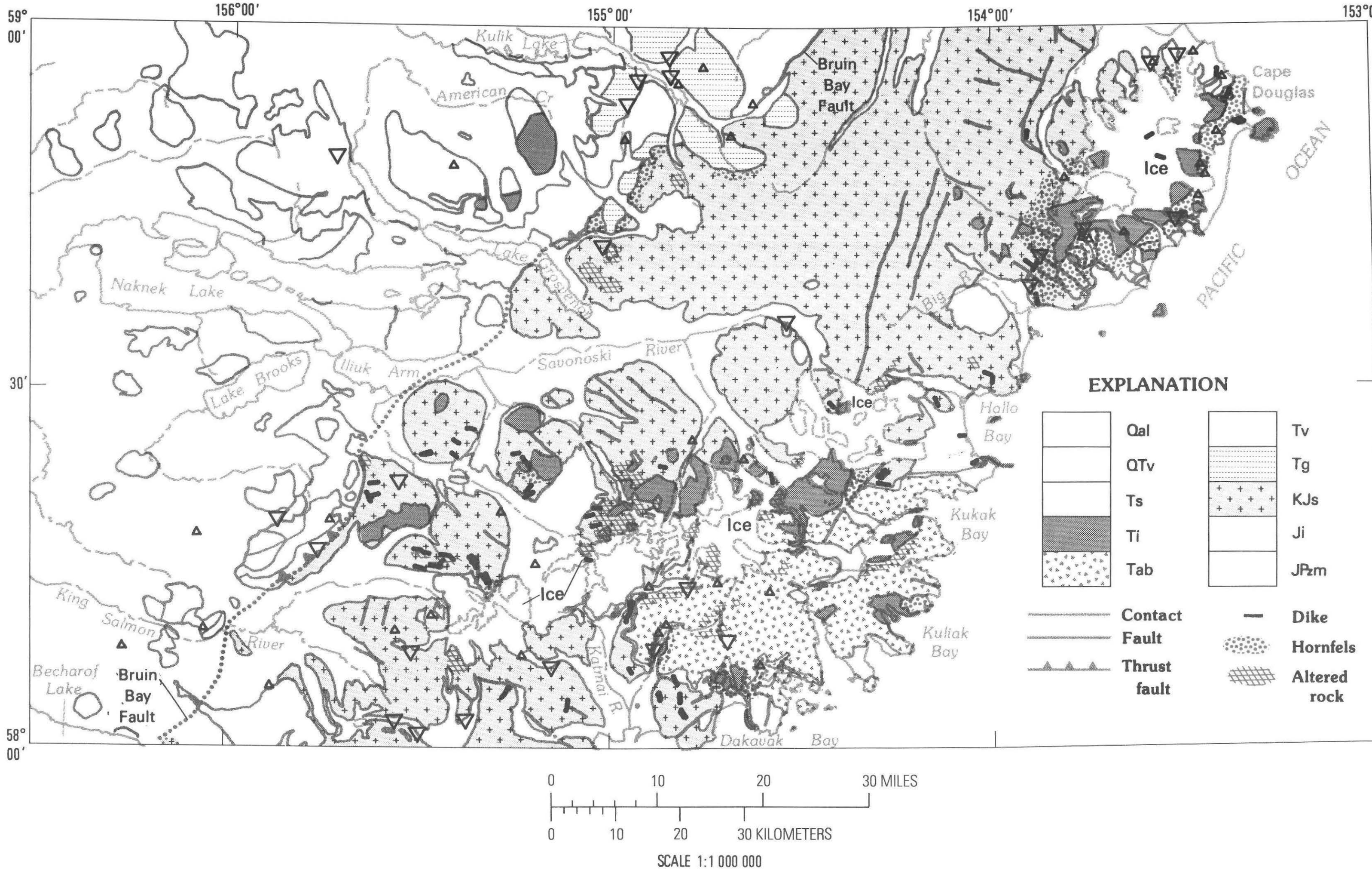

Figure 6. Map of the Katmai study area, Alaska, showing correlation of high aqua-regia-leachate factor 4 sample-scores (SSFP–4: Cu, Cr, Mg, Ni, [Pb?], [Mo?], and [As?]) sample-scores with zones of altered rock, particularly in the volcanic rocks of the Barrier Range (Tab), where SSFP–4 sample-scores are high for zones of propylitic(?) alteration. Open triangle represents locality for which the factor sample-score exceeds 95th percentile of the data. Open, inverted triangle represents locality for which factor sample-score exceeds 98th percentile. See figure 2 for explanation of other geologic map symbols.

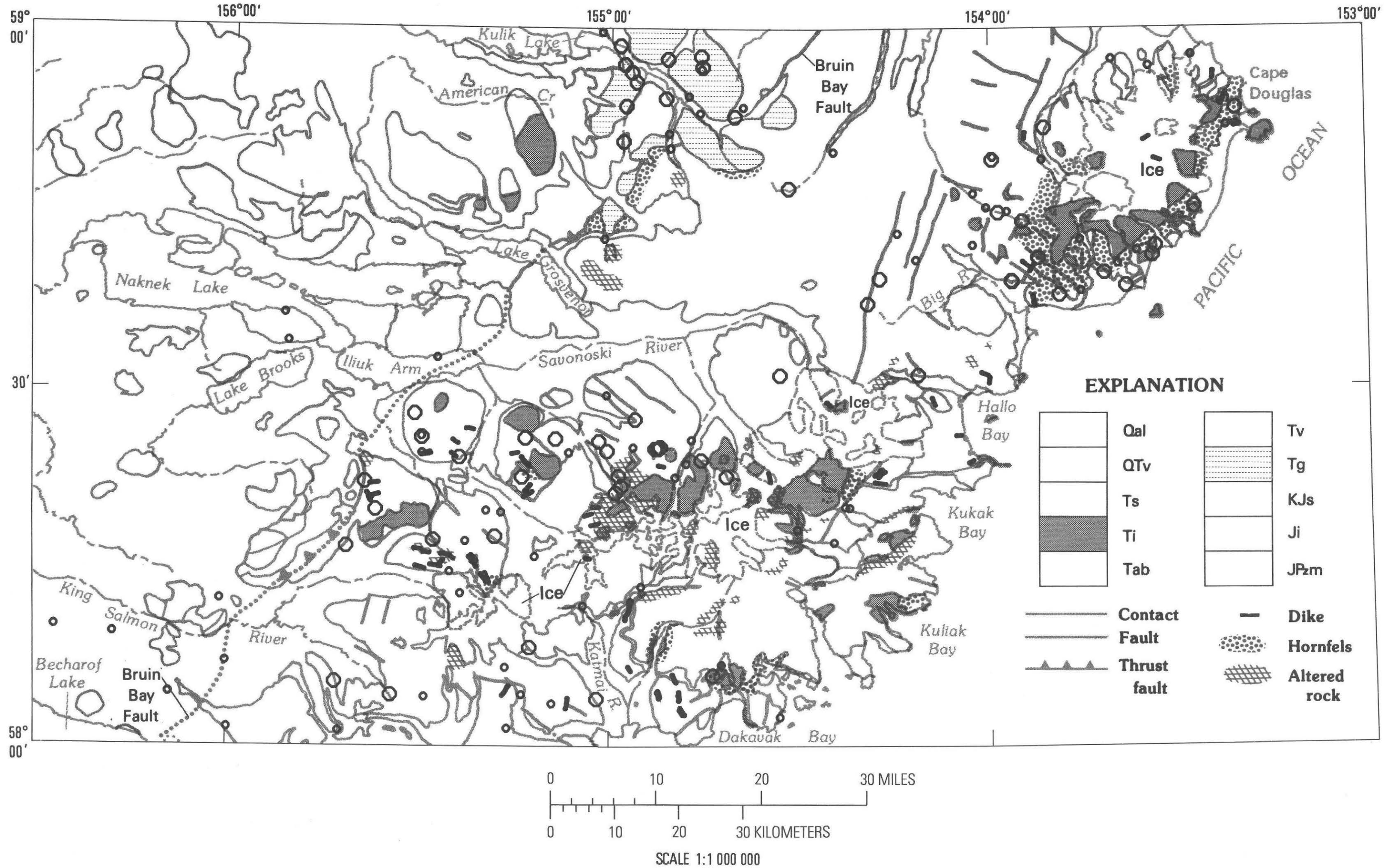

Figure 7. Map of the Katmai study area, Alaska, showing distribution of localities for which stream-sediment factor 2 (SSFT–2: Pb, Cu, B, Ba, [Mo] and [Zn]) sample-scores are high. This variable reflects a suite of elements that characterize areas in the Katmai study area favorable for undiscovered porphyry Cu and porphyry Cu-Mo deposits and for polymetallic vein deposits. SSFT–2 is shown as a point plot of high factor sample-scores; small open circle represents locality for which the factor sample-score exceeds 90th percentile, whereas larger open circle represents locality for which the factor sample-score exceeds 95th percentile. See figure 2 for explanation of other geologic map symbols.

Mesozoic sedimentary rocks (KJs, fig. 2). These geochemical anomalies are also delimited by localities for samples having high SSFT–2 factor sample-scores (fig. 7). Comparison of areas delimited by localities for samples having high SSFT–2 factor sample-scores with the rock geochemical anomalies (pls. 1 and 2) also suggests that this factor is indicative of areas that have potential for either undiscovered porphyry Cu or polymetallic-vein deposits.

Many of the metals that are potentially useful in defining specific types of mineral deposits are highly censored and were excluded from factor analysis of the data for the NMHMC samples. All of the chalcophile metals correlate with the elements that define PCF–1 (fig. 8). Samples having high PCF–1 factor sample-scores (PCF–1: Cu, Co, Fe, Pb, Ba, V, (Ti), [Ni], [Sn], [Mo], [As], [Ag?], [Au?], [Bi?], and [Cd?]) serve to augment the geochemical character of areas defined by high SSFT–2 factor sample-scores (fig. 7). Samples having the highest PCF–1 factor sample-scores were collected in the Buttress Range, the Ikagluik Creek valley east of Mount Griggs (Knife Peak), the area north of the Big River and south and east of Fourpeaked Mountain, and the Kulik Lake area. Samples that have high PCF–1 factor sample-scores also define areas underlain by volcanic rocks (Tab, fig. 2) in the northern part of the Barrier Range and by the Tertiary volcanic rocks north of Naknek Lake (Tv, fig. 2). Samples from scattered localities underlain by the Talkeetna Formation on Dumpling Mountain (JTRm, fig. 2) and from scattered localities underlain by the Naknek Formation (KJs, fig. 2) also have high PCF–1 factor sample-scores. Geochemical anomalies evident in the NMHMC samples also are present in these same areas (Church and Arbogast, 1989). Rock geochemical anomalies are also associated with these localities (pls. 1–3). A detailed discussion of the geology, rock geochemistry, and evidence for undiscovered mineral deposits is presented below.

Finally, areas of hydromorphic anomalies are outlined by the distribution of localities for which samples have high SSFP–3 factor sample-scores (Fe, Co, Mn, Zn, [Pb?], [As?], [Mo?], and [Cd?]; fig. 9). Areas defined by these sample localities expand the regional extent of the areas outlined by reconnaissance geochemical data for samples from an area east of Mount Griggs (Church and Motooka, 1989). Small clusters of localities for which samples have high SSFP–3 factor sample-scores also are present in the Big River–Fourpeaked Mountain area, the area east of Kulik Lake, and the area north of Kukak Bay on the north side of the Barrier Range. Rock geochemical data from each of these areas are indicative of polymetallic veins (pl. 2). In addition, the area of Tertiary volcanic rocks north of Naknek Lake (Tv, fig. 9) is also indicated by samples having high SSFP–3 factor sample-scores. We observed only one locality within this area where altered rocks are present. The recent discovery of the Pebble Beach porphyry Cu-Au deposit in the Iliamna quadrangle was defined on the basis of geochemical anomalies associated with Fe-oxide phases and small quartz veins (Phil St. George, oral commun., 1991; Danielson, 1991). The area north and west of Naknek Lake may likewise have potential for concealed porphyry Cu-Au deposits.

GEOLOGIC INTERPRETATION

We have identified eight discrete areas within the Katmai study area for detailed discussion and interpretation of the geology and reconnaissance geochemistry, and for the site-specific evaluations of mineral occurrences. These areas have been delineated on the basis of their geologic attributes, geochemistry of the rock and float samples, the geochemical data from the SS and NMHMC samples, and NMHMC mineralogy. Geochemical results for float and rock samples are shown, along with the summaries of the reconnaissance geochemical data, on plates 1–3. Elemental groupings are based on the geochemical attributes of the types of mineral deposits discussed above. Because more than 2,000 rock samples were collected, and because many samples were collected in areas where our followup studies indicated evidence of hydrothermal activity, we have combined the results from multiple samples taken at the same site. Furthermore, we have gridded the data to limit the number of sample localities plotted within a 500-m cell in order to reduce the sample density on the maps. This treatment of the data is necessary to allow visual presentation of the rock geochemical data at the map scale of the plates (1:250,000). This treatment also has the effect of reducing the number of sample localities in mineralized areas that have anomalous concentrations of metals. For the purposes of clarity, only those samples or groups of samples containing multiple-element anomalies have been individually numbered on plates 1–3. Single element anomalies have not, in general, been treated in this report. The 95th and 98th percentiles for each rock unit (table 4) are the two values plotted on plates 1–3, respectively (tables 8–10). Data for rock and float samples that contained anomalous concentrations of metals are given in tables 11–18. In these tables, we report, in general, only those elements present at anomalous concentrations in samples from localities or groups of localities that showed multielement anomalies. Furthermore, for many localities where multiple samples of the same rock type were collected, composite results are given by rock type and locality; for example, the high concentrations of elements measured in several samples of the Naknek Formation or a Tertiary intrusive rock would be reported as a single entry; the highest concentration for a given element was used in the composite entry. Complete listings of the analytical data were published in Riehle and others (1989).

On plate 1 we plotted the Cu-Mo-Sn-W element suite, which is indicative of porphyry Cu deposits not only on the Alaska Peninsula (for example, Hollister, 1978; Cox and others, 1981; Church, Detterman, and Wilson, 1989), but also in the Cascade Range (for example, Hollister, 1978;

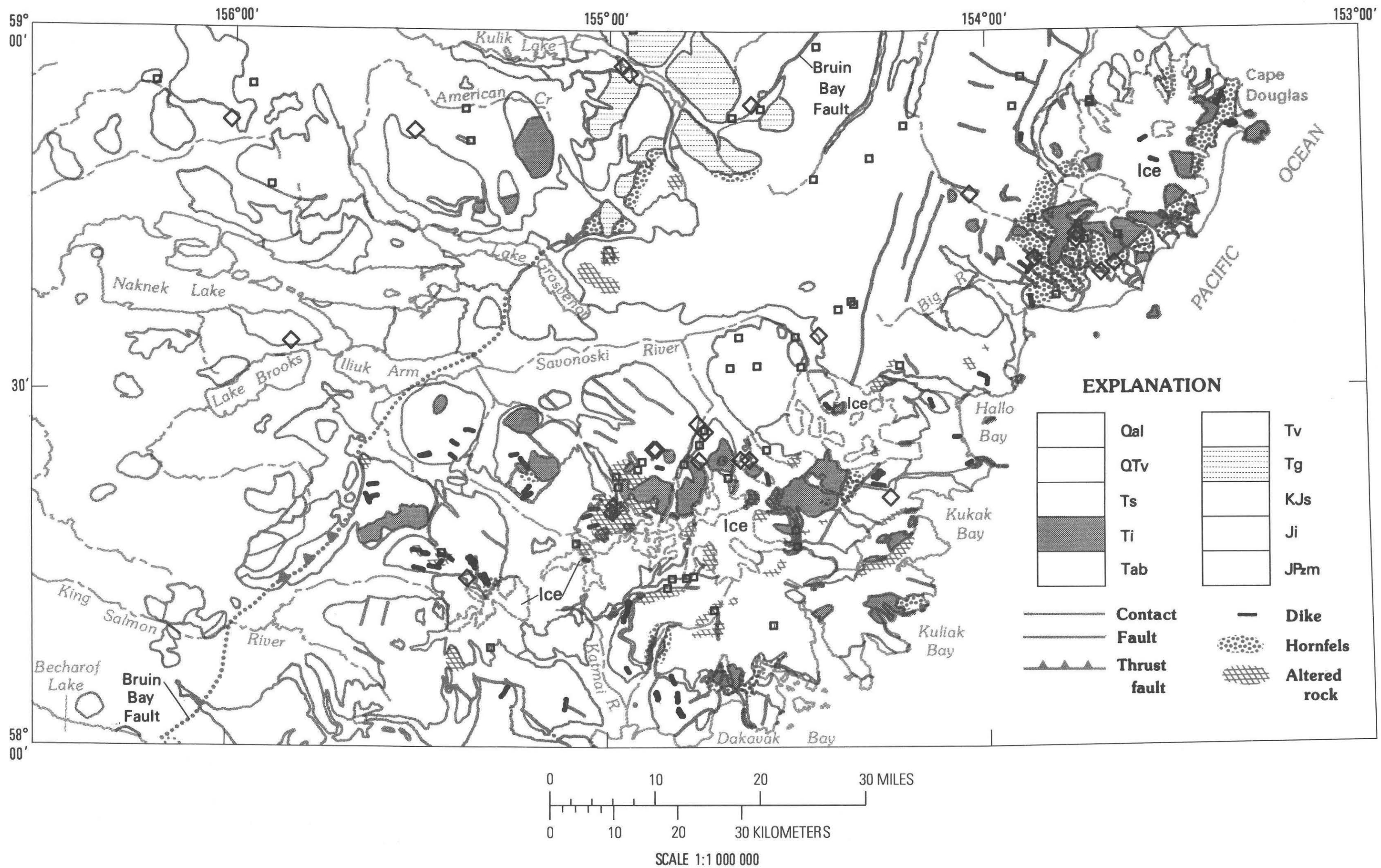

Figure 8. Map of the Katmai study area, Alaska, showing the distribution of localities for which heavy-mineral-concentrate factor 1 (PCF–1: Cu, Co, Fe, Pb, Ba, Vn, (Ti), [Ni], [Mo], [Sn], [As], [Ag?], [Au], [Bi?] and [Cd?]) sample-scores are high; PCF–1 reflects the presence of sulfide minerals in the nonmagnetic heavy-mineral-concentrate (NMHMC) samples. PCF–1 is shown as a point plot of high factor sample-scores; open square represents locality for which the factor sample-score exceeds 92nd percentile; open diamond represents locality for which the factor sample-score exceeds 97th percentile. See figure 2 for explanation of other geologic map symbols.

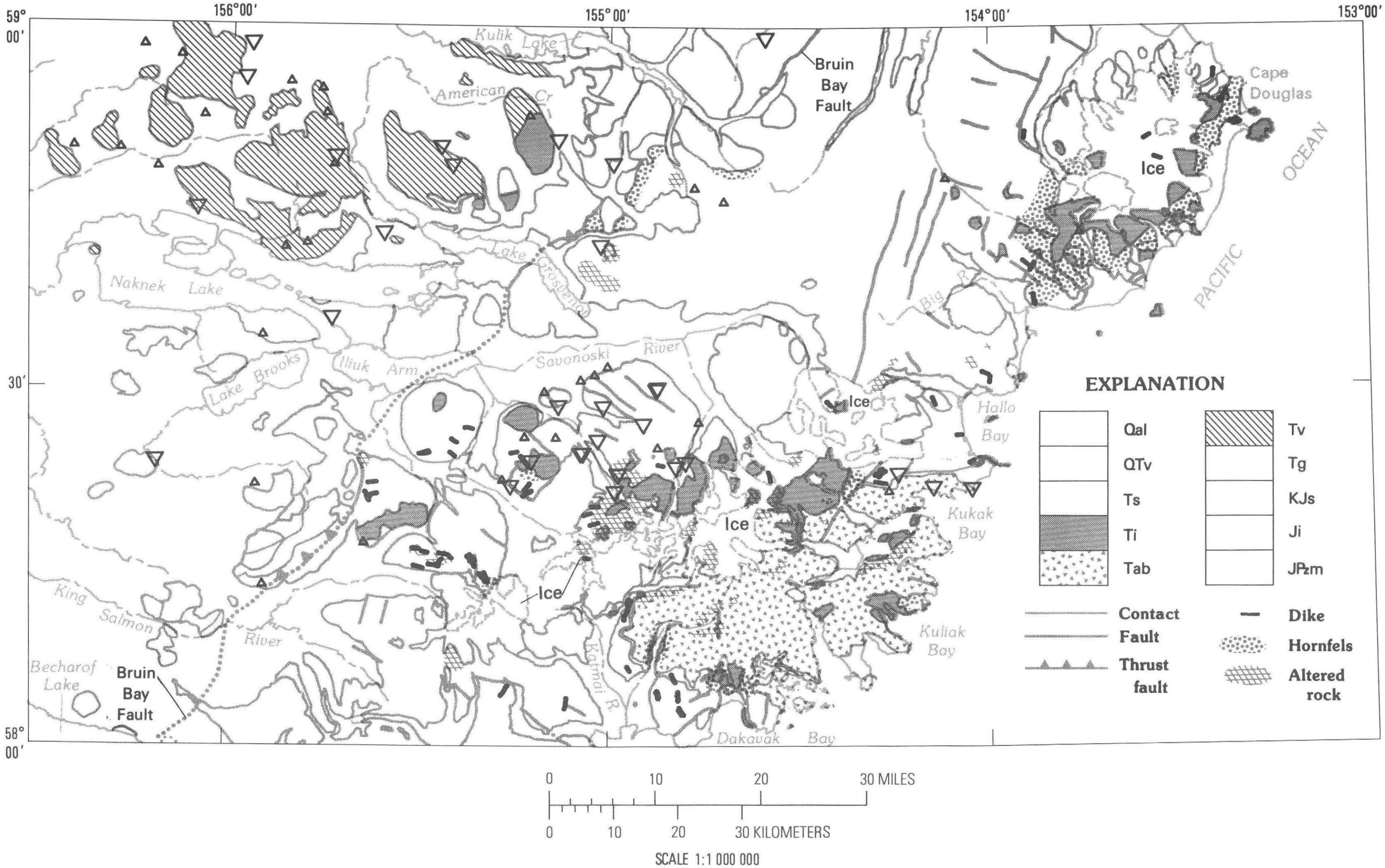

Figure 9. Map of the Katmai study area, Alaska, showing distribution of localities for which aqua-regia-leachate factor 3 (SSFP–3: Fe, Co, Mn, Zn, [Pb?], [Mo?], and [As?]) sample-scores, which are interpreted to represent hydromorphic anomalies, are high. Open triangle represents locality for which the factor sample-score exceeds 95th percentile, and open, inverted triangle represents locality for which the factor sample-score exceeds 98th percentile. See figure 2 for explanation of other geologic map symbols.

Church and others, 1984), where similar exploration geochemistry studies have been conducted. Rock and float samples containing anomalous concentrations of the elements Cu, Mo, W, and Sn are presented on the top part of the star diagram. Anomalous concentrations at the 95th percentile are indicated by the shorter vector length, whereas anomalous concentrations at the 98th percentile are indicated by the longer vector (table 8, pl. 1).

In addition, on plate 1 we use the B-Cr-Ni-Co suite to represent the propylitic alteration halos that surround these mineralized areas. Factor analysis of suites of rocks from these various alteration zones (S.E. Church, unpub. data, 1990) substantiates this interpretation. Chromium, manganese, and boron are present in the silicate minerals that make up the propylitic alteration suite. Manganese (not shown on pl. 1) substitutes for calcium in the epidote mineral structure (for example, see Church and others, 1987), whereas chromium and boron substitute in the tourmaline structure. Dravite, the magnesium-rich endmember of the tourmaline composition field (Conklin and Slack, 1983), and schorl, the iron- and manganese-rich endmember of the tourmaline composition field (Smith and others, 1987) have been shown to include significant amounts of chromium (as much as 560 and 300 ppm, respectively) in the crystal lattice. Anomalous concentrations of both cobalt and nickel are interpreted to reflect the minerals pyrite or pyrrhotite in propylitic alteration haloes, whereas both chromium and nickel also substitute into hydrothermal chlorite. The elements boron, chromium, nickel, and cobalt appear to represent the zone of propylitic alteration in the Katmai study area. Polymetallic-vein signatures of base-metal suites that commonly are present within these propylitic alteration halos also are shown for the reconnaissance geochemical data by the dashed blue outline of the drainage basins on plate 1.

On plate 2 we present the geochemical data for the polymetallic-vein mineral deposit type. Rock and float samples containing anomalous concentrations of the elements Cu, Mo, Ag, Pb, Zn, Cd, Bi, and As are shown with the star diagram. Threshold values used are shown in table 9 (pl. 2). This suite of metals is typical of base-metal polymetallic veins associated with porphyry Cu deposits on the Alaska Peninsula (Cox and others, 1981).

On plate 3 we present the geochemical data for precious-metal polymetallic and epithermal quartz-vein types of mineral deposits. Rock and float samples containing anomalous concentrations of the elements As, Sb, Ag, Au, Hg, and Mn are shown with the star diagram. Application of this metal suite is based on the mineral deposit models of Heald and others (1987), Mosier and others (1986), and Berger (1986), and on the metal suite found at the Apollo Mine and the Shumagin prospect on Unga Island (White and Queen, 1989). Because only a limited group of samples was analyzed for many of these elements, threshold values (table 10, pl. 3) used were derived from both statistical data and by comparison with results from other areas on the Alaska Peninsula.

Field descriptions of zones of altered rock are based on limited field observations. Most of the mineral identifications were based on hand-lens identifications, but X-ray diffraction and semiquantitative emission spectrographic data were used for selected samples. The term "pyrite" as used in this report is a field mineral-identification term and should be interpreted only to indicate the presence of a brass-colored sulfide mineral rather than a mineral having an exact stoichiometric formula of FeS_2.

The terminology we use to describe quartz veins also needs some explanation. The majority of the quartz veins seen in the field appeared to be small, anastomosing, single-generation quartz veins that contain finely disseminated pyrite, in most cases less than ten percent. We describe these simply as "quartz veins," or as "sulfide-bearing quartz veins." In some areas, the quartz veins are clearly banded and some of them also contain vugs near the center of the vein. In these cases, we describe the veins as "banded or vuggy quartz veins" and we indicate the sulfide mineralogy of the bands within the vein as we have determined by our hand-lens mineralogical identifications. In some cases, quartz veins are present along a series of parallel fractures; we use the term "sheeted quartz veins" to describe the structural control of this vein geometry. Finally, we use the term "stockwork" to describe a complex interlacing system of anastomosing and reticulate, commonly sulfide-bearing quartz veins. Feldspar was rarely identified in these veins, but potassium feldspar was observed along the borders of sulfide-bearing, quartz-vein stockwork in the zone of potassic altered rock described below from the Margot Creek copper occurrence. We refer the reader to Jensen and Batemen (1981, p. 111–133) for a more detailed description of the use of economic geology terms used herein.

Because this study is largely reconnaissance in scope, we have not studied the economic geology in detail in areas where mineral occurrences have been found. In summarizing our findings, we have considered an entire area having common geologic attributes rather than individual samples collected from a single area. We assume that samples that show similar metal anomalies and are from an area underlain by common geology also have a common origin. Furthermore, we assume that the conclusions reached from particular geologic observations and geochemical anomalies shown by rock samples from specific sites within that area generally apply to the entire area. Element suites that define a particular geochemical signature of an area are listed in decreasing order of frequency of occurrence for the group of samples given. In the following discussions, we use an areal approach rather than one based on mineral deposit type or on age. Generalized boundaries of each of the eight areas discussed are shown in figure 10.

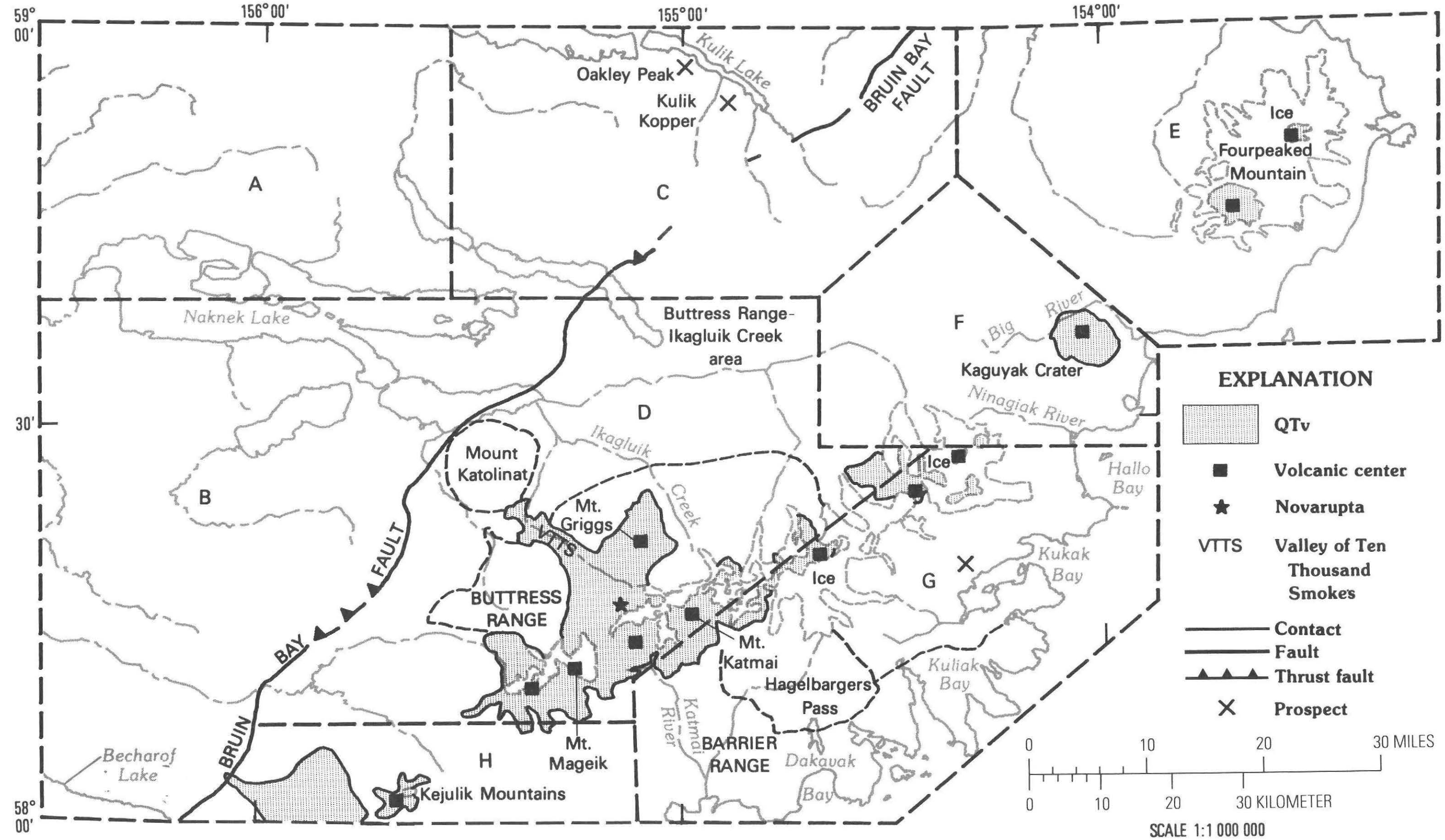

Figure 10. Map of the Katmai study area, Alaska, showing mineral occurrences and eight major areas (A–H) favorable for undiscovered mineral deposits. Approximate boundaries of areas shown by long-dashed lines; boundaries of subareas are shown by short-dashed lines; A, area north of Naknek Lake; B, area south of Naknek Lake and west of Bruin Bay fault; C, Kulik Lake area; D, Buttress Range–Ikagluik Creek area; E, Fourpeaked Mountain area; F, Ninagiak River area; G, Barrier Range–Kukak Bay area; and H, Kejulik Mountains area. High peaks of the Aleutian Range are identified, as are some additional physiographic features that are referenced in the text. QTv, Quaternary and latest Tertiary volcanic rocks of the Aleutian volcanic arc; VTTS, Valley of Ten Thousand smokes.

Table 11. Geochemical and geologic data for selected samples from the area north of Naknek Lake, Katmai study area, Alaska.

[Samples listed here have concentrations that exceed the 95th percentile for the respective lithologic units as defined in table 4. "Site No." is the locality shown on plates 1–3; map unit symbols are those on the geologic base map on plates 1–3. An "X" in columns headed "Vein," "Frac," or "Alt" indicates that veins, fracture fill, and (or) hydrothermally altered rock, including color anomalies caused by the oxidation of sulfide minerals, were observed at the sample site; "Int" indicates that the sample is an intrusive rock, or that there is a sill, dike, or pluton exposed nearby. "Lith" indicates the rock type of the sample: 1, sandstone or siltstone; 2, conglomerate; 3, volcaniclastic

Site No.	Sample No.	Map unit	Mn	Cr	Ni	Co	Cu	Mo	Sn	Pb	Ag	Bi	Zn	Cd
1	84YB101	Tva	---	---	---	---	---	---	---	100	---	---	---	---
2	84YB102	Tva	---	---	---	---	---	---	---	70	---	---	---	---
3	83RJ242	Tva	---	---	---	---	---	15	---	---	---	---	---	---
4	84RJ052C	Tva	---	1,000	200	70	---	---	---	---	---	---	---	---

AREA NORTH OF NAKNEK LAKE

Early Tertiary volcanic rocks, mainly flat-lying andesitic lava flows (Tva), but also including a few plugs and dikes of basalt (Tvb), crop out north of Naknek Lake and west of the Bruin Bay fault (fig. 10), within the Nushagak–Bristol Bay Lowland province. The terrain comprises low hills of only a few hundred meters relief. Many of the areas shown as outcrops are partially covered by extensive, although locally thin, glacial deposits (Riehle and Detterman, 1993). Except for incipient chlorite replacement of some mafic phenocrysts in the lava flows, little evidence of hydrothermal alteration was observed.

The reconnaissance geochemical data define scattered drainage basins yielding samples that contained anomalous concentrations of Mo, W, Cu, Zn, or Ag (pls. 1 and 2). The NMHMC samples from these drainage basins also contained scheelite, sphalerite, or gold at some localities. NMHMC samples from three drainage basins northwest of Sugarloaf Mountain contained anomalous concentrations of silver and gold (pl. 3). Aqua-regia-leachate data for the SS samples define an area of Fe-Mn-As anomalies in the King Salmon Creek drainage north of the west end of Naknek Lake (Church and Motooka, 1989). Fe-oxide coatings were observed in the lava flows throughout the area. Typically, they are thin, red hematite coatings along fractures within the flows. The origin of the hydromorphic oxide Fe-Mn-As anomaly pattern in the SS is best explained by the presence of these Fe-oxide coatings in the lava flows.

Hydrothermally altered rock, veins, and mineralized fractures are generally lacking in this area. Only a few rock samples are geochemically anomalous (sites 1–4, table 11). Six additional samples of mafic igneous rock contained high concentrations of nickel, chromium, or cobalt, such as those seen at site 4, and are not included in table 11. These samples contained one or more of these elements at concentrations just above the 95th percentile and are interpreted to reflect olivine and pyroxene present in basaltic rocks. We interpret these bedrock data to reflect a high background for nickel, chromium, and cobalt, rather than being an indication of mineralized rock.

A small outcrop at site 3, east of Sugarloaf Mountain (T. 15 S., R. 40 W.), is the only outcrop of intensely altered rock. The protolith was a foliated, probably silicic tuff or dome that is now completely recrystallized to quartz and zeolites and is cut by thin veinlets of quartz and chlorite. This altered rock sample contains 15 ppm Mo. SS samples from drainage basins on either side of site 3 also contained anomalous concentrations of molybdenum. SS samples from the drainage basin on the north side of Sugarloaf Mountain contained anomalous concentrations of copper. The NMHMC samples from the drainage basin on the south side of Sugarloaf Mountain contained anomalous concentrations of molybdenum and tungsten. Gold was detected in drainage basins both east and northwest of Sugarloaf Mountain (Church and Arbogast, 1989). Rock samples from sites 1 and 2 also contained anomalous concentrations of lead.

In summary, there is only sparse geologic or geochemical evidence for either undiscovered porphyry Cu (pl. 1) or polymetallic-vein (pl. 2) deposits in the Tertiary volcanic rocks north of Naknek Lake (Tva, Tvb). However, the geochemical data from this area are permissive for concealed deposits of these types. The Fe-oxide alteration is similar to that reported for the area surrounding the Pebble Beach porphyry Cu-Au deposit, in the Iliamna quadrangle (Danielson, 1991). The interpretation of the aeromagnetic data for the Naknek quadrangle (Church and others, 1992) suggests that Tertiary(?) plutons are present in the subsurface. A number of small gold placer claims were platted in the drainage basin immediately north of Sugarloaf Mountain (U.S. Bureau of Mines, unpub. data, 1990; Church and others, 1992). Gold and silver anomalies in NMHMC samples from the drainage basins east and northwest of Sugarloaf Mountain indicate areas that may be favorable for precious-metal-bearing epithermal quartz veins (pl. 3).

AREA SOUTH OF NAKNEK LAKE AND WEST OF THE BRUIN BAY FAULT

The rocks in this area are largely Jurassic intrusive rocks (Jgr, Jgd, Jqd, Jgb) of the Alaska–Aleutian Range

rock or tuff; 4, lava flow; 5, sill or dike; 6, plutonic rock; 7, metamorphosed rock/protolith; 8, limestone; and (*), float sample. Mineralogy is generally based upon field identifications of hand specimens: py, pyrite; cpy, chalcopyrite; asp, arsenopyrite; spl, sphalerite; gn, galena; mly, molybdenite; qtz, quartz; Fe ox., iron oxides; dissem., disseminated mineral grains in sample. Dashes (---), concentrations not anomalous or feature not observed; all concentrations expressed in parts per million (ppm); >, concentration is greater than reported value]

Site No.	Sample No.	Map unit	Au	As	Sb	Hg	Alt	Int	Lith	Frac	Vein	Mineralogy and mode of occurrence
1	84YB101	Tva	---	---	---	---	---	---	4	---	---	
2	84YB102	Tva	---	---	---	---	---	---	4	---	---	
3	83RJ242	Tva	---	---	---	---	X	---	3	---	X	Qtz veins
4	84RJ052C	Tva	---	---	---	---	---	---	4	---	---	

batholith, ranging from granitic to gabbroic in composition, and the older sedimentary and volcanic rocks of the Kamishak (TRk) and Talkeetna Formations (Jt), the Cottonwood Bay Greenstone (TRc), and the metamorphosed rocks of the Kakhonak Complex (JTRk). Samples of the intrusive rocks were taken where they were cut by quartz veins or contained disseminated pyrite. Many of the outcrops sampled are metamorphosed roof pendants within the batholith and are locally iron stained, presumably by the oxidization of pyrite. Rock samples from this area (sample localities 5–28, pls. 1–3) that contained anomalous concentrations of metals are summarized in table 12. On the basis of exploration studies in the Talkeetna Formation northeast of the study area (Newberry, 1986; Newberry and others, 1986), these iron-stained zones were sampled for possible stratabound mineral occurrences. Steefel (1987) subsequently described a Kuroko-type massive sulfide deposit in the Talkeetna Formation north of the Katmai study area.

On the south side of Naknek Lake east of Dumpling Mountain (T. 18 S., R. 38–39 W.; pl. 1), reconnaissance geochemical samples from a few scattered localities contained anomalous concentrations of Cu, Mo, Ag, Pb, Zn, W, Au, Bi, or Cd (Church, Bailey, and Riehle, 1989; Church and Arbogast, 1989). Most of these anomalies were from NMHMC samples collected in drainage basins that are underlain by rocks of the Talkeetna Formation (Jt). Wulfenite, galena, sphalerite, and gold were identified in some of the NMHMC samples (Church and Bennett, 1989). Rock samples from sites 5–7 contained anomalous concentrations of molybdenum, chromium, and nickel. One sample (site 6) contained anomalous concentrations of molybdenum in a small tourmaline-bearing quartz vein. In general, however, we observed little evidence of mineralized rock in this area.

We also found no consistent suite of geochemical anomalies in SS and NMHMC samples from drainage basins underlain by Jurassic batholith rocks or the roof pendants from the central part of the study area south of Naknek Lake and west of the Bruin Bay fault (T. 20 S., R. 39–40 W. to T. 24 S., R. 42–43 W.). Scattered, single-element anomalies of Cu, Co, Ag, Pb, or Au are shown by some NMHMC samples collected downstream from the iron-stained zones in the roof pendants (Church and Arbogast, 1989). Chalcopyrite was identified in one NMHMC sample, but sphene and rutile, both of which are associated with stratabound occurrences in the Talkeetna Formation farther northeast (Newberry, 1986), were not abundant (Bennett and Church, 1987). Occurrences of galena and sphalerite were noted in a few NMHMC samples from scattered localities in drainage basins that are cut by the Bruin Bay fault (Church and Bennett, 1989). Gold and silver were also found in a few NMHMC samples from scattered drainage basins within the batholith. However, one drainage basin on the north side of the King Salmon River east of Granite Creek (T. 23 S., R. 42 W.) had anomalous concentrations of Mo (Church, Bailey, and Riehle, 1989) as well as As, Ba, Mn, and Pb (Church and Motooka, 1989). This drainage basin is underlain largely by rocks of the Kakhonak Complex (JTRk) and the Kamishak Formation (TRk). Detterman and others (1979) described several dikes that cut the rocks, and they noted pyrite and magnetite in altered sedimentary wall rocks marginal to dikes in this area. We did not revisit this area during our followup sampling program; however, these data indicate the presence of mineralized rock in this drainage basin, possibly a skarn mineral assemblage.

Chip samples were taken across iron-stained zones in the roof pendants (sites 16–19). No quartz-vein stockworks were found. These chip samples were primarily from weathered, pyrite-rich zones that were generally barren of both base- and precious-metals. A few samples from scattered localities contained mostly single-element anomalies of Mo, Cu, Pb, Zn, or As. These samples appeared to be weakly altered and were cut by thin quartz veins. Small, pyrite-bearing quartz veins containing epidote were sampled at site 17. These iron-stained zones are similar to the stratabound, pyrite-rich zones at the Sheep Mountain occurrence in the Talkeetna Formation (Newberry, 1986). However, they may also result from contact metamorphism during the emplacement of the batholith. Whereas the Talkeetna Formation (Jt) in these roof pendants is permissive for undiscovered Kuroko-type massive sulfide deposits, our geologic mapping and geochemical data do not indicate areas favorable for undiscovered Kuroko-type massive sulfide deposits in the area south of Naknek Lake and west of the Bruin Bay fault.

Table 12. Geochemical and geologic data for selected samples from the area south of Naknek Lake and west of Bruin Bay fault, Katmai

[Samples listed here have concentrations that exceed the 95th percentile for the respective lithologic units as defined in table 4. "Site No." is the locality shown on plates 1–3; map unit symbols are those on the geologic base map on plates 1–3. An "X" in columns headed "Vein," "Frac," or "Alt" indicates that veins, fracture fill, and (or) hydrothermally altered rock, including color anomalies caused by the oxidation of sulfide minerals, were observed at the sample site; "Int" indicates that the sample is an intrusive rock, or that there is a sill, dike, or pluton exposed nearby. "Lith" indicates the rock type of the sample: 1, sandstone or siltstone; 2, conglomerate; 3, volcaniclastic

Site No.	Sample No.	Map unit	Mn	Cr	Ni	Co	Cu	Mo	Sn	Pb	Ag	Bi	Zn	Cd
5	83RJ213	Jt	---	---	---	---	---	20	---	---	---	---	---	---
6	84RJ180B	JTRk	---	---	---	---	---	10	---	---	---	---	---	---
7	86RJ090	Jt	---	500	100	---	---	---	---	---	---	---	---	---
8	83RJ223	Jt	---	---	---	100	---	---	---	---	---	---	---	---
9	84EM073C	Jqd	1,500	---	---	100	---	---	---	---	---	---	---	---
9	84RJ163C	Td	---	---	---	---	200	---	---	---	---	---	---	---
9	84RJ163D	Jgb	---	---	---	---	500	---	---	---	---	---	---	---
10	83RJ220	Jgb	---	---	---	---	---	---	---	50	---	---	---	0.2
11	83RJ221D	Jqd	---	---	---	100	---	---	---	---	---	---	---	---
12	K3075RA	Jqd	---	---	---	70	150	---	---	---	---	---	---	---
13	K3159RA	Jqd	---	---	---	---	---	10	---	---	---	---	---	---
14	85RJ042	Jgd	---	---	---	---	---	---	---	---	---	---	130	.2
15	K1075RA	Jqd	---	---	---	---	---	7	---	---	1.0	---	---	---
16	K2654RA	(*)	---	---	---	---	---	---	---	150	---	---	---	---
17	K3158RJ	Jqd	---	---	---	---	100	7	---	---	---	---	200	---
18	K3156RC	JTRk	---	---	---	---	---	---	---	---	---	---	---	---
19	K3157RA	JTRk	---	---	---	---	---	15	---	---	---	---	---	---
20	85RJ053	Jgr	1,500	300	---	---	---	---	---	---	---	---	---	---
21	85YB201	Jqd	---	---	---	---	---	---	---	---	---	---	---	---
22	85YB205	Qac	1,500	200	---	---	---	---	---	---	---	---	---	---
23	84YB094	Jgr	---	---	---	---	5,000	---	---	---	---	---	---	---
24	85RJ021	TRc	---	200	100	---	---	---	---	---	---	---	---	---
25	83RJ228	TRc	---	---	100	100	---	---	---	---	---	---	---	---
26	84YB095	TRc	---	---	100	100	---	---	---	---	1.0	---	---	---
27	85RJ029	TRc	---	---	100	---	200	---	---	---	---	---	---	---
28	83RJ229	TRc	---	1,000	500	100	---	---	---	---	---	---	---	---

Rock samples collected from Jurassic intrusive rocks (sites 9–15, 20, 23) contained anomalous concentrations of Cu, Co, Mo, Cd, or Mn, and, less commonly, of Pb, Zn, or Ag. Most of the samples contained only single-element anomalies and were rarely associated with alteration or fracture filling in the intrusive rocks. A sample containing 5,000 ppm Cu is from a zone of iron-stained quartz veins in a Jurassic granite (Jgr) that is cut by felsic dikes (site 23; T. 25 S., R. 43 W.). We found no continuous zones of mineralized rock within the Jurassic batholithic intrusive rocks (pl. 2). These data extend the observations of Detterman and Reed (1980) on the Jurassic intrusive rocks from the Iliamna quadrangle and confirm that, in general, the Jurassic intrusive rocks of the Alaska–Aleutian Range batholith do not constitute a favorable mineral exploration target on the Alaska Peninsula. However, site 23 warrants further investigation for an undiscovered polymetallic-vein deposit.

Samples of the Upper Triassic Cottonwood Bay Greenstone (TRc, sites 24–28) from Blue Mountain (or the east end of Whale Mountain; T. 24–25 S., R. 43–44 W.), on the north shore of Becharof Lake, contained anomalous concentrations of nickel, cobalt, copper, and chromium. One sample, in which pyrite and Fe-oxides were concentrated along vertical fractures, contained 1 ppm Ag. Some samples also contained small quartz or pyrite veins along fractures. Although these rocks are permissive for undiscovered Cyprus-type massive sulfide deposits (Singer, 1986b), we interpret this geochemical association as a reflection of the mafic composition of the rocks rather than as an indication of undiscovered Cyprus-type massive sulfide deposits.

KULIK LAKE AREA

In the north-central part of the Katmai study area, middle Tertiary granodiorite (Tgd) and quartz diorite (Tqd) intrude Jurassic plutons (Jgd, Jqd) and form contact-metamorphic aureoles in the surrounding rocks (units Jt, Jn, and Kh). This 400-km^2 area, referred to as the Kulik Lake area (T. 14–17 S., R. 31–38 W.), extends north from Lake Grosvenor to the boundary of the Mount Katmai quadrangle (fig. 10). Bedrock is well exposed, and the topographic relief of the area is as much as 600 m. Glacial deposits are sparse study area, Alaska.

rock or tuff; 4, lava flow; 5, sill or dike; 6, plutonic rock; 7, metamorphosed rock/protolith; 8, limestone; and (*), float sample. Mineralogy is generally based upon field identifications of hand specimens: py, pyrite; cpy, chalcopyrite; asp, arsenopyrite; spl, sphalerite; gn, galena; mly, molybdenite; qtz, quartz; Fe ox., iron oxides; dissem., disseminated mineral grains in sample. Dashes (---), concentrations not anomalous or feature not observed; all concentrations expressed in parts per million (ppm); >, concentration is greater than reported value]

Site No.	Sample No.	Map unit	Au	As	Sb	Hg	Alt	Int	Lith	Frac	Vein	Mineralogy and mode of occurrence
5	83RJ213	Jt	---	---	---	---	---	---	7/4	---	---	
6	84RJ180B	JPzk	---	---	---	---	---	X	7/1	---	X	Qtz-tourmaline veins
7	86RJ090	Jt	---	---	---	---	---	---	7/4	---	---	
8	83RJ223	Jt	---	---	---	---	---	X	7/1	---	---	
9	84EM073C	Jqd	---	---	---	---	---	X	6	---	---	
9	84RJ163C	Td	---	---	---	---	---	X	5	---	---	
9	84RJ163D	Jgb	---	---	---	---	---	X	6	X	---	Fe ox. on fractures
10	83RJ220	Jgb	---	---	---	---	---	X	6	---	---	
11	83RJ221D	Jqd	---	---	---	---	---	X	6	---	---	
12	K3075RA	Jqd	---	---	---	---	---	X	6	---	---	Dissem. py
13	K3159RA	Jqd	---	---	---	---	X	X	6	---	---	Dissem. py
14	85RJ042	Jgd	---	---	---	---	---	X	6	---	---	
15	K1075RA	Jqd	---	---	---	---	X	X	6	---	---	Dissem. py
16	K2654RA	(*)	---	---	---	---	---	X	7/1	---	---	Dissem. py
17	K3158RJ	Jqd	---	---	---	---	X	X	5	---	---	Dissem. py; qtz veins; epidote
18	K3156RC	JPzk	---	200	---	---	X	X	7/1	---	---	Dissem. py
19	K3157RA	JPzk	---	---	---	---	X	X	7/1	---	---	Dissem. py in hornfels
20	85RJ053	Jgr	---	---	---	---	---	X	6	---	---	
21	85YB201	Jqd	---	---	---	0.28	---	---	---	---	---	
22	85YB205	Qac	---	---	---	---	---	---	4	---	---	
23	84YB094	Jgr	---	---	---	---	---	X	6	---	X	Felsic dikes; Fe ox.
24	85RJ021	T̄Rc	---	---	---	---	---	---	---	---	---	
25	83RJ228	T̄Rc	---	---	---	---	---	---	7/4	---	---	
26	84YB095	T̄Rc	---	---	---	---	---	---	7/4	---	X	Dissem. py
27	85RJ029	T̄Rc	---	---	---	---	---	---	7/5	X	X	Fe ox. along vertical fractures
28	83RJ229	T̄Rc	---	---	---	---	---	X	6	---	---	

in this alpine terrain. Prospect pits (fig. 10) were found on Oakley Peak, at the west end of Kulik Lake, and at the Kulik Kopper [sic] prospect (MacKevett and Holloway, 1977; Church and others, 1992).

The SS and NMHMC geochemical data for the Kulik Lake area show a consistent suite of elements that are present at anomalous concentrations (Church, Bailey, and Riehle, 1989; Church and Arbogast, 1989). They indicate a geochemical anomaly pattern that is poorly zoned with respect to the outcrop pattern of the middle Tertiary intrusive rocks (Tgd, Tqd, Tgb). In the SS samples, Cu, Mo, Pb, and Ag commonly were present in anomalous concentrations, whereas Zn and B less commonly were present at anomalous concentrations; As, Sb, Sn, Bi, or Cd were present at anomalous concentrations in one drainage basin. In many of the NMHMC samples, Mo, Pb, Zn, and Ag were present at anomalous concentrations, whereas Cu, B, W, Ba, Bi, Cd, As, or Au anomalies were less common. Scheelite, pyrite, chalcopyrite, galena, wulfenite, sphalerite, barite, and gold were identified in the mineralogical studies of the NMHMC samples (Church and Bennett, 1989). Drainage basins that contain anomalous concentrations of copper, molybdenum, silver, and lead are commonly underlain by Tertiary granitic rocks. Peripheral to these central anomalies are drainage basins that contain anomalous concentrations of lead, silver, and, in some places, zinc. Many of the surrounding drainage basins, which are underlain primarily by rocks of the Naknek Formation (Jn), contain anomalous concentrations of gold, bismuth, tungsten, and arsenic. These drainage-basin anomaly patterns are generally indicative of undiscovered porphyry Cu deposits (pl. 1), base-metal-bearing polymetallic-vein deposits (pl. 2), or precious-metal-bearing polymetallic or epithermal quartz-vein deposits (pl. 3).

Samples of altered rock and float (table 13, sites 29–77) showed multi-element suites of metals at anomalous concentrations within many of the drainage basins, particularly those underlain by the Tertiary intrusive rocks (sites 48–49, 52, 57–58, 59, 63, 66, 68, and 69). Zones of altered igneous rock, as well as Fe-oxide-stained zones along the margins of plutons, are common in areas where we found anomalous concentrations of Cu, Pb, Zn, Bi, As, Mn, Ag, and Cd, and, less commonly, of Mo, Co, Ni, Sb, or Au (pls. 1–3). Finely disseminated and vein pyrite, predominantly deposited along fractures or in sheeted quartz veins, is abundant.

Table 13. Geochemical and geologic data for selected samples from the Kulik Lake area, Katmai study area, Alaska.

[Samples listed here have concentrations that exceed the 95th percentile for the respective lithologic units as defined in table 4. "Site No." is the locality shown on plates 1–3; map unit symbols are those on the geologic base map on plates 1–3. An "X" in columns headed "Vein," "Frac," or "Alt" indicates that veins, fracture fill, and (or) hydrothermally altered rock, including color anomalies caused by the oxidation of sulfide minerals, were observed at the sample site; "Int" indicates that the sample is an intrusive rock, or that there is a sill, dike, or pluton exposed nearby. "Lith" indicates the rock type of the sample: 1, sandstone or siltstone; 2, conglomerate; 3, volcaniclastic

Site No.	Sample No.	Map unit	Mn	Cr	Ni	Co	Cu	Mo	Sn	Pb	Ag	Bi	Zn	Cd
29	84RJ171B	Jt	---	---	---	---	---	---	---	70	---	---	---	---
30	84RJ055B	Jt	---	---	---	---	---	---	---	---	---	---	---	---
31	85YB248	JPzk	---	---	---	---	---	---	---	---	---	---	---	---
32	85YB249	Tiu	1,500	---	---	---	---	---	---	---	---	---	---	---
32	85YB250	Tiu	1,500	---	---	---	---	---	---	---	---	---	---	0.3
33	85YB251	Tiu	1,500	---	---	---	---	---	---	---	---	---	---	---
34	85YB254	Tva	2,000	---	---	---	200	---	---	---	---	---	---	---
35	85RJ105D	Jt	---	700	100	---	---	---	---	---	---	---	---	---
36	85YB231	Jt	---	500	---	---	---	---	---	---	---	---	---	---
37	85RJ065	Jt	---	---	---	---	---	---	---	---	---	---	---	---
38	83RJ216A	Jt	---	200	70	---	---	---	---	---	---	---	---	---
38	86RJ068A	Jt	---	---	---	100	200	---	---	---	---	---	---	---
38	K4197RB	(*)	1,500	---	---	---	---	20	---	---	---	---	90	---
39	85RJ075	Jt	---	---	---	---	1,000	---	---	---	2.0	---	120	.2
40	85RJ074C	Jt	---	---	---	---	---	---	---	---	---	---	340	.8
41	K4179RA	Tgd	---	---	50	70	300	7	---	100	---	---	70	---
41	K4573RD	(*)	---	---	100	150	2,000	10	---	---	3.0	---	---	---
41	K4574RA	(*)	5,000	---	---	70	---	---	---	300	---	10	360	---
41	K4574RB	(*)	---	150	---	---	200	---	---	70	---	---	---	---
42	86RJ088	Jqd	---	---	---	---	500	---	---	---	---	---	---	---
43	85RJ072A	Jgb	1,500	---	---	100	---	---	---	---	---	---	150	.6
44	85YB237B	Jn	2,000	200	---	---	---	---	---	---	---	---	---	---
45	85RJ062	JPzk	>5,000	---	---	---	---	---	---	---	---	---	300	---
46	K4194RA	(*)	---	---	---	---	---	10	---	---	---	---	---	---
47	K4596RA	(*)	---	---	---	---	---	20	20	---	---	---	---	---
48	85YB228	Tgd	3,000	---	---	---	---	---	---	50	---	---	165	---
49	K3607RA	Tgd	---	---	50	---	500	---	---	300	5.0	2	70	.2
49	K3607RB	Tgd	---	---	---	---	200	---	---	200	5.0	2	---	---
49	K3607RD	Tgd	---	---	---	---	150	---	---	30	---	---	95	.2
50	85RJ107D	Jt	---	---	---	---	---	7	---	---	---	---	---	---
50	85RJ107I	Jt	5,000	---	---	---	---	---	---	---	---	---	---	---
50	86RJ111	Jt	>5,000	---	---	---	300	---	---	---	1.0	23	---	---
50	K3608RA	Jqd	5,000	---	100	200	500	---	---	50	2.0	8	>10,000	16
50	K3608RB	Jt	3,000	---	---	---	---	---	---	300	3.0	38	230	.2
50	K4202RB	(*)	1,500	---	---	---	---	---	---	---	---	---	110	.3
50	K4202RC	(*)	5,000	---	---	70	500	15	---	200	2.0	2	660	3.6
51	86RJ109B	Jt	---	---	---	---	200	---	---	---	---	---	---	---
51	K3505RC	Jqd	---	---	---	70	---	50	---	---	---	---	---	.2
51	K3505RD	Jqd	---	---	---	---	1,000	70	---	30	1.0	---	---	---
51	K3505RE	Jqd	2,000	300	100	100	2,000	---	---	---	---	---	---	---
52	K3393RB	(*)	---	---	---	70	---	---	---	---	---	---	---	---
52	K3394RD	(*)	---	---	---	70	1,500	500	---	---	---	---	80	---
52	K3394RE	(*)	---	---	---	100	---	---	---	---	---	---	---	---
52	K3504RA	Tgd	---	---	---	---	1,000	---	---	---	---	2	---	---
53	85YB258	Jt	---	---	---	---	---	---	---	---	---	---	---	---

rock or tuff; 4, lava flow; 5, sill or dike; 6, plutonic rock; 7, metamorphosed rock/protolith; 8, limestone; and (*), float sample. Mineralogy is generally based upon field identifications of hand specimens: py, pyrite; cpy, chalcopyrite; asp, arsenopyrite; spl, sphalerite; gn, galena; mly, molybdenite; qtz, quartz; Fe ox., iron oxides; dissem., disseminated mineral grains in sample. Dashes (---), concentrations not anomalous or feature not observed; all concentrations expressed in parts per million (ppm); >, concentration is greater than reported value]

Site No.	Sample No.	Map unit	Au	As	Sb	Hg	Alt	Int	Lith	Frac	Vein	Mineralogy and mode of occurrence
29	84RJ171B	Jt	---	---	---	---	---	X	7/4	---	---	
30	84RJ055B	Jt	0.05	---	---	---	---	X	7/4	---	---	Aplite dikes with dissem. py.
31	85YB248	JPzk	---	---	---	0.24	---	X	7/4	---	---	
32	85YB249	Tiu	---	---	---	.16	X	X	5	---	---	
32	85YB250	Tiu	---	---	---	---	X	X	5	---	---	
33	85YB251	Tiu	---	---	---	.13	---	---	4	---	---	
34	85YB254	Tva	---	---	---	---	---	X	5	---	---	Dike cross-cutting Jt.
35	85RJ105D	Jt	---	---	---	---	X	---	7/1	X	---	
36	85YB231	Jt	---	---	---	---	---	---	3	---	---	
37	85RJ065	Jt	---	30	---	---	---	---	3	X	---	Py along fractures.
38	83RJ216A	Jt	---	---	---	---	---	X	5	---	---	
38	86RJ068A	Jt	---	---	---	---	X	---	7/4	---	---	
38	K4197RB	(*)	---	---	---	---	X	X	5/6	---	---	Py in breccia.
39	85RJ075	Jt	---	---	---	---	---	---	4	---	---	
40	85RJ074C	Jt	---	30	8	.32	X	---	3	---	---	Fe ox.
41	K4179RA	Tgd	---	---	---	---	---	X	6	---	X	Dissem. py; py in qtz veins.
41	K4573RD	(*)	.20	---	---	---	X	X	6	---	X	Py and sulfosalt in qtz vein stockwork.
41	K4574RA	(*)	---	---	---	---	---	X	6	---	---	Dissem. py.
41	K4574RB	(*)	---	---	---	---	---	X	6	X	---	Dissem. py; py in qtz vein.
42	86RJ088	Jqd	---	20	---	---	X	X	6	---	---	Fe ox.-stained mafic inclusions.
43	85RJ072A	Jgb	---	---	---	---	---	X	6	---	---	Aplitic veinlets.
44	85YB237B	Jn	---	---	---	---	X	X	2	---	---	Fe ox.
45	85RJ062	JPzk	---	---	---	---	X	X	7/4	---	---	
46	K4194RA	(*)	---	---	---	---	---	X	6	---	---	Dissem. py.
47	K4596RA	(*)	---	---	---	---	X	X	6	---	---	Dissem. py
48	85YB228	Tgd	---	---	---	---	X	---	6	---	---	Fe ox.
49	K3607RA	Tgd	---	140	34	---	X	X	---	---	X	Py, cpy in qtz veins as much as 10 cm wide.
49	K3607RB	Tgd	---	---	6	---	X	X	---	---	X	Py in qtz veins.
49	K3607RD	Tgd	---	---	---	---	---	X	6	X	---	Dissem. py.
50	85RJ107D	Jt	---	45	---	---	X	---	7/5	X	---	Fe ox. along fractures.
50	85RJ107I	Jt	---	210	20	---	X	---	7/1	X	---	Fe ox. along fractures.
50	86RJ111	Jt	---	55	20	---	X	---	7/1	---	X	
50	K3608RA	Jqd	.05	---	---	---	X	X	6	---	X	Dissem. py; py, spl in qtz veins.
50	K3608RB	Jt	---	---	---	---	X	X	7/1	---	X	Dissem. py; py in qtz veins.
50	K4202RB	(*)	---	10	---	---	---	X	7/1	---	---	Dissem. py.
50	K4202RC	(*)	.10	10	---	---	X	X	5/6	---	---	Py and epidote in qtz veins.
51	86RJ109B	Jt	---	30	---	---	X	---	7/1	X	X	Py in qtz veins and along fractures.
51	K3505RC	Jqd	.55	---	---	---	X	X	6	---	---	Dissem. py.
51	K3505RD	Jqd	.20	---	---	---	X	X	6	---	X	Dissem. py, cpy in qtz veins; malachite.
51	K3505RE	Jqd	.20	---	---	---	X	X	6	---	---	Banded dissem. magnetite and py.
52	K3393RB	(*)	.15	---	---	---	X	X	5/6	---	---	Dissem. py and magnetite; qtz vein.
52	K3394RD	(*)	.05	---	---	---	X	X	5/6	---	X	Cpy and epidote in qtz veins.
52	K3394RE	(*)	.10	---	---	---	X	X	5/6	---	---	Dissem. py.
52	K3504RA	Tgd	.05	---	---	---	X	X	6	---	---	Dissem. py.
53	85YB258	Jt	---	30	---	---	X	---	7/3	---	---	

Table 13. Geochemical and geologic data for selected samples from the Kulik Lake area, Katmai study area, Alaska—Continued.

Site No.	Sample No.	Map unit	Mn	Cr	Ni	Co	Cu	Mo	Sn	Pb	Ag	Bi	Zn	Cd
54	86RJ067	Jt	---	---	---	---	---	---	---	---	---	---	---	---
54	86YB315B	Jt	3,000	---	---	---	---	---	---	---	---	---	---	---
55	83RJ218	Jgd	---	---	---	100	---	---	---	---	---	---	---	---
56	86RJ112	Jgd	2,000	200	---	---	---	---	---	---	---	---	---	---
56	K3609RA	Jgd	---	---	---	---	200	---	---	70	0.7	2	---	---
56	K3609RB	(*)	---	---	---	---	---	---	---	---	---	6	---	---
56	K4597RA	Jgd	---	---	---	---	---	---	10	---	---	4	---	---
56	K4597RB	(*)	2,000	700	100	70	---	70	---	---	---	---	---	---
56	K4597RE	(*)	---	---	---	---	20,000	---	---	100	200	80	---	---
56	K4597RG	Jt	---	---	---	200	300	70	---	---	---	---	---	---
56	K4597RI	(*)	---	---	100	700	2,000	---	---	30	5.0	11	---	---
56	K4597RJ	(*)	---	---	---	100	15,000	20	---	---	5.0	---	60	---
57	K3613RA	Tgd	1,500	---	---	150	300	---	---	---	1.0	1	80	.2
57	K3613RC	Tgd	---	---	---	100	700	---	---	---	---	1	---	---
57	K3614RC	Tgd	---	---	---	---	200	10	---	30	---	---	60	---
58	K4549RA	Tgd	---	---	---	---	500	10	---	---	5.0	---	---	---
59	85RJ181	Tgd	---	---	---	---	500	---	---	---	---	---	---	---
60	K3384RA	(*)	2,000	---	---	---	---	---	---	---	---	---	---	.4
60	K4155RA	(*)	---	---	---	---	---	---	---	---	1.0	---	500	2.4
60	K4155RB	(*)	1,500	---	---	---	200	---	---	---	---	---	65	---
61	85YB243	Jn	>5,000	---	---	---	---	---	---	---	---	---	370	---
62	K3610RB	(*)	2,000	---	100	100	200	---	---	---	---	---	---	.2
62	K3610RD	(*)	>5,000	---	---	---	---	---	---	300	10	---	5,000	31
62	K3612RA	Jn	2,000	---	50	---	1,000	---	---	---	3.0	7	>10,000	>100
62	K3612RB	Kh?	>5,000	---	50	150	20,000	---	---	---	1.0	6	720	6.1
63	K3611RA	Jn	1,500	---	---	---	---	---	---	---	---	---	---	.2
63	K3611RB	Tgd	1,500	---	50	---	---	---	---	---	---	1	---	---
64	86RJ057A	Jn	---	---	---	70	200	---	---	---	---	---	---	---
65	86RJ058	Td	---	---	---	---	---	---	---	100	---	---	---	---
66	86YB318	Tgd	---	---	---	---	200	---	---	---	---	---	---	---
66	K3616RA	Jn	1,500	---	---	---	200	---	---	---	---	---	115	.2
66	K3616RB	Jn	1,500	---	---	---	---	---	---	---	---	---	130	.3
67	86RJ066A	Jn	---	200	---	---	---	---	---	---	---	---	---	---
68	86YB316	Jqd	---	---	---	---	---	---	---	---	---	---	60	---
68	K3617RD	Tgd	2,000	---	50	---	1,000	---	---	---	---	2	---	.2
69	K3405RA	(*)	2,000	---	---	70	500	---	---	---	---	---	---	---
69	K3406RC	(*)	2,000	---	---	---	---	---	---	---	---	---	---	---
69	K3406RD	(*)	---	150	50	70	300	---	---	---	---	---	---	---
69	K3406RE	Tgd	2,000	---	---	---	200	---	---	---	---	---	---	---
70	K3093	(*)	---	---	50	---	100	---	---	---	---	---	---	---
71	86JM196	Jn	---	150	70	50	---	---	---	---	---	---	---	---
72	K3303RB	(*)	1,500	---	---	---	---	---	---	---	---	---	100	---
73	K4508RC	(*)	1,500	---	---	---	---	---	---	---	---	---	205	.5
73	K4508RD	(*)	---	---	---	---	---	20	100	---	---	1	---	---
74	86DT259	Jn	---	200	---	50	100	---	---	---	---	---	---	---
75	86DT263	Jn	---	---	---	---	---	---	---	---	---	---	---	---
76	K4185RA	(*)	2,000	---	---	---	---	---	---	---	---	---	---	---
77	K4186RA	(*)	---	---	---	---	---	---	---	---	---	---	---	---

Site No.	Sample No.	Map unit	Au	As	Sb	Hg	Alt	Int	Lith	Frac	Vein	Mineralogy and mode of occurrence
54	86RJ067	Jt	---	---	---	1.10	X	---	7/1	---	X	
54	86YB315B	Jt	---	80	---	.22	---	---	7/8	---	---	
55	83RJ218	Jgd	---	---	---	---	---	X	6	---	X	Qtz veins, felsic dikes.
56	86RJ112	Jgd	---	---	---	---	X	X	7/4	X	---	Py, cpy along fractures.
56	K3609RA	Jgd	---	---	---	---	X	X	6	---	X	Dissem. py in vuggy qtz veins.
56	K3609RB	(*)	.05	---	---	---	X	X	---	---	X	Dissem. py in qtz veins; 50 ppm tungsten.
56	K4597RA	Jgd	.50	---	---	---	X	X	6	---	X	Finely dissem. py in qtz veins.
56	K4597RB	(*)	---	---	---	---	---	X	6	---	X	Dissem. py in qtz veins as much as 3 cm wide
56	K4597RE	(*)	4.4	---	---	---	X	X	6	---	X	Finely dissem. py in qtz veins 5 mm wide.
56	K4597RG	Jt	.10	---	---	---	X	X	7/1	---	X	Banded py in qtz vein.
56	K4597RI	(*)	.35	---	2	---	---	---	---	---	X	Py, cpy in qtz vein.
56	K4597RJ	(*)	.45	---	---	---	---	---	---	---	X	Py, tourmaline in qtz vein.
57	K3613RA	Tgd	.1	40	---	---	X	X	6	---	X	Py in qtz vein.
57	K3613RC	Tgd	---	20	---	---	---	X	6	---	---	Dissem. py.
57	K3614RC	Tgd	---	---	---	---	---	X	6	---	---	Dissem. py.
58	K4549RA	Tgd	---	---	---	---	X	X	5	---	---	Dissem. py.
59	85RJ181	Tgd	---	---	---	---	---	X	6	---	X	Veinlets of chlorite, py, chrysocolla.
60	K3384RA	(*)	---	20	---	---	---	X	5	---	---	Dissem. py.
60	K4155RA	(*)	---	---	---	---	---	X	6	---	---	Dissem. py.
60	K4155RB	(*)	---	---	---	---	X	X	6	---	---	Dissem. py.
61	85YB243	Jn	---	---	---	---	X	---	7/1	---	X	Qtz vein; Fe ox.
62	K3610RB	(*)	---	---	---	---	X	---	7/1	---	---	Dissem. py.
62	K3610RD	(*)	.05	7,000	48	---	---	---	7/1	---	X	Py in qtz veins; Fe ox.
62	K3612RA	Jn	---	---	2	---	X	X	8	---	---	Py, spl in tremolite-epidote tactite.
62	K3612RB	Kh?	.50	---	---	---	---	X	7/1	---	---	Malachite stained; dissem. cpy.
63	K3611RA	Jn	---	---	---	---	X	X	7/1	---	---	Py in breccia.
63	K3611RB	Tgd	---	---	---	---	---	X	6	---	---	Dissem. py.
64	86RJ057A	Jn	---	---	6	6	X	---	1	---	---	
65	86RJ058	Td	---	---	10	1.4	---	X	5	---	---	Dissem. py.
66	86YB318	Tgd	---	---	---	.2	---	X	6	---	---	
66	K3616RA	Jn	---	---	2	---	---	X	7/1	---	---	Dissem. py.
66	K3616RB	Jn	---	---	2	---	X	X	7/1	---	---	Dissem. py.
67	86RJ066A	Jn	---	20	---	.2	X	X	1	---	---	Fe ox.
68	86YB316	Jqd	---	20	---	---	---	X	6	---	---	
68	K3617RD	Tgd	---	10	---	---	X	X	6	---	---	Dissem. py.
69	K3405RA	(*)	.05	---	---	---	X	X	5	---	---	Dissem. py.
69	K3406RC	(*)	.25	---	---	---	---	X	5	---	---	Py along contact zone of dike.
69	K3406RD	(*)	.45	---	---	---	---	X	5	---	---	Dissem. py.
69	K3406RE	Tgd	---	---	---	---	X	X	5	---	X	Finely dissem. py in qtz veins.
70	K3093	(*)	---	---	---	---	X	X	1	---	---	Dissem. py.
71	86JM196	Jn	---	---	---	.5	---	---	1	---	---	
72	K3303RB	(*)	---	20	---	---	---	---	7/1	X	X	Py in vuggy qtz veins.
73	K4508RC	(*)	---	---	---	---	---	X	5/6	---	---	Dissem. py.
73	K4508RD	(*)	---	30	2	---	X	X	5/6	---	---	Dissem. py.
74	86DT259	Jn	---	---	---	---	---	---	1	---	---	
75	86DT263	Jn	---	---	---	.24	---	---	1	---	---	
76	K4185RA	(*)	---	---	---	---	---	---	---	---	---	Py and qtz in breccia.
77	K4186RA	(*)	.05	60	---	---	---	---	6	---	---	Dissem. py.

Oakley Peak (fig. 10), at the west end of Kulik Lake (T. 14 S., R. 34 W.), is underlain by slightly metamorphosed lava flows, sills, volcanic tuff, sandstone, and breccia of the Talkeetna Formation (Jt). Rocks in this area are marked by a prominent red-brown color anomaly. Nearby, the Talkeetna Formation is in contact with Tertiary equigranular to marginally porphyritic quartz monzodiorite to granodiorite (29.2±0.9 Ma, Shew and Lanphere, 1992). Bedrock samples of the Talkeetna Formation (sites 35–40) characteristically contained anomalous concentrations of Zn, Cr, Ni, Cu, As, and Cd; some samples also contained anomalous concentrations of Co, Mo, Ag, Sb, or Hg. Fracture-controlled pyrite was identified at site 37. At site 38, we collected a sample of float that showed a propylitic alteration assemblage and contained brecciated granodiorite in a pyritic matrix.

At a distance 10 km southeast of Oakley Peak (fig. 10), on a hillside overlooking Kulik Lake (T. 14 S., R. 34 W.), several prospect pits over several acres comprise the Kulik Kopper prospect (table 13, site 50; MacKevett and Holloway, 1977). At this locality metamorphosed lava flows and sills of probable andesitic composition compose a roof pendant of the Talkeetna Formation in equigranular quartz diorite of Jurassic age (173±5.2 Ma, Shew and Lanphere, 1992). The locality is marked by a weakly developed red-brown color anomaly. Samples collected from this prospect generally show a propylitic alteration assemblage and contained anomalous concentrations of Mn, As, Sb, Ag, and Bi. In addition, some samples also contained anomalous concentrations of copper, lead, zinc, or cadmium. Sulfide minerals, generally pyrite, are visible on minute fractures in quartz veins. Intrusive rocks of middle Tertiary age (ranging from about 27 to 29 Ma, Shew and Lanphere, 1992) crop out a few kilometers to the southeast (site 48; samples contained anomalous concentrations of Mn, Pb, and Zn) and to the west (site 52; samples contained anomalous concentrations of Cu, Co, As, Bi, and Au).

In the small stream valley immediately south of the Kulik Kopper prospect (site 49), we sampled a small Tertiary(?) granitic pluton that shows a phyllic alteration assemblage and is cut by numerous quartz veins. Samples from this site contained anomalous concentrations of Cu, Pb, Ag, Bi, Zn, Cd, Sb, As, Ba, and B. The plutonic rock contains disseminated pyrite; pyrite and chalcopyrite are also common in quartz veins in both the pluton and in the older rocks that it intruded. Quartz veins as much as 10 cm in width were observed. Open vugs lined with small quartz crystals are exposed in outcrop in the stream valley. We interpret the geologic observations and the geochemical data for site 49 as a base-metal-rich polymetallic-vein occurrence (pl. 2).

Gold and arsenic also were found in anomalous concentrations in samples of Tertiary(?) plutonic rocks (sites 51 and 52) that had been altered to a propylitic assemblage and were cut by quartz veins. Pyrite and chalcopyrite were present in both disseminated and vein form, and epidote was deposited along fractures. The rocks at site 51 contain abundant secondary malachite. At site 41 we collected samples of porphyritic intrusive rock, mainly from float and presumably from the Tertiary plutons (potassium-argon age from hornblende of 34.3±1.2 Ma, Shew and Lanphere, 1992), that contained anomalous concentrations of Co, Cu, Pb, Zn, and Ni; a few samples also contained anomalous concentrations of Mn, Cr, Ag, Bi, or Au. The sample from site 41 contained pyrite in stockwork. At sites 42–47, a somewhat similar suite of metals (Mn, Mo, Co, Cu, Zn, As, and Sn) also is present in anomalous concentrations in porphyritic igneous rocks. These data are interpreted to reflect small, base-metal polymetallic veins, but they may also be indicative of a concealed porphyry Cu deposit.

Farther south, at site 56 (pl. 3), Jurassic granodiorite and rocks of a small roof pendant are cut by sheeted quartz veins that occupy as much as fifty percent of the outcrop area. These sheeted quartz veins vary in width, ranging from a few millimeters to 3 cm, and contain varying amounts of pyrite; some also contain minor amounts of tourmaline. Samples of the veins (table 13, site 56) commonly contained anomalous concentrations of Au, Cu, Bi, Ag, Co, Mo, and Pb; one or two samples were anomalous in Mn, Cr, Ni, Zn, W, Sb, or Sn. As much as 4.4 ppm Au was measured, although most of the samples of the vein material contained gold concentrations ranging from 0.1 to 0.5 ppm. We interpret the geologic and geochemical data for site 56 as indicating a precious-metal-bearing polymetallic vein (pl. 3). Similar suites of metals are present in anomalous concentrations, although of lesser intensity, in quartz veins in Tertiary granitic rocks at sites 57–58 (table 13).

A rock sample (K3612A, table 13; site 62, pl. 1) from a contact aureole developed in the Naknek Formation adjacent to the middle Tertiary quartz diorite pluton (dated between 35 and 37 Ma, Shew and Lanphere, 1992), contained chalcopyrite, pyrite, and sphalerite in a matrix of tremolite, actinolite, and epidote. Metals determined at anomalous concentrations were Mn, Ni, Cu, Zn, Cd, Bi, Ag, Au, Co, and Sb. We interpret this sample as indicating a skarn mineral assemblage. A similar suite of metals in anomalous concentrations was found at site 63. The Naknek Formation (Jn) contains only small limestone concretions and minor amounts of carbonate-cemented siltstone. The Herendeen Formation (Kh) is a thin unit composed of about fifty percent siltstone and shale interbedded with calcareous sandstone (Detterman and others, in press). Because carbonate rocks represent only a small component of the stratigraphic column in the Katmai study area, we suggest that the presence of the skarn mineral assemblage is not important in terms of types of mineral deposits present in the Katmai study area.

Finally, at site 69 (pl. 1), Tertiary(?) dikes and sills intruded rocks of the Naknek Formation (Jn). Float samples of hornfels from these sites contained disseminated pyrite, showed propylitic alteration, and contained as much as 0.45 ppm Au. Drainage basins at these localities have such steep walls that it was not practical to collect NMHMC samples.

However, some reconnaissance geochemical samples from drainage basins underlain by rocks of the Naknek Formation adjacent to the Tertiary plutons or cut by Tertiary(?) dikes contained anomalous concentrations of gold and silver in pyrite and have gold visible in the pan. This Au-Ag geochemical anomaly may reflect the presence of pyrite in hornfels adjacent to small dikes in other drainage basins where similar geochemical suites are found.

In summary, we interpret the field observations and the geochemical data for the Kulik Lake area to be indicative of undiscovered base-metal polymetallic veins (pl. 2), commonly inferred at or near the margins of middle Tertiary calc-alkaline intrusive rocks (ages range from 26 to 38 Ma, Shew and Lanphere, 1992). However, the presence of associated concealed porphyry Cu deposits cannot be ruled out. We favor the base-metal polymetallic-vein mineral deposit model because of (1) the paucity of strongly porphyritic intrusive rocks, (2) the presence of base-metal-bearing sheeted quartz veins, (3) the small areal extent of the geochemical anomalies, and (4) the absence of large zones of propylitic alteration surrounding the Cu-Mo-Sn-W anomalies (pl. 1). Precious-metal-bearing polymetallic veins (pl. 3) are suggested both by the geologic relations and by the geochemical suites observed peripheral to the outcrop pattern of the middle Tertiary granitic plutons.

The possibility of undiscovered Kuroko-type massive sulfide deposits in rocks of the Talkeetna Formation, analogous to the Johnson River prospect (Steefel, 1987), cannot be ruled out for the Oakley Peak occurrence. However, Kuroko-type massive sulfide is an unattractive mineral deposit model for the Oakley Peak area because of (1) the absence of silicic tuffs in any of the volcanic lithologies exposed in the Kulik Lake area, (2) the presence of anomalous concentrations of molybdenum, arsenic, and antimony, (3) the paucity of sphene and rutile in the NMHMC samples, (4) the close similarities between the geochemical signatures of the SS and NMHMC samples from drainage basins throughout the Kulik Lake area regardless of the bedrock underlying the drainage basins, and (5) the spatial relationship with middle Tertiary plutons that contain very similar suites of anomalous metals and have similar mineralogy elsewhere in the vicinity of Tertiary plutons (pl. 2). Studies in the Iliamna quadrangle of mineral occurrences in quartz veins in similar geologic settings and having similar geochemical suites of metals suggest that polymetallic veins formed when plutons intruded rocks of the Talkeetna Formation (Jt) or older plutonic rocks (Detterman and Reed, p. 78, 1980). The Diamond Point claim on Iliamna Bay is an example of such a small polymetallic vein. Generally, the veins are pyritic, some are rich in gold, and some contain chalcopyrite and other sulfide minerals in minor amounts.

We have little geologic or geochemical evidence for undiscovered copper-rich iron-skarn deposits associated with the middle Tertiary plutons. The most favorable host rock, the Kamishak Formation (T̄Rk), is not found in the Kulik Lake area. A few samples of tactite were found where the middle Tertiary plutons (Tgd, Tqd) intrude the Naknek Formation (Jn) and Herendeen Formation (Kh), which reaches a maximum thickness of 50–100 m east of the middle Tertiary plutons in the Kulik Lake area. Nowhere have we seen the middle Tertiary plutons exposed in direct contact with the Herendeen Formation nor do we have good geochemical evidence of the presence of a skarn. Although undiscovered copper-rich iron-skarn deposits are permissible, we suggest that carbonate host rocks present in the Kulik Lake area are volumetrically insignificant and that, on the basis of the geology, the Katmai study area is not generally favorable for undiscovered copper-rich iron-skarn deposits.

BUTTRESS RANGE–IKAGLUIK CREEK AREA

West of the Aleutian Range crest and southeast of the Bruin Bay fault, near the center of the Katmai study area, base- and precious-metal anomalies are indicated by the reconnaissance geochemical data (Church, Bailey, and Riehle, 1989; Church and Motooka, 1989; Church and Arbogast, 1989). These anomalies are found in drainage basins where small hypabyssal dikes, sills, and plutons (Tiu, Td) intrude rocks of the Naknek Formation (Jn). Exposures in this area are good: relief is as much as several hundred meters locally. Unconsolidated deposits are confined to the floors of glacial valleys. Due to pervasive deuteric(?) alteration, potassium-argon radiometric ages of the intrusive rocks are not available, but a Tertiary age for the plutons is inferred from the geologic mapping (Riehle and others, in press). Trace amounts of disseminated pyrite are ubiquitous in the intrusive rocks. Areas of silicified rock and color anomalies are locally developed at the margins of exposed plutons and in the vicinity of dikes; thus, we conclude that other color anomalies present in the area are probably related to buried intrusive rocks. Dikes and fractures are common and are typically oriented northwest.

The geochemical data for the SS and NMHMC samples allow us to divide this area into four subareas (see fig. 10): the Mount Katolinat subarea, the Buttress Range subarea, the Ikagluik Creek subarea, and the area underlain by the Quaternary volcanic rocks of the Aleutian Range. The first three of these are areas where small plutons and dikes have intruded the Naknek Formation (Jn). The fourth subarea, the Aleutian Range, is not shown separately in fig. 10 because it is not continuous. It consists of the watersheds of the Quaternary volcanic rocks of the Aleutian Range and includes the fumaroles at Novarupta at the head of the Valley of Ten Thousand Smokes (VTTS, see fig. 10).

Table 14. Geochemical and geologic data for selected samples from the Butress Range–Ikagluik Creek area, Katmai study area., Alaska.

[Samples listed here have concentrations that exceed the 95th percentile for the respective lithologic units as defined in table 4. "Site No." is the locality shown on plates 1–3; map unit symbols are those on the geologic base map on plates 1–3. An "X" in columns headed "Vein," "Frac," or "Alt" indicates that veins, fracture fill, and (or) hydrothermally altered rock, including color anomalies caused by the oxidation of sulfide minerals, were observed at the sample site; "Int" indicates that the sample is an intrusive rock, or that there is a sill, dike, or pluton exposed nearby. "Lith" indicates the rock type of the sample: 1, sandstone or siltstone; 2, conglomerate; 3, volcaniclastic

Site No.	Sample No.	Map unit	Mn	Cr	Ni	Co	Cu	Mo	Sn	Pb	Ag	Bi	Zn	Cd
78	K4037RB	(*)	---	---	---	---	200	---	---	---	---	---	---	---
79	K3420RA	(*)	1,500	---	---	---	200	---	---	---	---	---	140	0.4
79	K3420RD	(*)	1,500	---	70	150	500	---	---	---	1.5	2	---	---
79	K3420RE	Tiu	---	---	---	---	300	---	---	---	---	---	---	---
80	84DT147	Jn	2,000	---	---	50	---	---	---	---	---	---	---	---
80	K3419RC	Tiu	1,500	---	---	---	---	---	---	---	---	---	65	---
81	K1005RA	(*)	---	---	50	---	---	---	---	50	---	---	---	---
82	K1020RA	(*)	---	---	---	---	---	---	---	70	---	---	---	---
83	K1014RA	(*)	---	150	---	---	---	---	---	50	---	---	---	---
84	K1017RA	(*)	---	---	---	---	---	---	---	---	5.0	---	---	---
84	K1017RC	(*)	---	150	50	---	200	7	---	---	0.7	---	---	---
84	K1018RA	(*)	---	---	---	---	---	---	---	---	7.0	---	---	---
85	K1023RB	(*)	---	---	---	---	500	7	---	---	.7	---	---	---
86	K3416RB	Tiu	1,500	---	---	---	500	---	---	30	---	---	250	.6
87	85RJ175A	Jn	---	---	---	---	700	20	---	---	.5	---	---	---
87	85RJ175B	Jn	---	---	---	---	---	10	---	---	---	---	---	---
87	86RJ124A	Tiu	---	---	---	---	2,000	2,000	---	---	---	---	---	---
87	86RJ124D	Tiu	---	---	---	---	700	150	---	---	---	---	---	---
87	86RJ124E	Jn	---	---	---	---	1,000	---	---	---	.5	---	---	---
87	86RJ124F	Tiu	3,000	---	---	500	20,000	100	---	200	50	---	1,900	10
87	K3413RA	(*)	---	---	---	---	300	20	---	---	---	3	---	---
87	K3414RA	(*)	---	---	---	---	---	---	---	---	---	---	---	---
87	K3414RC	Tiu	---	200	100	70	300	---	---	---	---	---	60	---
87	K3414RD	(*)	---	---	70	150	10,000	---	---	---	10	2	70	.2
87	K3414RG	Tiu	---	---	50	---	10,000	---	---	---	3.0	---	---	---
87	K3414RH	(*)	---	---	---	---	700	100	---	---	---	---	---	---
87	K3414RI	Tiu	---	---	---	---	300	>2,000	100	---	---	---	---	---
87	K3414RN	Tiu	---	---	70	100	5,000	15	---	---	5.0	2	200	.3
87	K3415RB	Jn	2,000	---	---	70	700	---	---	---	3.0	3	---	---
87	K3417RA	Tiu	---	200	50	---	---	---	---	---	---	---	---	---
88	K1008RA	(*)	---	---	---	---	---	---	---	70	.7	---	---	---
89	K3058RB	Jn	---	150	50	---	---	---	---	50	---	---	---	---
90	K2058RA	(*)	---	---	---	---	---	7	---	---	---	---	---	---
91	85YB219	Td	1,500	---	---	---	---	---	---	---	---	---	---	---
91	K4019RB	Jn	1,500	---	---	---	---	---	---	---	---	---	---	---
91	K4020RB	Jn	---	---	---	---	200	15	---	200	1.5	---	1,500	20
91	K4021RA	Jn	2,000	200	---	---	---	---	---	50	---	---	---	---
91	K4022RA	Jn	---	150	50	---	---	---	---	50	---	---	---	---
91	K4023RA	Jn	---	150	70	---	---	---	---	50	---	---	---	---
91	K4024RA	Jn	---	150	70	---	---	10	---	100	---	---	---	---
91	K4025RB	Jn	---	---	---	---	---	10	---	50	---	---	---	---
91	K4027RA	Tiu	---	---	70	---	---	---	---	30	---	---	500	---
91	K4028RA	Jn	1,500	---	---	---	---	---	---	---	---	---	---	---
91	K4029RA	Tiu	>5,000	---	---	---	---	---	---	---	---	---	---	---
91	K4031RA	Jn	---	---	---	---	150	---	---	50	---	---	---	---
92	K2009RA	Tiu	1,500	---	---	---	---	20	---	700	---	---	300	---
92	K2009RE	Jn	---	---	50	---	---	---	10	---	1.5	---	---	---
92	K3056RC	Tiu	1,500	---	---	---	---	---	---	100	---	---	300	---

rock or tuff; 4, lava flow; 5, sill or dike; 6, plutonic rock; 7, metamorphosed rock/protolith; 8, limestone; and (*), float sample. Mineralogy is generally based upon field identifications of hand specimens: py, pyrite; cpy, chalcopyrite; asp, arsenopyrite; spl, sphalerite; gn, galena; mly, molybdenite; qtz, quartz; Fe ox., iron oxides; dissem., disseminated mineral grains in sample. Dashes (---), concentrations not anomalous or feature not observed; all concentrations expressed in parts per million (ppm); >, concentration is greater than reported value]

Site No.	Sample No.	Map unit	Au	As	Sb	Hg	Alt	Int	Lith	Frac	Vein	Mineralogy and mode of occurrence
78	K4037RB	(*)	---	---	---	---	X	X	6	X	X	Py vein along fracture
79	K3420RA	(*)	---	---	---	---	X	X	1	X	X	Py vein along fracture
79	K3420RD	(*)	0.05	50	---	---	X	X	6	---	---	Dissem. py
79	K3420RE	Tiu	---	---	---	---	---	X	6	---	---	Dissem. py
80	84DT147	Jn	---	---	---	---	---	---	---	---	---	
80	K3419RC	Tiu	---	---	---	---	---	X	5	---	---	Dissem. py
81	K1005RA	(*)	---	---	---	---	---	---	1	---	---	Oxidized dissem. py
82	K1020RA	(*)	---	700	---	---	---	---	1	---	---	Veinlets of qtz with py
83	K1014RA	(*)	---	---	---	---	---	---	1	---	---	Oxidized dissem. py
84	K1017RA	(*)	---	---	---	---	X	X	6	---	---	Oxidized dissem. py
84	K1017RC	(*)	---	---	---	---	---	X	1	X	X	Py in qtz veinlets
84	K1018RA	(*)	---	---	---	---	---	---	1	---	---	Dissem. py
85	K1023RB	(*)	---	---	---	---	X	X	6	---	---	Oxidized dissem. py
86	K3416RB	Tiu	.15	---	---	---	---	X	6	---	X	Py veins along margin of stock.
87	85RJ175A	Jn	---	---	---	---	---	X	5	X	X	Py, cpy in qtz veins.
87	85RJ175B	Jn	---	---	---	---	X	X	1	X	X	
87	86RJ124A	Tiu	---	---	---	---	---	X	6	---	X	Py, cpy, mly in qtz veins.
87	86RJ124D	Tiu	---	---	---	---	X	X	6	X	---	Qtz, py veins.
87	86RJ124E	Jn	---	---	---	---	---	X	7/1	---	---	Py, chrysocolla in qtz vein.
87	86RJ124F	Tiu	---	50	50	0.24	---	X	6	---	X	
87	K3413RA	(*)	.15	40	4	---	X	X	6	---	X	Fe ox.-stained qtz veins with py.
87	K3414RA	(*)	.15	---	---	---	X	X	6	X	---	Dissem. py; py along fractures.
87	K3414RC	Tiu	---	---	---	---	X	X	6	---	---	Dissem. py.
87	K3414RD	(*)	.70	---	---	---	X	X	1	---	---	Pyritic breccia.
87	K3414RG	Tiu	.4	10	---	---	X	X	6	---	---	Dissem. py; py and cpy in stockwork.
87	K3414RH	(*)	.15	20	---	---	X	X	1	---	---	Hematitic breccia.
87	K3414RI	Tiu	.1	---	---	---	X	X	6	---	---	3-mm-wide mly veinlets in stockwork.
87	K3414RN	Tiu	---	---	---	---	---	X	6	X	X	Py in qtz veins.
87	K3415RB	Jn	.1	20	---	---	X	X	1	---	---	Dissem. py.
87	K3417RA	Tiu	.05	20	---	---	---	X	6	---	---	Dissem. py.
88	K1008RA	(*)	---	---	---	---	---	X	1	---	---	Py in breccia.
89	K3058RB	Jn	---	---	---	---	---	X	1	---	---	Dissem. py in hornfels.
90	K2058RA	(*)	---	---	---	---	---	X	5	---	---	Dissem. py.
91	85YB219	Td	---	---	---	---	---	X	5	---	---	
91	K4019RB	Jn	---	---	---	---	X	X	1	---	X	Dissem. py, minor qtz veins.
91	K4020RB	Jn	---	---	---	---	---	X	1	---	---	Dissem. py.
91	K4021RA	Jn	---	---	---	---	---	X	1	---	---	Dissem. py.
91	K4022RA	Jn	---	---	---	---	---	X	1	---	---	Dissem. py.
91	K4023RA	Jn	---	---	---	---	---	X	1	---	---	Dissem. py.
91	K4024RA	Jn	---	---	---	---	---	X	1	---	---	Dissem. py.
91	K4025RB	Jn	---	---	---	---	---	X	1	---	---	Dissem. py.
91	K4027RA	Tiu	---	---	---	---	X	X	5	---	X	Fe ox-stained vuggy qtz veins; py.
91	K4028RA	Jn	---	---	---	---	---	X	7	---	X	Hematitic breccia.
91	K4029RA	Tiu	---	---	---	---	---	X	5	---	X	Hematite, pyrolucite, py in vuggy qtz veins.
91	K4031RA	Jn	---	---	---	---	X	X	1	---	---	Oxidized dissem. py.
92	K2009RA	Tiu	---	---	---	---	X	X	5	---	X	Py, calcite, tourmaline in 2-cm-wide qtz veins.
92	K2009RE	Jn	---	---	---	---	X	X	1	---	X	Brecciated Jn with py and qtz matrix
92	K3056RC	Tiu	---	---	---	---	---	X	5	---	X	Hematitic breccia.

Table 14. Geochemical and geologic data for selected samples from the Butress Range–Ikagluik Creek area—Continued.

Site No.	Sample No.	Map unit	Mn	Cr	Ni	Co	Cu	Mo	Sn	Pb	Ag	Bi	Zn	Cd
92	K3057RA	Tiu	---	---	---	---	---	---	---	50	---	---	---	---
92	K3057RB	Jn	---	150	50	---	---	---	---	50	---	---	500	---
93	86RJ128A	Jn	---	---	---	---	200	5	---	---	---	---	---	---
93	86RJ128B	Td	2,000	---	---	---	---	---	---	---	---	---	850	2.0
93	86RJ128C	Jn	---	---	---	---	---	---	---	---	---	---	420	1.0
93	K2055RB	Jn	---	---	---	---	---	---	---	50	---	---	---	---
93	K3626RB	Jn	2,000	---	50	100	200	---	---	---	---	---	100	.3
94	K4011RA	(*)	---	---	---	---	---	30	---	---	---	---	---	---
94	K4011RC	Td	---	---	50	70	500	---	---	---	1.0	---	---	---
95	84JM120	Jn			70	50	100	---	---	---	---	---	---	---
96	84JM135	Jn	---	---	---	---	---	---	---	70	---	---	---	---
97	K1040RC	(*)	---	---	---	---	---	---	---	200	2.0	---	---	---
98	K3411RD	Jn	3,000	---	---	---	---	---	---	---	---	---	100	---
99	K3031RC	(*)	---	---	100	---	---	10	---	30	---	---	---	---
100	86DT264	Kk	---	300	---	---	---	---	---	---	---	---	---	---
100	K3410RA	Jn	3,000	---	---	---	---	---	20	---	---	6	---	---
100	K3410RB	Td	2,000	200	100	---	500	---	---	50	---	---	120	---
100	K3410RC	Td	2,000	---	50	100	>20,000	---	---	70	200	130	500	1.6
100	K3410RF	Jn	2,000	---	---	---	>20,000	---	---	---	100	---	500	.9
100	K3410RG	Jn	1,500	---	---	---	200	---	---	---	---	---	210	.4
100	K3410RJ	Jn	5,000	---	150	70	10,000	500	---	---	---	---	200	---
100	K3410RK	Jn	2,000	---	70	150	500	---	---	---	---	5	95	---
101	86RJ125A	Jn	---	---	---	100	2,000	---	---	---	---	---	---	.2
101	86RJ125B	Jn	---	---	---	---	500	---	---	---	1.0	---	---	---
101	86RJ125C	Tiu	2,000	---	---	---	5,000	---	---	---	5.0	---	---	---
101	86RJ125F	Tiu	---	---	---	---	5,000	---	---	---	5.0	---	---	---
101	86RJ125G	Tiu	2,000	---	---	200	>20,000	---	---	---	20	---	---	.9
101	K3409RA	Jn	3,000	---	---	---	10,000	---	---	100	2.0	---	1,500	7.0
101	K3409RB	Jn	---	---	---	---	300	---	---	200	50	330	310	2.0
101	K3409RD	Jn	---	---	---	---	500	15	---	50	---	---	830	3.2
102	K2531RA	(*)	---	---	50	---	---	---	---	50	---	---	---	---
102	K3412RB	Tiu	---	---	---	---	---	---	---	50	---	---	260	.6
102	K3412RC	Jn	---	---	---	---	300	---	---	---	---	---	---	---
103	86RJ126A	Tiu	---	---	---	---	300	15	---	---	---	---	---	---
103	86RJ126C	Jn	---	---	---	100	300	---	---	---	1.0	---	---	---
103	K3408RD	Tiu	---	---	---	---	---	---	---	700	15	36	460	.4
103	K3408RE	Jn	---	---	---	---	---	7	---	---	---	---	---	---
103	K3408RG	Jn	---	---	50	100	1,000	10	---	---	---	---	85	.5
103	K3408RJ	---	---	---	---	---	---	10	---	---	---	---	---	---
103	K3408RK	Jn	---	---	---	---	---	---	---	700	10	5	5,000	10
103	K3408RL	Tiu	---	---	---	---	---	15	---	5,000	15	31	5,000	13
103	K3408RM	---	1,500	---	50	200	2,000	---	---	---	---	5	---	---
103	K3408RP	---	---	---	---	---	---	10	---	500	150	42	10,000	100
103	K3408RS	---	>5,000	---	---	---	2,000	---	---	>20,000	100	10	>10,000	100
103	K3408RT	Jn	2,000	---	---	100	1,500	---	---	500	2.0	3	260	1.5
103	K3408RU	---	1,500	---	---	---	1,000	---	---	150	3.0	5	>10,000	54
104	K3147RA	Tiu	---	200	50	---	150	20	---	---	---	---	---	---
104	K3147RI	Jn	---	150	---	---	150	15	---	30	---	---	---	---
105	86JM213	Jn	---	200	70	50	150	---	---	---	---	---	---	---
106	K3422RE	(*)	2,000	---	---	---	---	50	---	---	2.0	---	---	---
107	K3423RA	Jn	1,500	150	50	---	---	---	---	---	---	---	100	---
107	K3423RI	Tiu	1,500	150	50	---	500	---	20	---	1.0	4	---	---
108	K2554RB	(*)	---	---	---	---	---	10	---	---	---	---	---	---

Site No.	Sample No.	Map unit	Au	As	Sb	Hg	Alt	Int	Lith	Frac	Vein	Mineralogy and mode of occurrence
92	K3057RA	Tiu	---	---	---	---	---	X	5	---	---	Dissem. py.
92	K3057RB	Jn	---	---	---	---	---	X	1	---	---	Dissem. py.
93	86RJ128A	Jn	---	---	---	---	---	X	7/1	---	X	Py vein.
93	86RJ128B	Td	---	---	---	---	---	X	5	---	---	Dissem. py.
93	86RJ128C	Jn	---	---	---	---	---	X	7/1	---	---	Dissem. py.
93	K2055RB	Jn	---	---	---	---	X	X	7/1	---	---	Dissem. py.
93	K3626RB	Jn	---	---	---	---	X	X	7/1	---	---	Dissem. py; epidote.
94	K4011RA	(*)	---	---	---	---	X	---	4	---	X	Py in qtz veins 1 cm wide.
94	K4011RC	Td	---	---	---	---	---	---	5	---	---	Dissem. py.
95	84JM120	Jn	---	---	---	---	---	---	---	---	---	
96	84JM135	Jn	---	---	---	---	---	---	1	---	---	
97	K1040RC	(*)	.1	---	---	---	X	X	5	---	X	Py in vuggy qtz veins.
98	K3411RD	Jn	.1	10	---	---	X	X	1	X	X	Dissem. py; py in qtz veinlets.
99	K3031RC	(*)	---	---	---	---	X	X	1	---	---	Dissem. py.
100	86DT264	Kk	---	40	---	---	---	---	7/1	---	---	
100	K3410RA	Jn	---	140	---	---	X	X	1	---	X	Fe ox. matrix in breccia.
100	K3410RB	Td	---	50	---	---	---	X	5	---	X	Dissem. py, epidote in qtz veins.
100	K3410RC	Td	.15	10	6	---	X	X	5	---	X	Py, cpy in 1 cm wide qtz vein, chrysocolla.
100	K3410RF	Jn	.05	---	2	---	X	X	---	---	X	Py, cpy in malachite-stained qtz veins.
100	K3410RG	Jn	---	10	4	---	X	X	1	---	X	Py in qtz veins.
100	K3410RJ	Jn	---	20	---	---	X	X	1	---	X	Malachite-stained qtz vein.
100	K3410RK	Jn	---	---	---	---	X	X	1	---	---	Dissem. py.
101	86RJ125A	Jn	---	---	---	---	---	X	7/1	X	X	Chrysocolla in qtz vein.
101	86RJ125B	Jn	---	---	---	---	---	X	7/1	X	X	Py vein.
101	86RJ125C	Tiu	---	---	---	---	X	X	6	X	X	Py vein.
101	86RJ125F	Tiu	---	---	---	---	---	X	6	X		
101	86RJ125G	Tiu	---	---	---	---	X	X	6	---	X	Py vein.
101	K3409RA	Jn	---	10	---	---	X	X	7/1	---	X	Malachite-stained qtz veins.
101	K3409RB	Jn	.1	300	8	---	X	X	---	---	---	Hematitic matrix breccia.
101	K3409RD	Jn	---	10	---	---	X	X	5/6	---	X	Epidote, malachite, py in qtz veins.
102	K2531RA	(*)	---	---	---	---	---	X	1	---	X	Py in qtz veins.
102	K3412RB	Tiu	.05	---	---	---	X	X	5	---	X	Py and qtz in breccia.
102	K3412RC	Jn	.05	---	---	---	X	X	1	X	---	Py veins along fractures.
103	86RJ126A	Tiu	---	---	---	---	---	X	6	X	X	Py vein.
103	86RJ126C	Jn	---	70	---	---	---	X	7/1	---	X	Py vein.
103	K3408RD	Tiu	.2	---	---	---	---	X	6	---	X	Hematite, gn, py in qtz vein.
103	K3408RE	Jn	.05	---	---	---	X	X	1	---	---	Py matrix in breccia.
103	K3408RG	Jn	.05	---	---	---	X	X	1	---	---	Dissem. py.
103	K3408RJ	---	---	---	---	---	X	X	---	---	---	Hematitic breccia.
103	K3408RK	Jn	.1	50	2	---	X	X	1	---	X	Spl, py in qtz vein.
103	K3408RL	Tiu	.25	120	4	---	X	X	6	---	X	Gn, spl in qtz vein.
103	K3408RM	---	.05	---	---	---	X	X	---	---	X	Py in qtz vein; epidote.
103	K3408RP	---	.35	---	8	---	X	X	---	---	X	Spl in qtz vein.
103	K3408RS	---	.7	30	2	---	---	X	---	---	X	Gn, spl in open vugs in qtz vein.
103	K3408RT	Jn	---	---	---	---	X	X	7/1	---	X	Py in qtz veins.
103	K3408RU	---	.05	20	---	---	X	X	---	---	X	Py in qtz veins.
104	K3147RA	Tiu	---	---	---	---	X	X	6	---	---	Dissem. py.
104	K3147RI	Jn	---	---	---	---	X	X	1	---	---	Dissem. py in silicified rock.
105	86JM213	Jn	---	---	---	---	---	---	---	---	---	
106	K3422RE	(*)	.15	230	24	---	X	X	5/6	---	X	Oxidized py in qtz vein; epidote.
107	K3423RA	Jn	---	10	---	---	---	X	1	---	---	Dissem. py.
107	K3423RI	Tiu	.15	10	---	---	X	X	5	---	---	Dissem. py.
108	K2554RB	(*)	---	---	---	---	X	X	---	---	X	Py in qtz veins.

Table 14. Geochemical and geologic data for selected samples from the Butress Range–Ikagluik Creek area—Continued.

Site No.	Sample No.	Map unit	Mn	Cr	Ni	Co	Cu	Mo	Sn	Pb	Ag	Bi	Zn	Cd
108	K3150RB	Tiu	---	300	100	---	---	---	---	50	---	---	---	---
108	K3150RI	Jn	---	---	---	---	300	10	---	30	1.0	---	---	---
108	K3151RD	Tiu	---	150	---	---	300	50	---	70	2.0	---	---	---
108	K4004RB	(*)	---	150	---	---	---	10	---	---	---	---	---	---
109	K1045RA	(*)	1,500	200	50	---	150	---	---	300	1.0	---	---	---
109	K3153RD	Tiu	---	---	---	---	---	10	10	---	---	---	---	---
110	K1051RA	(*)	---	---	---	---	---	15	---	100	---	---	---	---
111	K4003RA	(*)	---	---	---	---	150	10	20	---	.7	---	---	---
112	86JM214A	Kh	---	---	---	---	150	---	---	---	---	---	---	---
112	86JM214B	Td	---	500	---	---	---	---	---	---	---	---	---	---
113	86YB333	Qac	---	---	---	---	---	---	---	---	1.0	---	---	---
113	K1049RA	Qac	---	---	---	---	---	---	---	---	---	---	300	---
114	K0198RA	(*)	---	---	---	50	---	---	---	50	---	---	160	.5
115	K0282RD	(*)	---	---	---	---	---	15	10	50	---	9	---	---
115	K0282RG	Qac	---	150	50	---	150	---	---	---	---	1	---	---
116	84EM090B	Qac	---	---	---	---	---	---	---	50	---	---	---	---
117	K2616RB	(*)	---	---	---	---	---	---	---	50	---	---	---	---
118	83RJ092	Qac	---	---	---	---	---	---	10	---	---	---	---	---
119	84EM091B	Qad	---	---	---	---	---	10	---	70	---	5	---	---
Novarupta:														
120	K3059RA	Qap	---	---	---	50	100	---	---	70	---	500	---	---
120	K3059RC	Qap	---	---	---	---	100	15	20	1,500	---	200	---	---
120	K3060RD	Qap	---	---	---	---	---	10	---	50	---	50	---	---
120	K3060RE	Qap	---	---	---	---	---	---	10	100	---	20	---	---
120	K3060RF	Qap	---	---	---	---	---	100	---	50	---	20	---	---
120	K3061RC	Qap	---	---	---	---	---	---	---	70	---	50	---	---
120	K3061RD	Qap	---	---	---	---	---	---	---	50	---	20	---	---
120	K4033RA	Qad	---	---	---	---	---	10	---	50	---	---	---	---

MOUNT KATOLINAT SUBAREA

The geochemical data for the SS samples from the Mount Katolinat subarea (T. 19–20 S., R. 37–38 W.) indicate only scattered lead anomalies in two drainage basins. However, the data for the NMHMC samples indicate anomalous concentrations of Au, Ag, W, As, and Sn in several of the drainage basins sampled (Church and Arbogast, 1989). Gold, galena, and scheelite were identified in the NMHMC samples from two drainage basins, and sphalerite and chalcopyrite(?) were identified in NMHMC samples from one drainage basin (Church and Bennett, 1989). Followup sampling at two sites on Mount Katolinat (79–80; geochemical data given in table 14), identified areas where the Naknek Formation was metamorphosed by dikes and a small pluton. Samples of fine-grained plutonic rock collected at site 79 showed evidence of weak propylitic alteration and commonly contained anomalous concentrations of copper and manganese. Anomalous concentrations of Zn, Co, Ni, Ag, Au, Bi, Cd, or As were also found in rock samples from Mount Katolinat (pl. 2). Small veins of pyrite were observed in hornfels derived from the Naknek Formation; disseminated pyrite was observed in the intrusive rocks. We interpret the geologic data to indicate small pyritic veins and disseminated pyrite confined to the contact-metamorphic zones adjacent to the dikes and plutons at Mount Katolinat.

BUTTRESS RANGE SUBAREA

The SS samples collected from the Buttress Range subarea (T. 21–23 S., R. 37–38 W.) commonly contained anomalous concentrations of Cu, Mo, Zn, Co, and Pb, and, less commonly, As, Cd, Bi, or Sn (Church, Bailey, and Riehle, 1989; Church and Motooka, 1989). The NMHMC samples also contained anomalous concentrations of Au, Ag, W, Ba, or Sb (Church and Arbogast, 1989). The minerals pyrite, chalcopyrite, scheelite, wulfenite, sphalerite, galena, cinnabar, arsenopyrite, and barite were identified in the NMHMC samples (Church and Bennett, 1989). Rock samples from sites 81–86 and 88–91 (pl. 2; geochemical data given in table 14) commonly contained anomalous concentrations of Pb, Zn, Mn, Ni, Mo, Cu, Ag, and Cr, whereas anomalous concentrations of Cd, Co, or Sn were less common. Followup

Site No.	Sample No.	Map unit	Au	As	Sb	Hg	Alt	Int	Lith	Frac	Vein	Mineralogy and mode of occurrence
108	K3150RB	Tiu	---	---	---	---	---	X	6	---	---	Dissem. py.
108	K3150RI	Jn	---	---	---	---	X	X	1	---	X	Oxidized dissem. py in qtz veinlets; malachite.
108	K3151RD	Tiu	---	---	---	---	X	X	6	---	---	Dissem. py.
108	K4004RB	(*)	---	---	---	---	---	---	1	---	X	Dissem. py; py in qtz veinlets.
109	K1045RA	(*)	---	---	---	---	X	X	1	---	X	Py in vuggy qtz veins 1 cm wide.
109	K3153RD	Tiu	---	---	---	---	X	X	4	---	---	Dissem. py and vuggy qtz.
110	K1051RA	(*)	---	---	---	---	X	X	5	---	X	Fe-ox.-stained breccia.
111	K4003RA	(*)	---	---	---	---	X	X	5	---	---	Dissem. py.
112	86JM214A	Kh	---	30	---	---	---	---	1	---	---	
112	86JM214B	Td	---	---	---	---	---	X	5	---	---	
113	86YB333	Qac	---	---	---	---	---	---	4	---	---	
113	K1049RA	Qac	---	1,000	---	---	X	X	4	X	X	Fe ox.-rich hot springs sinter.
114	K0198RA	(*)	---	---	---	---	---	---	---	---	---	Dissem. py in siliceous hot-springs sinter.
115	K0282RD	(*)	---	20	---	.3	X	X	4	---	---	Bleached, silicified volcanic rock.
115	K0282RG	Qac	---	10	---	.44	---	X	4	---	---	Fe ox.-stained breccia adjacent to dike.
116	84EM090B	Qac	---	---	---	---	---	---	4	---	---	
117	K2616RB	(*)	---	---	---	---	X	X	4	---	---	Oxidized volcanic breccia.
118	83RJ092	Qac	---	---	---	---	---	---	4	---	---	
119	84EM091B	Qad	---	---	---	---	---	---	4	---	---	
Novarupta:												
120	K3059RA	Qap	---	---	---	---	X	X	3	---	---	Hematite-rich siliceous sinter.
120	K3059RC	Qap	---	200	---	---	X	X	3	---	---	Hematite-rich siliceous sinter.
120	K3060RD	Qap	---	---	---	---	X	X	3	---	---	Hematite-rich siliceous sinter.
120	K3060RE	Qap	---	---	---	---	X	X	3	---	---	Hematite-rich siliceous sinter.
120	K3060RF	Qap	---	500	---	---	X	X	3	---	---	Hematite-rich siliceous sinter.
120	K3061RC	Qap	---	700	---	---	X	X	3	---	---	Hematite-rich siliceous sinter.
120	K3061RD	Qap	---	300	---	---	X	X	3	---	---	Hematite-rich siliceous sinter.
120	K4033RA	Qad	---	---	---	---	---	X	6	---	---	Dissem. py.

studies at sites 85–86 indicate that the geochemical anomalies shown by the SS and NMHMC data are spatially associated with small dikes and sills that have intruded and metamorphosed Mesozoic sedimentary rocks. Anomalous metal concentrations (site 86: Mn, Cu, Pb, Au, Zn, and Cd; table 14) were determined in samples of pyrite veins from an aphanitic border phase of a pluton. We suggest that the anomalies at other sites discussed above have a similar origin.

At the headwaters of Margot Creek (site 87, pl. 1), a Tertiary(?) pluton intruded and metamorphosed the Naknek Formation. At its outer margins, the stock is surrounded by a zone of propylitic alteration. The intensity of the alteration increases and grades inward to localized areas of potassically altered granodiorite that has a weakly developed stockwork containing thin veins of chalcopyrite and molybdenite as much as 3 mm in width. Potassium feldspar selvages are found along the margins of some molybdenite-bearing quartz veins in the central zone of potassic alteration. Exposures of the pluton crop out only in the uppermost part of the stream valley, and the exposed area of stockwork does not exceed more than a few hundred square meters. Samples from site 87 commonly contained anomalous concentrations of Cu, Mo, Au, Ag, and As, and, less commonly, Ni, Co, Zn, Bi, Cd, Sb, Mn, Cr, Pb, or Sn (pls. 1 and 2). The geologic and geochemical data observed here are best explained as an undiscovered porphyry Cu-Mo deposit.

During the geochemical reconnaissance work in the upper part of Windy Creek, we found anomalous concentrations of copper, cobalt, lead, and zinc in the SS and NMHMC samples (Church, Bailey, and Riehle, 1989; Church and Motooka, 1989; Church and Arbogast, 1989). We also sampled pyrite-bearing float at sites 88 and 90 that contained anomalous concentrations of molybdenum, lead, and silver. During followup studies of this area, we sampled hornfels derived from the Naknek Formation that contained disseminated pyrite and thin (1–2 mm thick) quartz veins. At site 92, we sampled sulfides, mainly pyrite, that were present as pyrite-rich veins and as disseminated grains in quartz-calcite veins and as matrix material in breccia fragments in talus. Exposed in the cliff face above site 92 is a large breccia body, measuring 10 m or more in thickness and 30 m or more in length, composed of brecciated rock fragments of the Naknek Formation and intrusive rocks in a pyritic matrix.

The fine-grained pyritic matrix forms as much as 30 percent of the breccia; only lead, silver, and zinc were present at anomalous concentrations in the samples we collected from talus (pl. 2; table 14). Tourmaline was also observed. Quartz veins and breccias of this type are commonly associated with porphyry Cu-Mo deposits (Cox, 1986d).

IKAGLUIK CREEK SUBAREA

The suite of geochemical anomalies indicated by the SS and NMHMC samples from the Ikagluik Creek subarea (T. 19–21 S., R. 33–35 W.) does not differ significantly from those from the Buttress Range subarea; only the frequency of occurrence is different (Church, Bailey, and Riehle, 1989; Church and Motooka, 1989; Church and Arbogast, 1989). In the SS samples anomalous concentrations of Pb, Zn, Cu, Co, and As were common, whereas Mo, Ag, Ni, Bi, or Cd were less commonly anomalous. In addition to the suite given above, barium, gold, or tungsten were also present at anomalous concentrations in the NMHMC samples from a few drainage basins. Pyrite was ubiquitous, galena, chalcopyrite, and sphalerite were common, and arsenopyrite, wulfenite, scheelite, and gold were identified in a few of the NMHMC samples (Church and Bennett, 1989).

Followup sampling was done at many localities in this area (sites 97–112; geochemical data given in table 14) in an attempt to understand the source of the geochemical anomalies. On both sides of Ikagluik Creek near its headwaters a moderately to strongly porphyritic tonalite to quartz diorite pluton intrudes Mesozoic sedimentary rocks, primarily the Naknek Formation. There are numerous small outlying stocks and sills in this area. The groundmass of the intrusive rocks is pervasively altered to chlorite and calcite and contains minor epidote. The veins, fractures, and minor faults in these rocks are nearly vertical, and the wallrocks are locally silicified or altered to propylitic assemblages. Most of the mineralized rock samples from the Ikagluik Creek subarea, excluding site 103, contained anomalous concentrations of Cu, Ag, Pb, Mn, As, Mo, Zn, Cr, Ni, Au, and Cd, and, less commonly, Sb, Bi, Co, or Sn. Multiple generations of quartz veins containing pyrite, molybdenite, and chryscolla, together with epidote and chlorite, are common. An Fe-Mn-oxide breccia containing fragments of siltstone was also sampled (site 100). Quartz veins in the breccia contain epidote, pyrite, and chalcopyrite. We observed similar quartz veins and breccia material at many of the other sites within this subarea. Quartz-vein samples from site 103, largely collected from float, commonly contained anomalous concentrations of Au, Ag, Zn, Bi, Cd, Pb, Cu, and Mo, whereas anomalous concentrations of As, Sb, Co, Ni, or Cr were less common. Pyrite, sphalerite, and galena were the common ore minerals identified in these vein samples. We interpret these data to be indicative of polymetallic veins; this deposit model (Cox, 1986f) best fits the geologic and geochemical data from this subarea (pl. 2). However, a concealed porphyry Cu deposit cannot be ruled out, particularly in light of the geologic and geochemical observations in the Margot Creek valley described for the Buttress Range subarea.

QUATERNARY VOLCANIC ROCKS OF THE ALEUTIAN RANGE SUBAREA

On the flanks of the active volcanoes (sites 108, 113–119; data given in table 14), we collected a small suite of altered rock and float samples that contained anomalous concentrations of lead, bismuth, or arsenic. One or two samples also contained anomalous concentrations of Hg, Zn, Mo, Sn, Co, Cu, Ag, or Cd. Followup studies were largely unrewarding because most of the anomalous samples were collected from float in streams at the terminus of alpine glaciers. Our observations made at Mount Mageik, located at the headwaters of Martin Creek (T. 23 S., R. 37 W.), are typical of the active volcanic centers in the Katmai study area: Mount Mageik contains a small, water-filled, steaming crater at its summit. Volcanic rocks exposed along Martin Creek (site 115) are silicified and bleached. They consistently contain 300–500 ppb Hg and as much as 2,900 ppm F. Goldfarb and others (1988) pointed out that this area is favorable for undiscovered precious-metal-bearing hot-springs deposits. Deposits from hot springs were also sampled along the crest of the Aleutian Range at sites 108 and 113 during this study (pl. 3). A precious-metal-bearing hot-springs or epithermal quartz-vein mineral deposit model (model 25b; Mosier and others, 1986) best describes the geologic and geochemical data for sites 108 and 113–119 (table 14).

Samples of the small fumarolic vents exposed at Novarupta (T. 22 S., R. 36 W.; site 120, table 14) were analyzed to evaluate the metal anomalies associated with the rootless fumaroles that formed following the eruption of 1912 (Fenner, 1920). Keith (1984) reported on zones of argillic alteration in the fumarole vents and observed alunite in active hot springs at Novarupta in 1982. Anomalous concentrations of Pb, Bi, Tl, Sb, and As were common in these samples, whereas Cu, Mo, Sn, or Co were less common, and Au and Ag were detected in trace amounts (Keith, 1984). Hydrothermal activity at Novarupta represented a single, short-lived geologic event resulting in vent areas of small areal extent, each generally only a few meters in any one dimension. As such, they may constitute a feature of general academic interest rather than one of economic significance. Nevertheless, the metal zonation, mineralogy, and alteration suites observed in the fumaroles at Novarupta, as well as at fumaroles sampled in the lower part of the Valley of Ten Thousand Smokes, are instructive in the study of vapor-transport processes (Keith, 1991). Many of these geologic and geochemical features have been reported as guides to gold and silver mineralization associated with volcanic domes in the Andes (Cunningham and Ericksen, 1991). The Novarupta dome area is an ideal study area for a single-event, gold-bearing epithermal quartz-alunite system (mineral deposit model 25e, Berger, 1986).

In summary, the Buttress Range–Ikagluik Creek area may contain both an undiscovered porphyry Cu-Mo deposit and one or more undiscovered polymetallic-vein deposits. The geologic and geochemical data also indicate additional areas, discussed in detail above, that have potential for undiscovered polymetallic-vein, precious-metal-bearing hot springs or epithermal quartz-alunite veins.

FOURPEAKED MOUNTAIN AREA

The Fourpeaked Mountain area (T. 14–18 S., R. 24–29 W.) is underlain by Mesozoic sandstone and siltstone (Jn, Kh, Kp, Kk) and by Tertiary sandstone, conglomerate, and tuff (Tc, Th). The rocks of the area are broadly folded and pervasively fractured. The area is an alpine terrain that is generally free of snow and ice below an elevation of 1,000 m during the summer field season. Because glacial drift is thin, exposures are good. A late Tertiary pluton underlies Fourpeaked Mountain (unit Ti, ages are generally 4–8 Ma, Shew and Lanphere, 1992). Sills, dikes, and small plugs also crop out in the sedimentary rocks beyond the margins of the pluton. The main pluton is tonalite to granodiorite and is locally porphyritic, having a fine- to medium-grained groundmass. Areas of hornfels are locally prominent adjacent to intrusive rocks, and thin quartz veins and red-brown color anomalies are present throughout the Fourpeaked Mountain area. Northwest-trending fractures and minor faults cut both sedimentary and intrusive rocks, but they are more prominent in the sedimentary rocks. The Tertiary sedimentary rocks are plastically deformed locally at the margins of sills. Fourpeaked Volcano tops Fourpeaked Mountain and forms the prominent high on Cape Douglas (pl. 1).

The SS and NMHMC geochemical data define a broad zone of base-metal anomalies (pl. 2) in the southern part of the area (Church and Arbogast, 1989; Church, Bailey, and Riehle, 1989; Church and Motooka, 1989). Many SS samples contained anomalous concentrations of Cu, Co, Pb, Zn, and As. Anomalous concentrations of silver, molybdenum, nickel, or boron were present in some drainage basins. This geochemical suite differs from that associated with the Tertiary intrusive rocks (Tiu) in the Buttress Range and Ikagluik Creek subareas as well as the suite from the Kulik Lake area (Tgd, Tqd) in that anomalous concentrations of arsenic are ubiquitous in the Fourpeaked Mountain area. Pyrite was abundant in NMHMC samples from these drainage basins; chalcopyrite and arsenopyrite were common. Galena, sphalerite, and barite were less commonly observed (Church and Bennett, 1989).

The most prominent group of geochemical anomalies is in the southwestern part of the Fourpeaked Mountain area, northeast of the mouth of the Big River (pl. 1). In addition to the base-metal anomalies described above, the SS and NMHMC samples from these drainage basins also contained anomalous concentrations of molybdenum, boron, or tungsten. Pyrite was ubiquitous; chalcopyrite, wulfenite, scheelite, and arsenopyrite were common; and sphalerite, barite, and gold were less common in the NMHMC samples.

On the west and northwest side of the Fourpeaked Mountain area, a large As-Sb-Au-Ag anomaly was defined by the SS and NMHMC geochemical data (pl. 3). Within these drainage basins pyrite and chalcopyrite are common, and arsenopyrite, galena, and barite were identified in some NMHMC samples. Gold was observed in the NMHMC sample collected from the drainage basin containing sample locality 135 (pl. 3).

Rock and float samples from the Fourpeaked Mountain area that contained anomalous concentrations of metals are summarized in table 15 (sites 121–168). Most of the rock samples listed were collected in drainage basins containing base-metal anomalies (sites 141–156, 159, 160, 163–167, 173, 174, 176; sites shown on pl. 2). Samples, generally from either dikes or plutonic rocks but also from hornfels, commonly contained anomalous concentrations of As, Zn, Pb, Sb, Ag, and Bi; less commonly, they contained anomalous concentrations of Mn, Cd, Co, Cu, or Mo, and a few contained anomalous concentrations of Ni, Cr, Au, or Hg. Samples generally were altered to epidote and chlorite assemblages typical of a propylitic alteration suite. Pyrite, chalcopyrite, and arsenopyrite are common in quartz veins and along fractures. In the northwestern part of the Fourpeaked Mountain area (T. 14–15 S., R. 26–28 W.) similar bedrock geochemical anomalies were also observed (sites 132–134, 136–138). Quartz veins containing pyrite were observed at many of these localities. A polymetallic-vein mineral deposit model best accounts for these geologic and geochemical observations.

Southwest of Fourpeaked Mountain, samples of hornfels and hydrothermally altered Mesozoic and Tertiary sedimentary rocks and Tertiary intrusive rocks were collected from sites within drainage basins where the reconnaissance geochemical data indicated a potential for undiscovered porphyry Cu-Mo deposits (T. 16–18 S., R. 27–28 W.; pl. 1). Rocks from these sites (138–139, 157–158, 161–162, 168–172, 175) are closely associated with intrusive plugs, dikes, or sills. Most of the mineralized rock samples contained anomalous concentrations of As, Zn, Cu, Mo, Sb, Ni, Co, and Mn, and, less commonly, of Cr, Ag, Au, Bi, Pb, Cd, or Sn. Zones of argillic and sericitic alteration are commonly associated with abundant quartz veins. Zones of propylitic alteration are associated with the Tertiary intrusive rocks as indicated by the higher frequency of chromium and nickel anomalies in igneous samples. Quartz veins are common in open spaces; fractures in the sedimentary rocks appear to be radial to intrusive centers. Locally, iron-stained zones are found around thin pyrite veins. Exposed in the stream

Table 15. Geochemical and geologic data for selected samples from the Fourpeaked Mountain area, Katmai study area, Alaska.

[Samples listed here have concentrations that exceed the 95th percentile for the respective lithologic units as defined in table 4. "Site No." is the locality shown on plates 1–3; map unit symbols are those on the geologic base map on plates 1–3. An "X" in columns headed "Vein," "Frac," or "Alt" indicates that veins, fracture fill, and (or) hydrothermally altered rock, including color anomalies caused by the oxidation of sulfide minerals, were observed at the sample site; "Int" indicates that the sample is an intrusive rock, or that there is a sill, dike, or pluton exposed nearby. "Lith" indicates the rock type of the sample: 1, sandstone or siltstone; 2, conglomerate; 3, volcaniclastic

Site No.	Sample No.	Map unit	Mn	Cr	Ni	Co	Cu	Mo	Sn	Pb	Ag	Bi	Zn	Cd
121	85JM175	Kk	---	---	---	---	---	---	---	---	1.0	---	---	---
122	K4171RA	(*)	2,000	---	---	70	300	---	---	---	---	---	---	---
123	K4145RA	(*)	2,000	---	---	70	300	---	---	---	---	---	95	---
124	86DT255	Kk	---	---	---	---	---	---	---	---	---	---	---	---
125	85DT213	Jn	---	---	---	---	---	---	---	---	---	---	---	---
126	85DT214	Jn	---	---	---	---	---	---	---	---	---	---	---	0.2
127	86YB313	Td	2,000	---	---	---	200	---	---	---	---	---	---	---
128	86DT256	Jn	---	---	---	---	---	---	---	---	---	---	---	---
129	K4165RA	(*)	---	---	50	---	---	50	---	---	---	---	200	---
130	86DT254	Jn	---	---	---	50	100	---	---	---	---	---	---	---
131	86JM192	Jn	---	---	---	---	---	---	---	---	---	---	---	---
131	86JM193B	Jn	5,000	---	---	---	---	---	---	---	---	---	---	---
132	K4148RA	(*)	---	---	---	---	---	---	---	---	---	---	200	.6
133	K3336RA	(*)	---	---	---	---	---	---	---	---	3.0	---	---	---
134	86JM189	Kk	---	300	---	---	100	---	---	---	---	---	190	---
135	86DT250	Kk	---	---	---	---	---	---	---	---	---	---	---	---
135	86DT251	Kk	---	---	---	---	---	---	---	---	---	---	---	---
136	K4528RA	(*)	---	500	100	100	200	---	---	---	---	1	---	---
137	K3321RA	(*)	1,500	---	50	---	150	---	---	500	1.0	---	730	1.3
138	K4527RB	(*)	---	---	---	---	---	200	---	---	---	---	---	---
139	85DT203	Tc	---	---	---	70	500	---	---	---	---	---	---	---
140	K4131RA	(*)	---	---	---	---	---	---	---	50	1.0	---	250	.7
141	86RJ044A	Td	---	---	---	70	---	---	---	---	---	---	---	---
141	86RJ044B	Tc	---	---	---	---	---	5	---	---	---	---	---	---
142	K4519RA	(*)	---	---	---	---	---	---	---	---	---	---	---	---
143	84RJ148C	Ti	---	---	---	---	---	---	---	---	---	---	---	---
144	84YB079	Ti	---	---	---	---	---	---	---	---	1.0	---	---	---
145	84EM064C	Ti	---	---	---	---	---	---	---	---	0.7	---	100	.5
145	84EM064E	Tc	---	---	---	---	---	---	---	100	.5	---	---	.7
146	K4518RA	(*)	1,500	---	100	70	1,000	---	---	---	---	2	165	---
147	84RJ154D	Tc	2,000	---	---	---	---	---	---	---	---	---	400	1.7
148	84YB080C	Ti	---	---	---	---	---	---	---	70	---	---	---	---
149	84JM113	Tc	---	---	---	---	---	---	---	---	---	---	230	---
150	84DT139	Ti	---	---	---	700	---	---	---	---	.7	---	---	---
150	86RJ049A	Ti	---	---	---	200	---	---	---	---	1.0	---	---	---
150	86RJ049B	Ti	---	300	---	---	---	---	---	---	---	---	95	---
151	K4128RA	(*)	---	---	---	---	---	---	---	100	---	1	---	---
152	86RJ048	Ti	---	---	---	---	---	---	---	200	---	---	---	---
153	K3313RA	(*)	3,000	---	---	---	---	---	---	50	---	4	205	---
154	84DT142	Tc	---	---	---	---	---	---	---	---	---	---	200	1.0
155	84JM072	Ti	---	---	---	---	---	---	---	---	---	---	100	---
156	84JM068B	Tc	---	---	---	---	---	---	---	150	.5	---	420	---
156	84JM069	Tc	---	---	---	---	---	---	---	---	---	---	270	.7
157	K4126RA	(*)	2,000	---	---	150	1,000	100	---	---	5.0	6	145	---
158	86RJ052A	Tc	---	---	---	---	---	---	---	---	---	---	---	---
158	86RJ052C	Tc	3,000	---	---	---	---	---	---	---	---	---	200	---
158	86RJ052D	Tc	---	---	---	---	500	20	---	---	---	---	---	---

rock or tuff; 4, lava flow; 5, sill or dike; 6, plutonic rock; 7, metamorphosed rock/protolith; 8, limestone; and (*), float sample. Mineralogy is generally based upon field identifications of hand specimens: py, pyrite; cpy, chalcopyrite; asp, arsenopyrite; spl, sphalerite; gn, galena; mly, molybdenite; qtz, quartz; Fe ox., iron oxides; dissem., disseminated mineral grains in sample. Dashes (---), concentrations not anomalous or feature not observed; all concentrations expressed in parts per million (ppm); >, concentration is greater than reported value]

Site No.	Sample No.	Map unit	Au	As	Sb	Hg	Alt	Int	Lith	Frac	Vein	Mineralogy and mode of occurrence
121	85JM175	Kk	---	---	---	---	---	---	1	---	---	
122	K4171RA	(*)	---	10	---	---	---	X	1	X	X	Py and Fe ox. in qtz vein.
123	K4145RA	(*)	---	10	---	---	---	X	5	---	---	Dissem. py.
124	86DT255	Kk	---	---	---	0.9	---	---	1	---	---	
125	85DT213	Jn	---	---	---	.38	---	---	1	---	---	
126	85DT214	Jn	---	---	---	.46	---	---	1	---	---	
127	86YB313	Td	---	---	---	---	---	---	5	---	---	
128	86DT256	Jn	---	---	2	1.4	---	---	1	---	---	
129	K4165RA	(*)	---	300	4	---	---	X	1	---	---	Marcasite nodule.
130	86DT254	Jn	---	---	---	---	---	---	1	---	---	
131	86JM192	Jn	---	---	---	.24	---	---	1	---	---	
131	86JM193B	Jn	---	---	---	.30	---	---	1	---	---	
132	K4148RA	(*)	---	---	12	---	X	X	5	---	X	Py in qtz veins.
133	K3336RA	(*)	0.10	120	---	---	X	X	1	---	X	Vuggy qtz and py in breccia.
134	86JM189	Kk	---	---	---	---	---	X	1	X	---	
135	86DT250	Kk	---	---	6	---	---	---	1	---	---	
135	86DT251	Kk	---	---	2	.9	---	---	1	---	---	
136	K4528RA	(*)	---	10	4	---	---	X	5	---	---	Dissem. py.
137	K3321RA	(*)	---	10	---	---	---	X	1	X	X	Py vein along fractures.
138	K4527RB	(*)	---	---	2	---	X	X	4	---	X	Dissem. py.
139	85DT203	Tc	---	120	---	---	X	X	3	---	---	
140	K4131RA	(*)	.50	60	10,000	---	X	X	5	---	---	Py and stibnite in qtz vein.
141	86RJ044A	Td	---	---	---	---	---	---	5	---	---	
141	86RJ044B	Tc	---	40	---	---	---	X	7/1	X	---	
142	K4519RA	(*)	---	180	2	---	X	X	5	---	---	Dissem. py; tourmaline.
143	84RJ148C	Ti	---	---	---	.10	---	---	5	---	---	
144	84YB079	Ti	---	---	---	---	---	---	5	---	X	Qtz veins.
145	84EM064C	Ti	---	100	---	---	---	---	5	---	---	Dissem. py.
145	84EM064E	Tc	---	---	6	---	X	X	7/1	---	---	Dissem. py.
146	K4518RA	(*)	---	10	---	---	---	X	1	---	---	Dissem. py.
147	84RJ154D	Tc	---	---	---	---	---	---	1	---	---	
148	84YB080C	Ti	---	---	---	---	---	---	5	---	---	
149	84JM113	Tc	---	---	---	---	---	X	1	---	---	
150	84DT139	Ti	.60	40	---	---	X	---	5	---	X	
150	86RJ049A	Ti	---	70	---	---	X	X	7/4	---	X	Qtz vein, Fe ox..
150	86RJ049B	Ti	---	---	---	---	X	X	7/4	---	X	Py in veins.
151	K4128RA	(*)	---	10	---	---	X	X	---	---	X	Vuggy qtz vein with py.
152	86RJ048	Ti	---	---	---	---	---	---	5	---	X	Qtz veins.
153	K3313RA	(*)	---	10	2	---	X	X	5	---	---	Dissem. py.
154	84DT142	Tc	---	---	---	---	---	---	1	---	---	
155	84JM072	Ti	---	---	---	---	---	---	5	---	---	
156	84JM068B	Tc	---	---	---	---	---	---	1	---	---	
156	84JM069	Tc	---	---	---	---	---	---	1	---	---	
157	K4126RA	(*)	.10	40	2	---	---	X	4	---	X	Py, chlorite, amethyst in qtz vein.
158	86RJ052A	Tc	---	120	4	---	X	X	7/2	---	---	
158	86RJ052C	Tc	---	---	---	---	---	---	7/1	---	X	Qtz vein.
158	86RJ052D	Tc	---	80	4	---	---	---	7/1	---	X	

Table 15. Geochemical and geologic data for selected samples from the Fourpeaked Mountain area—Continued.

Site No.	Sample No.	Map unit	Mn	Cr	Ni	Co	Cu	Mo	Sn	Pb	Ag	Bi	Zn	Cd
159	K0162RA	(*)	---	---	50	---	---	20	---	---	---	4	---	---
160	K0163RA	(*)	---	---	---	---	---	15	---	70	---	1	85	---
161	K0160RA	(*)	---	---	---	---	---	---	---	50	---	---	---	---
161	K0160RB	(*)	---	---	---	---	200	10	---	70	---	---	---	---
161	K3605RE	Ti	---	---	50	---	150	---	---	50	1.0	---	500	---
162	K0157RB	(*)	---	---	70	---	---	20	---	---	---	8	---	---
163	84RJ141E	Tc	---	---	---	---	---	---	---	---	---	---	---	---
164	K4514RB	(*)	1,500	---	---	---	300	---	---	---	---	---	215	---
164	K4514RC	(*)	---	---	---	---	---	---	---	---	---	2	70	---
165	84RJ086A	Tc	---	---	---	---	---	---	---	50	---	---	---	---
166	84EM018C	Ti	---	---	---	---	70	---	---	---	---	---	---	---
166	84YB028	Kk	---	---	---	---	100	---	---	70	---	---	---	---
167	84JM067	Kk	---	200	---	---	---	---	---	100	---	---	---	---
168	K4515RC	(*)	5,000	---	---	---	---	100	---	---	---	---	---	---
169	K3309RA	(*)	---	---	---	---	---	---	---	---	---	---	---	---
169	K3604RB	Ti	5,000	---	---	150	>20,000	50	---	200	200	2	2,000	6.4
169	K3604RC	Ti	---	---	50	200	2,000	100	---	100	20	2	200	1.5
169	K4123RA	(*)	1,500	---	---	---	---	---	---	---	---	---	65	---
170	86RJ106A	Kh	---	---	---	---	200	---	---	---	---	---	---	---
170	K3603RB	Kk	---	300	50	70	500	---	---	---	1.0	---	---	---
171	86JM182C	Ti	---	---	---	---	---	---	---	---	---	---	270	---
172	K3352RA	(*)	---	300	70	---	---	---	---	---	---	---	---	---
172	K4168RA	(*)	---	150	50	---	---	---	---	---	---	---	---	---
173	86RJ055B	Kh	2,000	---	---	70	---	---	---	---	---	---	---	---
174	K4562RA	(*)	2,000	---	---	---	300	---	---	500	2.0	3	5,000	---
175	86RJ103A	Ti	---	---	500	---	---	---	---	---	---	---	---	---
175	K3600RA	Ti	2,000	500	---	---	200	---	100	---	1.0	3	200	.4
175	K3600RI	Kk	5,000	150	50	---	---	---	---	---	---	---	---	---
175	K3601RA	Ti	2,000	---	---	100	---	15	---	---	---	---	200	---
175	K3601RD	Kk	---	---	---	---	200	15	---	---	---	---	---	---
176	K4511RA	(*)	---	---	---	---	---	---	---	---	---	---	100	---

drainage at site 169 is a small, pervasively altered plug containing both disseminated and vein sulfides, mainly pyrite, chalcopyrite, and molybdenite(?). Samples of quartz veins as much as 6 cm wide from this locality contained copper concentrations greater than 20,000 ppm and molybdenum concentrations as much as 100 ppm. Both the geochemical suite of metals and the geologic observations indicate that undiscovered polymetallic-vein and porphyry Cu deposits, associated with local extension and fracturing of the overlying sedimentary and volcanic rocks during the emplacement of hypabyssal intrusive rocks, may be present.

Rock samples were collected from only three sites (135, 140, and 168; pl. 3) within drainage basins characterized by the As-Sb-Au-Ag anomaly suite defined by the SS and NMHMC geochemical data. The samples of sedimentary and volcanic rocks were cut by small quartz veins that contained anomalous concentrations of Sb, As, and Hg; scattered samples also contained anomalous concentrations of Mn, Zn, Pb, Mo, Au, or Ag. A float sample from site 140, cut by quartz veins containing stibnite and pyrite, contained 0.5 ppm Au (pl. 3). A precious-metal-bearing polymetallic-vein model would best account for these observations.

Samples of veins and sedimentary rocks from the west side of the Fourpeaked Mountain area, west of the zones of anomalies defined by the SS and NMHMC samples (sites 121–131; pl. 3), generally contained anomalous concentrations of two or three of the following elements: Hg, Mn, Zn, Cu, As, or Sb. The elements Co, Cd, Au, Ag, or Mo were present in anomalous concentrations in only one or two samples (pls. 2 and 3). Sample 122, which contained 1 ppm Ag, was collected from a small quartz vein in rocks of the Kaguyak Formation. These samples were not associated with obvious zones of altered rock or with intrusive rocks; we provisionally interpret these geochemical anomalies as poorly developed polymetallic veins associated with regional fractures and faults that are similar to those described elsewhere in the Fourpeaked Mountain area.

Site No.	Sample No.	Map unit	Au	As	Sb	Hg	Alt	Int	Lith	Frac	Vein	Mineralogy and mode of occurrence
159	K0162RA	(*)	---	10	---	.12	---	X	---	---	---	Silicified hypabyssal with dissem. py.
160	K0163RA	(*)	---	10	---	---	---	X	---	---	---	Andesite with dissem. py.
161	K0160RA	(*)	---	---	---	---	---	---	---	---	---	Oxidized and dissem. py.
161	K0160RB	(*)	---	10	---	---	---	X	---	---	---	Hematite-cemented breccia.
161	K3605RE	Ti	---	30	---	---	X	X	5	---	---	Fe ox. in silicified rock
162	K0157RB	(*)	---	80	8	.54	---	X	---	---	---	Oxidized and dissem. py.
163	84RJ141E	Tc	.05	---	---	---	X	---	7/1	X	---	Fe ox.
164	K4514RB	(*)	---	---	4	---	---	X	5	---	X	Oxidized py in qtz vein.
164	K4514RC	(*)	---	10	2	---	---	X	7/1	---	---	Dissem. py.
165	84RJ086A	Tc	---	---	---	---	---	X	7/1	---	---	
166	84EM018C	Ti	---	---	---	---	---	---	5	---	---	
166	84YB028	Kk	---	---	---	---	X	---	1	---	---	
167	84JM067	Kk	---	---	---	---	X	X	1	---	---	
168	K4515RC	(*)	---	20	2	---	X	X	5	---	X	Py in qtz vein.
169	K3309RA	(*)	.10	---	2	---	X	X	5	---	X	Dissem. py; py in qtz veinlets.
169	K3604RB	Ti	1.1	10	---	---	X	X	5	---	X	Py, cpy, spl in qtz veins as much as 6 cm wide.
169	K3604RC	Ti	.40	60	8	---	X	X	5	---	X	Py in qtz veins.
169	K4123RA	(*)	---	---	2	---	X	X	4	---	---	Dissem. py.
170	86RJ106A	Kh	---	---	---	---	X	X	1	X	---	Oxidized py veins.
170	K3603RB	Kk	.10	10	---	---	---	X	7/1	---	---	Dissem. py.
171	86JM182C	Ti	---	50	---	---	---	X	5	---	---	
172	K3352RA	(*)	---	---	---	---	X	X	5	---	---	Dissem. py.
172	K4168RA	(*)	---	10	---	---	X	X	5	---	---	Dissem. py.
173	86RJ055B	Kh	---	90	---	---	X	X	7/1	---	---	Fe ox.
174	K4562RA	(*)	---	80	6	---	---	X	---	---	X	Fe ox. in breccia; spl.
175	86RJ103A	Ti	---	---	---	---	---	X	5	---	---	
175	K3600RA	Ti	.30	10	4	---	X	X	5	---	X	Fe ox. in vuggy qtz veins.
175	K3600RI	Kk	---	---	---	---	X	X	7/1	---	---	Dissem. py.
175	K3601RA	Ti	---	---	---	---	X	X	5	---	X	Py in qtz veins; calcite veins.
175	K3601RD	Kk	---	---	---	---	X	X	7/1	---	---	Dissem. py in silicified hornfels; calcite veins.
176	K4511RA	(*)	---	20	10	---	---	X	8	---	X	Py in qtz veins.

In summary, the Fourpeaked Mountain area contains undiscovered polymetallic veins in the area between Fourpeaked Mountain and the Big River. In addition, the Fourpeaked Mountain area has potential for undiscovered polymetallic-vein deposits and for concealed porphyry Cu deposits associated with middle to late Tertiary hypabyssal and plutonic rocks.

NINAGIAK RIVER AREA

The Ninagiak River area is south of the Big River and runs from east of the crest of the Aleutian Range to the north shore of Hallo Bay (T. 18–19 S., R. 28–31 W.). The area is underlain by sandstone and siltstone of the Naknek Formation (Jn), which, in turn, is overlain either by Quaternary (Qac, Qad, Qap) or late Tertiary and Quaternary (QTac, QTap) volcanic rocks near the range crest. Except for vertical dikes (Td) having a northwesterly trend, exposures of Tertiary volcanic and hypabyssal rocks (Ti) are uncommon in the Ninagiak River area.

The SS and NMHMC geochemical data identified scattered drainage basins containing geochemical anomalies of Cu, Pb, Zn, Ni, or Ag; anomalous concentrations of Mo, As, Au, and Bi were also observed (Church, Bailey, and Riehle, 1989; Church and Motooka, 1989; Church and Arbogast, 1989). In drainage basins west of Kaguyak Crater the rocks are cut by large north-south-trending normal faults. Commonly, NMHMC samples from watersheds west of Kaguyak Crater contained anomalous concentrations of boron, suggesting the presence of tourmaline in the drainage basin. Pyrite, chalcopyrite, sphalerite, and arsenopyrite were common in NMHMC samples collected from several drainage basins west of Kaguyak crater and near the Aleutian Range crest, whereas wulfenite and galena were identified in NMHMC samples from only a few localities (Church and Bennett, 1989).

Table 16. Geochemical and geologic data for selected samples from the Ninagiak River area, Katmai study area, Alaska.

[Samples listed here have concentrations that exceed the 95th percentile for the respective lithologic units as defined in table 4. "Site No." is the locality shown on plates 1–3; map unit symbols are those on the geologic base map on plates 1–3. An "X" in columns headed "Vein," "Frac," or "Alt" indicates that veins, fracture fill, and (or) hydrothermally altered rock, including color anomalies caused by the oxidation of sulfide minerals, were observed at the sample site; "Int" indicates that the sample is an intrusive rock, or that there is a sill, dike, or pluton exposed nearby. "Lith" indicates the rock type of the sample: 1, sandstone or siltstone; 2, conglomerate; 3, volcaniclastic

Site No.	Sample No.	Map unit	Mn	Cr	Ni	Co	Cu	Mo	Sn	Pb	Ag	Bi	Zn	Cd
177	84DT106A	Td	---	---	---	70	---	---	---	---	---	---	---	---
178	K0175RA	(*)	---	---	---	---	---	15	---	---	---	1	---	---
179	86JM206	Jn	2,000	---	---	---	70	---	---	---	---	---	---	---
179	86JM210	Jn	---	200	---	---	---	---	---	---	---	---	---	---
180	K3402RA	(*)	2,000	---	---	---	70	15	---	---	---	---	120	---
180	K3402RD	(*)	2,000	---	---	70	---	---	---	---	---	---	150	---
181	K3403RE	(*)	---	200	50	---	---	20	---	---	0.7	---	130	---
182	86YB326	QTac	---	300	50	50	100	---	---	---	---	---	---	---
183	K3404RA	(*)	5,000	---	---	---	150	20	---	---	---	---	---	---
184	K0166RB	(*)	---	---	---	---	---	50	---	---	---	---	---	---
185	K0171	(*)	---	---	---	---	---	---	---	---	---	---	---	---
186	84YB033A	Jn	---	---	---	---	---	7	---	---	---	---	---	---
187	84JM084	Jn	---	---	---	---	---	---	---	---	---	---	---	---
188	84JM058A	Jn	---	---	---	---	---	---	---	---	2.0	---	---	---
188	84JM58A	Jn	---	---	---	---	---	---	---	---	2.0	---	---	---
189	84JM061A	Jn	---	---	---	---	---	---	---	---	---	---	70	---
190	84JM066	Jn	---	---	200	---	---	---	---	---	---	---	150	---
191	84JM064	Jn	---	---	70	---	150	---	---	---	.5	---	140	---
192	84JM065	Jn	2,000	---	---	---	---	---	---	---	---	---	160	---
193	84RJ068B	Td	---	---	---	---	100	---	---	50	---	---	---	---
194	84RJ070B	Jn	---	---	---	---	---	5	---	---	---	---	---	---
194	84YB018B	Td	---	---	---	---	---	---	50	---	1.0	3	---	---
195	84RJ067B	Jn	---	---	---	---	200	---	---	---	---	---	130	---
196	84DT074	Jn	---	---	---	---	---	---	---	70	---	---	135	---
196	84DT075	Ti	2,000	---	---	---	---	---	---	---	---	---	120	0.4
197	84DT081	Jn	---	---	---	---	---	10	---	100	---	---	---	---
198	83RJ145B	Jn	---	200	---	---	---	5	---	---	---	---	---	.3
199	83RJ144A	Jn	---	---	---	---	---	---	---	---	.5	---	---	---
199	83RJ144C	Ti	1,500	---	---	---	---	---	---	---	---	---	---	.6
199	84YB023B	Ti	---	---	---	---	200	20	---	70	---	---	---	.4
200	84RJ091B	Ti	---	---	---	---	---	---	---	---	---	---	120	---
201	83PB010	Qac	---	---	---	---	---	---	---	---	---	---	---	---
201	83PB054B	Qtap	1,500	---	70	---	---	---	---	---	---	---	180	.8
201	K4135RB	(*)	2,000	200	50	70	150	---	---	---	---	---	120	.5
202	83DT002B	Jn	---	---	---	---	---	---	---	---	---	---	---	---

Anomalous concentrations of metals (sites 177–202; geochemical data given in table 16) were found in samples that are predominantly sedimentary rocks, but most were not highly enriched in base or precious metals (pls. 2 and 3). Anomalous concentrations of Zn, As, Mo, Cu, and Cd, and, less commonly, Mn, Ni, Pb, Ag, Au, or Sb were found. A single dike sample (site 199) also contained an anomalous concentration of tin. Most rock samples contained anomalous concentrations of only one or two elements. Hornfels and quartz veins were not commonly observed in the field where the samples were collected in the Ninagiak River area.

At site 193, we sampled a narrow breccia dike at the margin of a large color anomaly in the Naknek Formation on the north side of Hallo Bay that contained anomalous concentrations of copper, lead, and gold (0.1 ppm). The breccia dike contains angular and rounded clasts derived from the Naknek Formation. Quartz veins are concentrated along its margins. A number of small igneous plugs crop out within a few kilometers of this locality.

Sites 194–197 are closely adjacent sites within a color anomaly developed in fractured, homoclinally dipping blocks of the Naknek Formation. These sites are along the axis of the Aleutian volcanic arc in a gap between the volcanic deposits from Devils Desk and Kaguyak Crater. The SS and NMHMC samples from the drainage basin where rock samples 194 and 195 were col-

rock or tuff; 4, lava flow; 5, sill or dike; 6, plutonic rock; 7, metamorphosed rock/protolith; 8, limestone; and (*), float sample. Mineralogy is generally based upon field identifications of hand specimens: py, pyrite; cpy, chalcopyrite; asp, arsenopyrite; spl, sphalerite; gn, galena; mly, molybdenite; qtz, quartz; Fe ox., iron oxides; dissem., disseminated mineral grains in sample. Dashes (---), concentrations not anomalous or feature not observed; all concentrations expressed in parts per million (ppm); >, concentration is greater than reported value]

Site No.	Sample No.	Map unit	Au	As	Sb	Hg	Alt	Int	Lith	Frac	Vein	Mineralogy and mode of occurrence
177	84DT106A	Td	---	---	---	---	---	---	5	---	---	
178	K0175RA	(*)	---	10	---	---	X	---	1	---	---	Oxidized dissem. py.
179	86JM206	Jn	---	---	---	---	---	X	1	---	---	
179	86JM210	Jn	---	---	6	---	---	---	1	---	---	
180	K3402RA	(*)	---	---	---	---	---	X	---	---	X	Carbonate vein.
180	K3402RD	(*)	0.05	50	2	---	X	X	5	---	---	
181	K3403RE	(*)	.2	---	---	---	---	---	1	---	---	
182	86YB326	QTac	---	---	---	---	---	---	4	---	---	
183	K3404RA	(*)	.2	50	---	---	---	---	1	---	---	
184	K0166RB	(*)	---	10	---	---	---	---	1	---	---	Calcite and qtz veins 1–3 mm wide.
185	K0171	(*)	---	10	2	4.6	---	---	---	---	---	
186	84YB033A	Jn	---	---	---	---	X	---	1	X	---	Fe ox.
187	84JM084	Jn	---	20	---	---	---	---	1	---	---	
188	84JM058A	Jn	---	1,600	42	---	X	---	1	---	---	
188	84JM58A	Jn	---	2,000	42	---	---	---	1	---	---	
189	84JM061A	Jn	---	---	---	---	---	---	1	---	---	
190	84JM066	Jn	---	---	---	---	---	---	1	---	---	
191	84JM064	Jn	---	---	---	---	---	---	1	---	---	
192	84JM065	Jn	---	---	---	---	---	---	1	---	---	
193	84RJ068B	Td	.1	---	---	---	---	---	5	---	X	Fe ox.
194	84RJ070B	Jn	---	---	---	---	X	X	1	---	---	Fe ox.
194	84YB018B	Td	---	---	---	---	X	---	5	---	---	Dissem. py.
195	84RJ067B	Jn	.15	---	---	---	X	X	1	X	---	Oxidized py veins.
196	84DT074	Jn	---	---	---	---	X	X	1	---	---	
196	84DT075	Ti	---	---	---	---	X	---	5	---	---	
197	84DT081	Jn	---	---	---	---	X	---	1	---	---	
198	83RJ145B	Jn	---	---	---	---	---	---	1	---	---	
199	83RJ144A	Jn	---	14	---	---	---	X	1	---	X	Py and hematite in fractures.
199	83RJ144C	Ti	---	---	---	---	---	---	5	---	---	
199	84YB023B	Ti	---	---	---	---	X	X	5	---	---	Py veins.
200	84RJ091B	Ti	---	---	---	0.14	---	---	5	---	---	Oxidized py veins.
201	83PB010	Qac	---	---	2	---	---	---	4	---	---	
201	83PB054B	Qtap	---	10	---	---	X	X	3	---	---	Dissem. py.
201	K4135RB	(*)	---	10	---	---	X	---	5	---	---	Dissem. py.
202	83DT002B	Jn	.05	---	---	---	---	---	1	---	---	

lected contained a large number of metals in anomalous concentrations (Cu, Pb, Zn, As, Ag, Bi, and Ba) and ore-related minerals (pyrite, wulfenite, sphalerite, and galena). A sample from a dike at site 194 contained anomalous concentrations of silver, bismuth, and tin. Pyrite veins in the Naknek Formation at site 195 contained anomalous concentrations of copper, zinc, and gold. A sample from a sill at site 196 contained anomalous concentrations of manganese, zinc, and cadmium, whereas a sample of the Naknek Formation from this site contained anomalous concentrations of lead and zinc.

Samples of highly altered sills (Ti; sites 199–200) contained anomalous concentrations of Mn, Cu, Mo, Pb, Zn, Cd, and Hg. At site 200 vertical fractures in rocks of the Naknek Formation are lined by pyrite and hematite after pyrite.

Red-brown color anomalies are locally well developed in the sedimentary rocks owing to oxidation of pyrite distributed along vertical fractures. At site 199 these highly altered sills are cut by less altered, northwest-trending dikes.

Samples from a late Tertiary to early Quaternary volcanic tuff (site 201) contained anomalous concentrations of Mn, Cu, Zn, Co, Cd, and As (pl. 2). These geochemical anomalies are spatially associated with an area where geologic mapping suggests emplacement of a resurgent dome in a series of thick ash flows, perhaps indicating a small caldera at this locality.

Table 17. Geochemical and geologic data for selected samples from the Barrier Range–Kukak Bay area, Katmai study area, Alaska.

[Samples listed here have concentrations that exceed the 95th percentile for the respective lithologic units as defined in table 4. "Site No." is the locality shown on plates 1–3; map unit symbols are those on the geologic base map on plates 1–3. An "X" in columns headed "Vein," "Frac," or "Alt" indicates that veins, fracture fill, and (or) hydrothermally altered rock, including color anomalies caused by the oxidation of sulfide minerals, were observed at the sample site; "Int" indicates that the sample is an intrusive rock, or that there is a sill, dike, or pluton exposed nearby. "Lith" indicates the rock type of the sample: 1, sandstone or siltstone; 2, conglomerate; 3, volcaniclastic

Site No.	Sample No.	Map unit	Mn	Cr	Ni	Co	Cu	Mo	Sn	Pb	Ag	Bi	Zn	Cd
203	83YB002	Tab	---	200	100	---	---	---	---	---	---	---	---	---
204	83JM050B	Jn	---	500	100	70	---	---	---	---	---	---	280	---
205	83PB009B	Jn	---	---	---	---	---	---	---	---	0.5	---	---	---
206	84JM086	Jn	---	---	100	---	---	---	---	---	.5	---	---	---
207	84YB015	Qac	---	---	---	---	---	---	---	50	---	---	---	---
208	84YB016	Qac	---	---	---	---	---	---	---	---	---	---	90	---
209	84YB017	Ti	---	---	---	---	---	---	---	50	---	---	---	---
210	83JM051	Kk	---	---	100	---	---	---	---	---	---	---	170	0.5
211	84EM022C	Tab	---	---	---	---	---	---	---	---	---	---	350	---
212	84EM026A	Kk	---	---	100	---	100	---	---	100	---	---	180	---
212	84EM026C	Td	1,500	---	100	---	---	---	---	---	---	---	---	---
213	84RJ064B	Th	---	---	---	---	200	5	---	---	---	---	---	---
214	K0139R	(*)	---	200	---	---	---	10	---	---	---	---	---	---
215	K0021RA	(*)	2,000	---	---	---	---	---	---	---	---	---	---	---
216	K0135RA	(*)	2,000	---	---	---	---	---	---	---	1.0	---	---	---
217	K0190RB	(*)	---	---	---	---	---	10	---	---	---	---	---	---
218	84RJ099D	Tab	---	---	---	---	200	---	---	---	---	---	---	---
218	84RJ101B	Tab	---	---	---	100	---	---	---	---	---	---	---	---
219	84RJ100A	Tab	---	---	---	---	---	50	---	---	---	---	---	---
220	83RJ141B	Tab	---	---	---	---	---	10	---	---	---	---	---	.4
221	84EM003C	Tab	2,000	200	100	50	---	7	---	---	---	---	---	---
222	83YB007	Tab	---	200	100	50	---	---	---	---	---	---	---	---
223	83PB058A	Tab	---	---	---	---	---	---	---	---	---	---	130	---
224	84EM066A	Tab	3,000	---	---	---	---	---	---	---	5.0	100	---	---
225	84EM014C	Ti	2,000	---	---	---	---	---	---	100	---	---	1,150	7.7
226	84RJ081D	Ti	2,000	---	---	---	200	---	---	200	10	15	580	2.3
227	K0178R	(*)	---	---	---	---	---	10	---	---	1.0	1	---	---
228	K4524RA	(*)	---	---	---	---	500	20	---	70	20	10	---	---
229	84EM012G	Td	---	300	70	---	---	---	---	---	---	---	---	---
230	K0181RA	(*)	---	---	---	---	---	---	---	50	---	4	---	---
231	K3500RA	Tab	---	---	---	---	---	---	---	---	10	---	---	---
232	84RJ095C	Tab	---	300	200	100	---	---	---	---	---	---	---	---
233	84YB063	Jn	---	200	---	---	---	---	---	---	---	---	---	---
234	84EM039C	Tab	---	---	---	---	---	20	---	---	2.0	---	---	---
234	84EM040C	Tab	---	---	---	---	---	---	---	---	1.0	---	---	---
235	84RJ121B	Jn	---	---	---	---	---	---	---	---	.5	---	---	---
236	84RJ120D	Tab	---	---	---	---	---	---	---	---	---	---	---	---
236	K0254RA	(*)	---	---	---	---	---	---	---	---	.7	---	---	---
236	K0255RA	Tab	---	---	---	---	---	---	---	---	---	1	---	---
237	84EM038C	Tab	---	---	---	---	---	---	---	---	.7	---	---	---
238	86RJ121A	Tab	---	---	---	---	---	50	---	---	1.0	---	---	---
238	86RJ121B	Tab	---	---	---	---	---	500	---	---	2.0	---	---	---
238	K0250R	(*)	---	---	---	---	---	100	---	---	2.0	1	---	---
238	K3619RA	Tab	---	---	---	---	---	---	---	---	5.0	---	---	.3
238	K3619RB	Tab	---	---	---	---	---	100	---	---	1.0	---	---	---
238	K3619RD	Tab	---	---	---	---	---	100	---	---	3.0	---	---	---

rock or tuff; 4, lava flow; 5, sill or dike; 6, plutonic rock; 7, metamorphosed rock/protolith; 8, limestone; and (*), float sample. Mineralogy is generally based upon field identifications of hand specimens: py, pyrite; cpy, chalcopyrite; asp, arsenopyrite; spl, sphalerite; gn, galena; mly, molybdenite; qtz, quartz; Fe ox., iron oxides; dissem., disseminated mineral grains in sample. Dashes (---), concentrations not anomalous or feature not observed; all concentrations expressed in parts per million (ppm); >, concentration is greater than reported value]

Site No.	Sample No.	Map unit	Au	As	Sb	Hg	Alt	Int	Lith	Frac	Vein	Mineralogy and mode of occurrence
203	83YB002	Tab	---	---	2	---	---	---	4	---	---	
204	83JM050B	Jn	---	70	---	---	---	---	7/1	---	---	
205	83PB009B	Jn	---	---	---	---	---	---	7/1	---	---	
206	84JM086	Jn	---	---	---	---	---	X	7/1	---	---	
207	84YB015	Qac	---	---	---	---	---	---	4	---	---	
208	84YB016	Qac	---	---	---	---	---	---	4	---	---	
209	84YB017	Ti	---	---	---	---	---	---	5	---	---	
210	83JM051	Kk	---	---	---	---	---	X	1	---	X	
211	84EM022C	Tab	---	---	---	---	X	---	5	---	---	Qtz veins.
212	84EM026A	Kk	---	---	---	---	---	X	1	---	---	
212	84EM026C	Td	---	---	---	---	---	---	5	---	---	
213	84RJ064B	Th	---	---	---	---	---	X	7/1	---	---	
214	K0139R	(*)	---	400	4	---	X	---	5/6	---	---	Dissem. py; py in qtz veins.
215	K0021RA	(*)	---	---	---	0.45	X	---	---	---	---	Dissem. py.
216	K0135RA	(*)	---	---	---	.16	X	---	---	---	---	Calcite veins.
217	K0190RB	(*)	---	---	---	.20	---	---	---	---	---	Oxidized dissem. py in breccia.
218	84RJ099D	Tab	---	---	---	---	X	---	4	---	---	Dissem. py.
218	84RJ101B	Tab	---	---	---	---	---	X	7/4	---	---	Oxidized dissem. and vein py.
219	84RJ100A	Tab	---	---	---	---	---	X	7/4	---	---	Dissem. py.
220	83RJ141B	Tab	---	---	---	---	X	---	4	X	---	
221	84EM003C	Tab	---	---	---	---	---	X	4	---	---	
222	83YB007	Tab	---	---	---	---	---	---	4	---	---	
223	83PB058A	Tab	---	---	---	---	X	---	4	---	---	
224	84EM066A	Tab	---	---	---	---	---	X	7/4	---	---	Dissem. py.
225	84EM014C	Ti	---	---	---	---	X	---	5	---	---	Qtz-epidote veins.
226	84RJ081D	Ti	---	80	2	---	X	---	5	X	---	Fe ox.
227	K0178R	(*)	---	---	---	---	X	---	5	---	---	Dissem. py.
228	K4524RA	(*)	1.9	120	82	---	X	---	5	---	X	Py in qtz vein.
229	84EM012G	Td	---	---	---	---	---	---	5	---	---	
230	K0181RA	(*)	---	---	---	---	X	---	5	---	---	
231	K3500RA	Tab	0.15	310	8	---	X	X	4	---	X	Py in breccia.
232	84RJ095C	Tab	---	---	---	---	X	---	3	X	---	Fe ox.
233	84YB063	Jn	---	150	---	---	---	---	1	---	---	
234	84EM039C	Tab	---	70	---	---	X	---	4	---	X	Fe ox.
234	84EM040C	Tab	---	---	---	---	X	X	4	---	X	
235	84RJ121B	Jn	---	---	---	---	---	---	1	---	---	
236	84RJ120D	Tab	---	---	6	.42	X	X	4	X	---	Fe ox.
236	K0254RA	(*)	.05	210	---	---	X	X	4	---	---	Oxidized dissem. py.
236	K0255RA	Tab	---	10	---	---	X	X	4	---	---	Dissem. py.
237	84EM038C	Tab	---	210	2	.14	---	X	4	X	---	Fe ox.; qtz veins.
238	86RJ121A	Tab	---	---	---	---	X	---	4	X	X	Fe ox.; qtz veins.
238	86RJ121B	Tab	---	160	2	---	X	---	3	X	X	Fe ox.; qtz veins.
238	K0250R	(*)	.05	300	6	---	X	X	4	---	---	Py in 2-mm-wide qtz veins; some brecciated.
238	K3619RA	Tab	2.0	800	16	---	X	X	4	---	---	Finely dissem. py in breccia.
238	K3619RB	Tab	.35	500	2	---	X	X	4	---	X	Banded qtz veins 3-5 mm wide; py, jordisite.
238	K3619RD	Tab	.35	800	36	---	X	X	---	---	X	Py in qtz veins as much as 10 cm wide.

Table 17. Geochemical and geologic data for selected samples from the Barrier Range–Kukak Bay area—Continued.

Site No.	Sample No.	Map unit	Mn	Cr	Ni	Co	Cu	Mo	Sn	Pb	Ag	Bi	Zn	Cd
238	K3619RG	Tab	---	---	---	---	---	20	---	---	---	---	---	---
238	K3619RL	Tab	---	---	---	---	---	100	---	---	1.0	---	---	---
238	K3620RB	Tab	---	---	---	---	---	1,000	---	---	5.0	---	---	---
239	83PB037B	Tab	---	---	---	---	---	15	---	---	---	---	---	---
240	83RJ096A	Tab	---	---	---	---	---	30	---	---	1.0	---	---	---
240	83RJ120	Tab	---	---	---	---	---	15	---	---	---	4	---	---
241	K0051R	(*)	---	---	100	50	---	15	---	---	.7	---	---	.2
241	K0069RA	(*)	---	---	---	---	---	20	---	---	---	---	---	---
242	83RJ079	Tab	---	---	---	---	---	---	---	---	---	---	---	---
243	K0109RA	Tab	1,500	---	---	---	---	---	---	---	---	---	140	---
244	83PB014B	Tab	---	---	---	---	---	---	---	---	---	---	---	---
245	83RJ168	Tab	---	---	---	---	---	---	---	---	---	10	---	---
246	K0153RA	(*)	---	---	---	---	---	10	---	---	---	---	---	---
247	83PB064C	Tab	---	---	---	---	---	---	---	---	---	---	---	---
248	83RJ063	Tab	---	---	---	---	---	---	---	---	---	10	---	---
249	84YB083	Tab	---	---	---	---	---	10	---	---	---	---	---	---
250	83RJ102B	Ti	---	---	---	---	---	---	---	---	---	---	---	.9
251	84EM067B	Tab	---	---	---	---	---	20	---	70	---	---	---	---
252	K0122RB	(*)	---	---	---	---	300	150	---	300	7.0	2	---	.2
253	83RJ154	Tab	---	---	---	---	---	---	---	---	---	---	100	---
254	83RJ032E	Tab	---	300	100	50	---	---	---	---	---	---	---	---
255	84RJ073A	Th	2,000	---	---	---	---	---	---	70	---	---	---	---
255	84RJ073C	Th	>5,000	---	---	100	---	---	---	---	---	---	---	---
255	K0147RA	Th	5,000	---	---	---	---	---	---	---	---	---	---	.3
256	83AL043B	Ti	1,500	---	---	---	---	---	---	---	---	---	95	---
257	83RJ116	Tab	---	---	---	---	---	---	---	---	---	---	180	---
257	84YB061	Th	---	---	---	---	---	---	---	---	---	---	---	---
258	84YB042A	Tab	---	---	---	---	---	---	---	70	---	---	---	---
259	83PB025	Th	---	---	---	---	---	---	---	---	---	---	160	---
260	83PB024	Th	---	---	---	---	---	10	---	---	.5	---	---	---
261	83RJ054	Ti	---	---	---	---	---	---	---	---	---	---	130	.3
262	K0113RA	(*)	---	---	---	---	---	---	---	---	---	---	---	.2
263	K0073RA	(*)	---	---	---	---	---	7	---	---	---	---	---	---
264	83RJ097C	Tab	---	---	---	---	---	---	---	---	10	---	---	---
264	84RJ135C	Tab	---	500	---	---	---	---	---	---	---	---	---	---
264	84RJ135E	Tab	---	---	---	---	---	---	---	---	---	---	---	---
264	84RJ135H	Tab	---	---	---	---	---	10	---	---	.5	---	100	.7
264	84RJ135I	Tab	---	---	---	---	---	---	---	---	---	---	---	---
264	84RJ135M	Tab	---	---	---	---	---	---	---	---	---	---	---	---
264	84RJ135R	Tab	---	---	---	---	---	---	---	---	---	---	---	---
264	84RJ135S	Ti	---	300	100	---	---	---	---	---	---	---	---	---
264	84RJ135T	Tab	---	---	---	---	---	10	---	---	.5	---	---	---
265	83RJ122A	Tab	---	300	---	---	---	---	---	---	---	---	---	---
265	K0103R	(*)	---	---	---	---	---	15	---	---	---	---	---	.2
266	84EM051B	Tab	---	---	---	---	---	70	---	---	---	---	---	---
267	K3618RB	Ti	2,000	---	---	50	---	30	---	30	---	3	200	---
267	K3618RD	Ti	---	300	100	50	500	---	---	---	---	---	200	---
267	K3618RF	Tab	---	---	---	---	---	---	---	---	---	---	200	---
267	K3618RG	Tab	3,000	---	---	---	---	---	---	---	---	---	200	---
268	83RJ126	Tab	---	---	---	---	---	---	---	---	---	---	---	---
268	K0105RA	(*)	---	---	---	---	---	50	---	---	---	---	---	---

Site No.	Sample No.	Map unit	Au	As	Sb	Hg	Alt	Int	Lith	Frac	Vein	Mineralogy and mode of occurrence
238	K3619RG	Tab	.20	170	4	---	X	X	---	---	---	Finely dissem. py in brecciated qtz veins.
238	K3619RL	Tab	.45	90	---	---	X	X	---	---	X	Finely dissem. py in qtz veins.
238	K3620RB	Tab	.15	600	2	---	X	X	---	---	X	Jordisite, py in qtz veins.
239	83PB037B	Tab	---	---	---	---	---	---	4	X	X	
240	83RJ096A	Tab	---	40	---	---	X	---	4	X	X	Qtz veins.
240	83RJ120	Tab	---	---	---	---	X	---	4	---	---	
241	K0051R	(*)	.80	30	---	.18	---	---	---	---	---	Dissem. py and qtz in breccia.
241	K0069RA	(*)	.25	---	6	---	---	---	---	---	---	Qtz matrix breccia.
242	83RJ079	Tab	---	40	---	---	X	---	4	---	---	
243	K0109RA	Tab	---	---	---	---	---	---	4	---	---	Dissem. py.
244	83PB014B	Tab	---	40	6	2.2	X	X	4	---	---	
245	83RJ168	Tab	---	90	2	.68	X	---	4	---	---	
246	K0153RA	(*)	---	---	---	.16	---	---	4	---	---	Oxidized dissem. py.
247	83PB064C	Tab	---	40	---	---	---	X	7/4	---	---	
248	83RJ063	Tab	---	---	---	---	X	---	4	X	---	Fe ox.
249	84YB083	Tab	---	300	2	---	X	---	4	---	---	Fe ox.
250	83RJ102B	Ti	---	---	---	---	---	---	5	---	---	
251	84EM067B	Tab	---	---	---	---	X	X	3	---	---	Fe ox.
252	K0122RB	(*)	---	75	30	---	---	---	4	---	---	Fe ox. in vuggy qtz vein.
253	83RJ154	Tab	---	---	---	---	X	---	4	---	---	
254	83RJ032E	Tab	---	---	---	---	---	---	4	---	---	
255	84RJ073A	Th	.05	---	---	---	---	X	2	---	---	Fe ox. in conglomerate matrix.
255	84RJ073C	Th	---	---	---	---	---	X	1	---	---	Fe ox. in sandstone matrix.
255	K0147RA	Th	.05	---	---	---	---	---	1	---	---	Fe ox. in sandstone matrix.
256	83AL043B	Ti	---	---	---	---	---	---	5	---	---	
257	83RJ116	Tab	---	---	---	---	---	---	3	---	---	Qtz veins.
257	84YB061	Th	---	---	---	.34	---	---	1	---	---	
258	84YB042A	Tab	---	---	---	---	---	X	4	---	---	
259	83PB025	Th	---	---	---	---	---	---	7/1	---	---	
260	83PB024	Th	---	---	---	---	---	---	1	---	---	
261	83RJ054	Ti	---	---	---	---	X	---	5	---	---	
262	K0113RA	(*)	---	50	---	---	X	---	---	---	---	
263	K0073RA	(*)	---	50	---	---	X	---	4	---	---	
264	83RJ097C	Tab	5.0	---	---	.15	X	---	4	---	X	Qtz veins.
264	84RJ135C	Tab	---	---	---	---	X	---	4	X	---	Dissem. py.
264	84RJ135E	Tab	---	50	---	---	---	---	4	X	X	Oxidized py, other sulfides in qtz vein.
264	84RJ135H	Tab	---	50	---	---	X	---	4	---	X	Oxidized py in qtz veins.
264	84RJ135I	Tab	---	560	10	---	X	---	4	X	---	Oxidized py in qtz veins.
264	84RJ135M	Tab	.20	---	---	---	X	---	4	X	---	Dissem. py.
264	84RJ135R	Tab	.20	800	---	---	X	---	4	X	---	
264	84RJ135S	Ti	---	---	---	---	X	---	5	---	---	Dissem. py.
264	84RJ135T	Tab	---	---	---	---	---	---	4	---	X	Qtz veins.
265	83RJ122A	Tab	---	---	---	.8	---	---	1	---	---	
265	K0103R	(*)	---	100	2	.10	---	---	4	---	---	Fe ox. in breccia.
266	84EM051B	Tab	---	---	---	---	X	---	4	---	---	Oxidized dissem. py in qtz veins.
267	K3618RB	Ti	---	130	---	---	X	X	6	---	---	Dissem. py; epidote.
267	K3618RD	Ti	---	40	---	---	X	X	6	---	---	Dissem. py.
267	K3618RF	Tab	---	80	---	---	X	X	4	---	---	Dissem. py.
267	K3618RG	Tab	---	---	---	---	X	X	4	---	---	Dissem. py.
268	83RJ126	Tab	---	---	8	---	X	---	4	---	---	
268	K0105RA	(*)	---	---	---	---	---	---	4	---	---	Oxidized dissem. py.

Table 17. Geochemical and geologic data for selected samples from the Barrier Range–Kukak Bay area—Continued.

Site No.	Sample No.	Map unit	Mn	Cr	Ni	Co	Cu	Mo	Sn	Pb	Ag	Bi	Zn	Cd
269	83RJ110	Td	---	---	---	---	---	---	---	---	---	---	95	---
270	84EM043D	Jn	---	---	---	---	---	---	---	---	---	---	110	---
271	83JM038A	Kk	---	---	---	---	---	---	---	---	---	---	---	---
271	83RJ107C	Jn	---	---	---	---	---	---	---	---	---	---	---	---
272	83DT051B	Kk	---	---	---	---	---	---	---	---	.7	---	---	---
273	83JM036A	Kk	---	---	---	---	---	---	---	---	---	---	---	---
274	83PB042	Tab	---	---	---	---	---	---	---	---	.7	---	---	---
275	83PB043B	Th	---	---	---	---	---	---	---	---	---	---	---	---
276	83PB044	Tab	---	---	100	100	---	---	---	---	---	---	---	---
277	K3621RD	(*)	---	200	100	---	---	10	---	---	---	---	90	.3
277	K3621RE	(*)	---	---	---	50	150	---	---	---	---	---	---	---
278	86RJ122B	Ti	---	---	---	---	---	---	---	---	---	---	---	---
278	K3622RC	Ti	---	---	---	---	200	---	---	100	---	---	180	.4
278	K3622RE	Ti	---	200	100	50	150	---	---	30	---	---	370	1.2
279	83JM039B	Td	---	---	---	---	---	15	---	---	---	---	---	---
280	83AL016C	Jn	---	---	---	---	---	100	---	---	---	2	---	---
281	83DT021	Kk	---	---	---	70	---	---	---	---	---	---	---	---
282	83DT014A	Jn	---	---	---	---	---	---	---	---	---	---	130	.6
283	83JM020A	Jn	---	200	---	---	---	15	---	---	.5	---	---	---

The geochemical anomalies and outcrops of brecciated sedimentary rocks adjacent to small igneous bodies suggest that undiscovered polymetallic veins may be present in the Ninagiak River area (pls. 1–3). Although the geochemical anomaly patterns are not as persistent throughout the Ninagiak River area as they are in either the Fourpeaked Mountain area or the Barrier Range–Kukak Bay area (see the following discussion), the geology and geochemistry of this area are very similar to the Fourpeaked Mountain and Barrier Range–Kukak Bay areas and may reflect an area of similar plutonic and hydrothermal history that has not been as well exposed by erosion.

BARRIER RANGE–KUKAK BAY AREA

The Barrier Range–Kukak Bay area extends east from just west of the Aleutian Range crest to the shore of Shelikof Strait, and from Hallo Bay on the north to the mouth of the Katmai River on the south. The area has as much as several hundred meters of relief; bedrock exposures are generally good due to a paucity of glacial and alluvial deposits, except along the ice- and snow-covered crest of the Aleutian Range. Late Tertiary volcanic rocks (Tab) crop out along the axis of a northeast-plunging syncline; underlying Oligocene (Th), Cretaceous (Kk, Kp, Kh), and Jurassic (Jn) sedimentary rocks are exposed successively outward from the axis of the syncline. These sedimentary and volcanic rocks were intruded by a variety of late Tertiary sills, dikes, and small plutons (Ti, Td). Color anomalies are widespread, and zones of pervasive propylitic alteration are common in the volcanic rocks. Numerous quartz veins, fractures, and dikes trend northwest. We interpret these widespread zones of alteration, quartz veins, and dike systems to be related to exposed and inferred subsurface plutons.

To facilitate discussion of this area, we have divided it into three subareas (fig. 10). The northernmost of these, called the Kukak Bay subarea (T. 20–22 S., R. 29–33 W.), contains the fewest drainage basins that have anomalous concentrations of base and precious metals in the reconnaissance samples. Furthermore, rock samples from sites within this subarea generally show fewer metals at anomalous concentrations than do samples from the southern part of the Barrier Range. NMHMC samples from the coastal area of the Barrier Range, called the Kuliak Bay–Katmai River subarea (T. 22 S., R. 30–31 W. to T. 25 S., R. 32–35 W.), contained most of the occurrences of cinnabar found in the Katmai study area. Finally, the Katmai Lakes–Hagelbargers Pass–Dakavak Lake subarea (T. 22–24 S., R. 32–34 W.), 5–10 km east of Mount Katmai, also has a distinctive epithermal-quartz-vein geochemical signature.

KUKAK BAY SUBAREA

SS samples from several scattered drainage basins, or small groups of adjacent drainage basins, on either side of Kukak Bay contained anomalous concentrations of Co, Mo, Ni, or Zn (Church, Bailey, and Riehle, 1989; Church and Motooka, 1989). In addition to the elements listed above, the NMHMC samples commonly contained anomalous concentrations of Cu and Pb, less commonly of Ag, Cd, or Ba; a few contained Sn, Bi, or Au (Church and Arbogast, 1989). Pyrite

Site No.	Sample No.	Map unit	Au	As	Sb	Hg	Alt	Int	Lith	Frac	Vein	Mineralogy and mode of occurrence
269	83RJ110	Td	---	---	---	---	X	X	5	X	X	
270	84EM043D	Jn	---	---	---	---	---	---	1	---	---	
271	83JM038A	Kk	---	---	4	---	---	---	1	---	---	
271	83RJ107C	Jn	---	---	2	---	---	X	1	---	---	
272	83DT051B	Kk	---	---	10	---	X	---	1	---	X	
273	83JM036A	Kk	.10	---	---	---	---	X	1	---	---	
274	83PB042	Tab	---	---	2	---	---	---	4	X	---	
275	83PB043B	Th	---	---	4	---	---	X	1	---	---	
276	83PB044	Tab	---	---	4	---	---	---	5	---	X	
277	K3621RD	(*)	---	50	2	---	X	---	6	---	X	Py in qtz veins.
277	K3621RE	(*)	---	---	---	---	X	---	4	---	---	Dissem. py.
278	86RJ122B	Ti	---	---	4	---	---	---	5	---	X	Qtz vein.
278	K3622RC	Ti	---	10	2	---	X	X	6	---	---	Dissem. py.
278	K3622RE	Ti	---	30	---	---	X	X	5	---	---	Dissem. py, spl in qtz veins.
279	83JM039B	Td	---	---	---	---	---	---	5	---	---	
280	83AL016C	Jn	---	360	6	.55	---	---	1	---	---	
281	83DT021	Kk	---	---	4	---	---	X	1	---	---	
282	83DT014A	Jn	---	---	---	---	---	X	1	---	---	
283	83JM020A	Jn	---	---	2	---	---	---	4	---	---	

and chalcopyrite were common in the NMHMC samples, arsenopyrite and sphalerite were less common, and wulfenite, galena, and gold were identified in one or more drainage basins (Church and Bennett, 1989).

Rock samples from the north side of Kukak Bay (sites 203–232; geochemical data given in table 17) contained anomalous concentrations of Zn, Ag, Pb, Mo, Ni, Mn, Cu, Bi, and As; samples from some localities also contained anomalous concentrations of Sb, Cd, Hg, or Au (pls. 2 and 3). Cobb (1972) gave an approximate location on the northwest side of Kukak Bay for a Cu-Au-Ag prospect reported by Martin (1920). Geochemical data for the SS and NMHMC samples from drainage basins near this locality were not anomalous except for those from two small drainage basins on the north side of the ridge near site 211. Silver, lead, zinc, and barium were present in anomalous concentrations in the reconnaissance geochemical samples from this drainage basin, and barite was identified in the NMHMC sample. Gold was seen in the NMHMC sample from the drainage basin immediately east of site 211. Samples of propylitically altered Tertiary volcanic rock (Tab) and hornfels derived from rocks of the Kaguyak Formation (sites 210–212, 217, and 218) contained anomalous concentrations of copper, molybdenum, lead, and zinc. These propylitically altered rocks are generally marginal to small hypabyssal plugs and dikes.

The SS and NMHMC samples, as well as intrusive rock samples collected from zones of propylitic and argillic alteration at the head of Kukak Bay (from sites 224–228), had higher metal contents than did samples from the north side of Kukak Bay. The NMHMC samples from the drainage basins near the head of Kukak Bay contained anomalous concentrations of Ag, Cd, Pb, As, Zn, and Ba. Pyrite and arsenopyrite were identified in the NMHMC samples. An NMHMC sample collected from the terminus of the glacier near sites 224–226 also contained 150 ppm Au! Rock samples from sites 247–249 were collected along the margin of a small tonalitic pluton dated at 2.45±0.07 Ma (Shew and Lanphere, 1992). This pluton is slightly porphyritic, and the fine- to medium-grained groundmass is moderately altered to chlorite and calcite. Anomalous concentrations of Mn, Zn, Pb, Ag, Bi, and Cd were determined in samples of plutonic rock collected within a few hundred meters of a stoped contact between the pluton and interbedded lava flows and breccias (pl. 2). Layers of volcanic rocks can be recognized for as much as 100 m into the pluton as strings of partly assimilated inclusions. Local color anomalies in the pluton are associated with small fractures or veins. A sample of a quartz vein from site 226 contained anomalous concentrations of Mn, Pb, Zn, Ag, Bi, Cd, As, and Sb. The presence of mineralized veins in the pluton suggests that this area is favorable for polymetallic veins near the margins of shallow intrusive rocks in the vicinity of Kukak Bay. We suggest that the locality of the Kukak Bay prospect is probably marginal to the Kukak Bay pluton, most likely near the head of Kukak Bay rather than in the uncertain locality reported by Cobb (1972).

The SS, NMHMC, and rock geochemical data suggest that similar base- and precious-metal veins may also extend along the range crest from near Mount Denison southwest to Snowy Mountain and from the Aleutian Range crest east into the outlying volcanic rocks. A sample of volcanic breccia collected from an outcrop on the southeast side of Snowy Mountain (site 231) contained anomalous concentrations of arsenic, antimony, silver, and gold. A sample of pyrite-bearing volcanic rock collected at site 232 contained anomalous concentrations of cobalt and nickel. The inferred extension of the west Kukak Bay pluton south and west beneath the Aleutian Range crest implies that geologic conditions are favorable for additional hydrothermally altered rock there. Goldfarb and others (1988) identified this area as favorable for undiscovered precious-metal-bearing epithermal quartz veins, but we have reclassified them as precious-metal-rich polymetallic veins because of the presence of intrusive rocks associated with these geochemical anomalies.

KULIAK BAY–KATMAI RIVER SUBAREA

Geochemical data for the SS and NMHMC samples from the coastal part of the Barrier Range area identify drainage basins that commonly contain anomalous concentrations of Co, Ag, Zn, and Mo. Anomalous concentrations of Pb, Cu, or Ni are less common, and As, Bi, Sn, or Cd were present in a few samples (Church and Arbogast, 1989; Church, Bailey, and Riehle, 1989; Church and Motooka, 1989). Mineralogical studies of the NMHMC samples indicate that sphalerite was common whereas pyrite, chalcopyrite, molybdenite, and arsenopyrite were less commonly observed. Cinnabar was identified in five drainage basins and galena in one (Goldfarb and others, 1988; Church and Bennett, 1989).

Float samples of volcanic and sedimentary rocks (sites 276–279; table 17), as well as samples from the Tertiary pluton (Ti), contained anomalous concentrations of Ni, Co, Cu, Zn, Pb, As, and Mo. Both disseminated pyrite and radial pyrite- and sphalerite-bearing quartz veins are present in zones of propylitic alteration in and adjacent to the Tertiary pluton. At site 267, just north of Painted Mountain on Soluka Creek, zones of propylitically altered volcanic rock containing disseminated pyrite contained anomalous concentrations of Zn, As, Co, Cu, Mn, Pb, Cr, Ni, Mo, and Bi. These data indicate that the zones of propylitic alteration exposed near plutons in the southern part of the Barrier Range are favorable for undiscovered polymetallic veins.

Samples of Tertiary conglomerate and sandstone from site 255 in the Kuliak Bay area contained anomalous concentrations of manganese, cobalt, lead, and gold (table 17). All of the sedimentary rock samples from this site have Fe-oxides in the matrix. On the basis of the geologic observations at this locality, we interpret the geochemical anomalies at site 255 to be synsedimentary in origin.

The NMHMC samples from five drainage basins between Amalik Bay and the mouth of the Katmai River contained cinnabar (Goldfarb and others, 1988; Church and Bennett, 1989). All of these drainage basins are underlain by sedimentary rocks, some of which are now hornfels, and have been cut by dikes (Td) or by faults. A sedimentary rock sample (site 280) contained anomalous concentrations of Mo, As, Sb, Bi, and Hg (pls. 2 and 3). Goldfarb and others (1988) suggested that this area is favorable for the occurrence of undiscovered precious-metal-bearing hot-springs or epithermal quartz-vein deposits.

KATMAI LAKES–HAGELBARGERS PASS–DAKAVAK LAKE SUBAREA

In this subarea, north of Dakavak Bay, we identified three localities that are favorable for the occurrence of epithermal quartz veins: the Katmai Lakes, Hagelbargers Pass, and Dakavak Lake localities. All three localities are characterized by zones of banded quartz veins that strike approximately northwest. In the SS and NMHMC samples from these subareas, anomalous concentrations of Co, Zn, Ni, and Cu were common and anomalous concentrations of Pb, Mo, Sn, As, Sb, Bi, Cd, or Ag were less commonly observed (Church and Arbogast, 1989; Church, Bailey, and Riehle, 1989; Church and Motooka, 1989). Pyrite and chalcopyrite were abundant, and sphalerite, arsenopyrite, and wulfenite were identified in the NMHMC samples from specific localities (Church and Bennett, 1989).

Altered volcanic rocks (Tab) from the Katmai Lakes locality are cut by quartz veins (sites 234–236; geochemical data given in table 17). These samples commonly contained anomalous concentrations of Ag, As, and Zn, and, less commonly, of Mo, Au, Bi, Sb, or Hg. Propylitically altered volcanic rock and float samples from the Katmai Lakes locality contained both oxidized, disseminated pyrite as well as pyrite in thin quartz veins. No followup work was done at this locality.

At the Hagelbargers Pass locality, reconnaissance geochemical samples from drainage basins near sites 237–238 showed consistent anomalies of arsenic, silver, and copper. Altered and fractured lava flows and tuffs are cut by northwest-trending quartz veins and are marked by a prominent color anomaly. Samples of the quartz vein collected along a short traverse (site 238, sample K3619) at the Hagelbargers Pass locality were consistently anomalous in Ag, As, Mo, Sb, and Au. Gold has a maximum detected concentration of 2.2 ppm; most vein samples range from 0.15 to 0.45 ppm Au. Individual sulfide-rich bands within the quartz vein range in thickness from 1 to 5 mm; samples of the quartz vein were as much as 10 cm thick. Pyrite and jordisite (5-micron grains of amorphous MoS_2) were identified in thinly banded, fine-grained quartz veins that were later brecciated; kaolinite and smectite were identified in the quartz vein by means of X-ray diffraction. Semiquantitative emission spectrographic analysis of the jordisite-bearing quartz vein gave the following results: 7,000 ppm Fe, 300 ppm As, 200 ppm Mo, 50 ppm Sn, 100 ppm Cu, and 3 ppm Ag. Stilbite, kaolinite, and quartz also were observed on late-formed fractures that cut the quartz veins and postdate the brecciation event. In this later stage vein, we detected 20,000 ppm Fe, 1,000 ppm As, 100 ppm Sb, 50 ppm Mo, 15 ppm Cu, and 2 ppm

Ag. Additional outcrops of the quartz vein were sampled 0.5 km away (site 238, sample K3620), indicating that the vein is continuous over that distance. Samples of altered volcanic rock cut by quartz veins that were collected from sites 239–242 (table 17) also have a similar geochemical signature (pls. 2 and 3).

Geochemical data for samples of quartz veins that cut altered volcanic rocks at the Dakavak Lake locality (sites 264–266), as well as float samples collected from the streams draining south into Dakavak Lake (sites 262, 263, and 265), also show a similar geochemical signature (As, Zn, Mo, Ag, and Au). Subhorizontally bedded volcanic flows and tuffs were intruded by sills and dikes. These dikes and sills are cut by northwest-trending quartz veins and by younger, unaltered dikes. Both X-ray and optical mineral identifications show that the volcanic rocks are moderately to intensely altered to propylitic, argillic, phyllic, and potassic mineral assemblages. Samples of quartz veins collected along a 2-km traverse in altered volcanic rocks (unit Tab; site 264) within one of the areas marked by a color anomaly contained as much as 5 ppm Au, the highest concentration of gold found in bedrock samples from the Katmai study area (pl. 3).

The presence of molybdenum, seen in epithermal quartz vein samples from all of these sites, is unusual. We suggest that these quartz veins may represent a shallow expression of an undiscovered low-fluorine porphyry molybdenum deposit. At the Mike prospect, in the Ugashik quadrangle, a porphyry Mo deposit in Pliocene rocks (2.8–4 Ma, Wilson and Shew, 1988) was described (Church, Frisken, and Wilson, 1989; Church, Detterman, and Wilson, 1989) that contained anomalous concentrations of Cu, Mo, Pb, Zn, Ba, Au, and Ag. Lead and zinc are found primarily in the outer sericitic alteration halo that surrounds the Mike prospect. Pyrite is abundant in the ore zone, and fine-grained molybdenite occurs along small quartz-filled fractures forming stockworks. Likewise, the Cape Kubugakli prospect, which is only 35 km south of the Hagelbargers Pass locality, is characterized by Cu, Mo, Pb, Zn, Ag, and Au anomalies in dike and vein samples (Wilson and O'Leary, 1986, 1987). Unlike the Cape Kubugakli prospect, however, no sulfosalt minerals were noted in our field investigations. Church, Detterman, and Wilson (1989) classified the Cape Kubugakli prospect as a polymetallic-vein deposit, but noted that molybdenum was usually not found in other deposits that are included in this mineral deposit model (Cox, 1986f).

The mineralogy and morphology of the vein samples, and the alteration assemblage from the Hagelbargers Pass locality, also bear some similarity to those described by Kimura and others (1976) for the Endako porphyry Mo deposit. Thin, brecciated and annealed quartz veins are common; the sulfide minerals at Endako are pyrite and fine-grained molybdenite. Quartz-pyrite-sericite and quartz-kaolinite are prominent alteration assemblages at Endako. A shallow expression of such a system, however, has not been described. On the basis of thermodynamic studies of hydrothermal systems, Bowers and others (1984, p. 2) indicated that the mineral assemblage quartz-laumontite-kaolinite or laumontite-kaolinite will coexist with quartz in a chloride-rich hydrothermal fluid at a temperature of 150° C and 5 bars pressure. However, at 300° C and 5 bars pressure, the stability field of pyrophyllite is significantly larger, and laumontite is replaced by wairakite, which is a calcium analogue of analcite. Kaolinite and wairakite would not coexist. Thus, we suggest that the zeolite stilbite, which is structurally very similar to laumontite (the zeolite used to construct the equilibrium activity diagrams referenced above) may be a lower temperature phase formed in the near-surface hydrothermal environment represented by the veins described here.

Finally, additional geochemical evidence supports our hypothesis that these veins might represent epithermal quartz veins above a concealed porphyry Mo deposit: several of the high-field-strength and small-ion-lithophile elements, which one might expect to be concentrated in the late-magmatic liquidus phase of a low-fluorine porphyry Mo magma (Westra and Keith, 1981), are also present in these samples, but are significantly diluted by quartz. We emphasize the geochemical suite of metals rather than the elemental concentrations present. Boron ranged from 10 to 70 ppm, titanium ranged from 1,000 to 7,000 ppm, and zirconium ranged from 50 to 500 ppm; no beryllium, niobium, or tin were detected in the bulk sample of the vein system, but tin was detected in the jordisite-bearing bands within these quartz veins. Barium ranged from 50 to 700 ppm, manganese ranged from 100 to 1,000 ppm, and vanadium ranged from 30 to 200 ppm (Riehle and others, 1989). The elements Cu, Mo, Pb, Zn, Au, and Ag are the base- and precious-metal suite associated with low-fluorine porphyry Mo deposits (Theodore, 1986) such as Endako, and the Mike prospect. Argentiferous tetrahedrite, such as that found at Cape Kubugakli (Smith, 1925, p. 207), is also indicated as an accessory sulfide phase associated with some examples of the low-fluorine porphyry Mo mineral deposit model (Theodore, 1986). We suggest that these quartz veins may be indicative of undiscovered low-fluorine porphyry Mo deposits at depth in the Barrier Range area of the Katmai study area.

KEJULIK MOUNTAINS AREA

The Kejulik Mountains area is underlain by latest Tertiary and Quaternary volcanic rocks (QTac, QTap) extruded on sandstone and siltstone of the Naknek Formation (Jn). Stream-sediment and NMHMC data indicate anomalous concentrations of Cu, Mo, Pb, Zn, Ag, Cd, and Ba (pl. 1; Church and Arbogast, 1989; Church, Bailey, and Riehle, 1989; Church and Motooka, 1989). Anomalous concentrations of copper, molybdenum, silver, and lead were also

Table 18. Geochemical and geologic data for selected samples from the Kejulik Mountains area, Katmai study area, Alaska.

[Samples listed here have concentrations that exceed the 95th percentile for the respective lithologic units as defined in table 4. "Site No." is the locality shown on plates 1–3; map unit symbols are those on the geologic base map on plates 1–3. An "X" in columns headed "Vein," "Frac," or "Alt" indicates that veins, fracture fill, and (or) hydrothermally altered rock, including color anomalies caused by the oxidation of sulfide minerals, were observed at the sample site; "Int" indicates that the sample is an intrusive rock, or that there is a sill, dike, or pluton exposed nearby. "Lith" indicates the rock type of the sample: 1, sandstone or siltstone; 2, conglomerate; 3, volcaniclastic

Site No.	Sample No.	Map unit	Mn	Cr	Ni	Co	Cu	Mo	Sn	Pb	Ag	Bi	Zn	Cd
284	83DT031	Jn	---	---	70	---	---	---	---	---	---	---	130	---
285	K3623RA	Jn	2,000	---	50	---	100	20	---	---	---	---	120	0.2
285	K3623RC	Td	2,000	---	---	50	---	50	---	---	---	18	140	1.3
286	K3624RA	Jn	2,000	200	50	---	---	---	---	---	---	---	65	.2
287	K0239RC	(*)	5,000	---	---	---	---	---	---	30	---	---	---	---
288	85DT189	Jn	---	---	---	---	---	---	---	---	---	---	70	---
288	K2066	(*)	---	70	---	---	---	15	---	---	---	---	---	---
289	85JM137	QTac	1,500	---	---	---	---	---	---	---	---	---	90	---
289	85YB213	QTac	1,500	---	---	---	---	---	---	---	---	---	---	---
290	K4059RB	(*)	---	---	---	---	---	10	---	---	---	---	---	---
291	K0219RB	(*)	2,000	---	---	---	150	100	20	70	---	---	200	.2
292	K3625RC	Jn	5,000	---	---	50	300	---	---	---	---	---	150	2.7
292	K3625RD	QTac	---	150	50	50	100	10	---	---	---	---	150	.8
293	84DT130	QTac	---	---	---	---	---	7	---	---	---	---	---	---
294	K0218RB	(*)	---	---	---	---	---	---	---	---	---	1	160	---
295	84DT133	Jn	---	---	---	---	---	---	---	---	0.5	---	---	---

reported for the Kejulik Mountains in the Karluk quadrangle immediately to the south (Church and others, 1988; Frisken and others, 1988). Pyrite, chalcopyrite, barite, and sphalerite were observed in the NMHMC samples (Church and Bennett, 1989; Frisken, Church, and Willson, 1988). This geochemical anomaly is in the headwaters of drainage basins that surround an exposed volcanic plug. Samples of bleached and altered siltstone of the Naknek Formation (sites 291 and 292; geochemical data given in table 18) contained anomalous concentrations of Cu, Mo, Zn, Cd, Co, and Mn. Single-element anomalies of Pb, Sn, As, Sb, Cr, or Ni were also found (pls. 1 and 2). Analyses of altered volcanic and sedimentary rock samples, as well as float samples (sites 290, 293–295, table 18) show that these rocks contained anomalous concentrations of molybdenum, arsenic, silver, or mercury. We interpret the geologic and geochemical data to be favorable for undiscovered polymetallic veins or a concealed porphyry Cu deposit emplaced just below the volcanic plug.

SUMMARY

Mineralized areas on the Alaska Peninsula, chiefly epithermal quartz and polymetallic veins associated with porphyry Cu and porphyry Cu-Mo deposits, have long been recognized. Hollister (1978, p. 72–73) summarized published geologic descriptions for eight porphyry Cu and porphyry Cu-Mo occurrences on the Alaska Peninsula south of Iliamna Lake. Mineral resource appraisals in the Chignik and Sutwik Island quadrangles (Cox and others, 1981) and the Ugashik and Karluk quadrangles (Church, Detterman, and Wilson, 1989), immediately south of the Katmai study area, also delineated additional areas on the Alaska Peninsula that have potential for undiscovered porphyry Cu, porphyry Cu-Mo, porphyry Cu-Au, porphyry Mo, polymetallic-vein, and epithermal quartz-vein deposits.

Geochemical analyses of the stream-sediment and the nonmagnetic heavy-mineral concentrates collected from the Mount Katmai, western Afognak, and eastern Naknek quadrangles delineate several areas where these same geochemical suites were found. Areas that have potential for undiscovered porphyry Cu and porphyry Cu-Mo deposits have been delineated on the basis of geochemical anomaly patterns of Cu-Mo-Sn-W and Pb-Ag-Zn-Cd-Bi-As in stream-sediment and nonmagnetic heavy-mineral concentrates as well as anomalous concentrations of these same metals in bedrock samples (pl. 1). Areas that have potential for undiscovered polymetallic-vein deposits have been delineated on the basis of geochemical anomaly patterns of Cu-Pb-Ag-Zn-Cd-Bi-As in stream-sediment and nonmagnetic heavy-mineral concentrates as well as anomalous concentrations of these same metals in bedrock samples (pl. 2). Areas that have potential for undiscovered precious-metal-bearing polymetallic and epithermal quartz-vein deposits have been evaluated on the basis of geochemical anomaly patterns of Mn-Au-Ag-Hg-Sb-As in stream sediment and nonmagnetic heavy-mineral concentrates as well as anomalous concentrations of these same metals in bedrock samples (pl. 3).

rock or tuff; 4, lava flow; 5, sill or dike; 6, plutonic rock; 7, metamorphosed rock/protolith; 8, limestone; and (*), float sample. Mineralogy is generally based upon field identifications of hand specimens: py, pyrite; cpy, chalcopyrite; asp, arsenopyrite; spl, sphalerite; gn, galena; mly, molybdenite; qtz, quartz; Fe ox., iron oxides; dissem., disseminated mineral grains in sample. Dashes (---), concentrations not anomalous or feature not observed; all concentrations expressed in parts per million (ppm); >, concentration is greater than reported value]

Site No.	Sample No.	Map unit	Au	As	Sb	Hg	Alt	Int	Lith	Frac	Vein	Mineralogy and mode of occurrence
284	83DT031	Jn	---	---	---	---	---	---	1	---	---	
285	K3623RA	Jn	---	30	---	---	---	X	1	---	---	Dissem. py.
285	K3623RC	Td	---	---	---	---	X	X	5	---	X	Dissem. py in qtz veins and breccias.
286	K3624RA	Jn	0.25	---	---	---	---	---	1	---	X	Py in qtz veins.
287	K0239RC	(*)	---	---	---	---	---	---	1	---	---	Py in calcite vein.
288	85DT189	Jn	---	10	---	---	X	X	1	---	---	
288	K2066	(*)	---	---	---	---	X	X	5	---	---	Dissem. py.
289	85JM137	QTac	---	---	---	0.16	---	---	4	---	---	
289	85YB213	QTac	---	---	---	.14	---	---	4	---	---	
290	K4059RB	(*)	---	300	---	---	---	---	4	---	X	Fe ox. in qtz veins.
291	K0219RB	(*)	---	20	4	---	X	---	4	---	---	Py in oxidized breccia.
292	K3625RC	Jn	---	---	---	---	X	X	1	---	---	Dissem. py.
292	K3625RD	QTac	---	---	---	---	X	X	5	---	X	Py in qtz veins.
293	84DT130	QTac	---	---	---	---	---	---	4	---	---	
294	K0218RB	(*)	---	10	---	.4	X	---	4	---	---	Fe ox.-stained breccia.
295	84DT133	Jn	---	---	---	---	---	---	1	---	---	

We found no compelling geologic and geochemical evidence suggesting the presence of undiscovered Kuroko-type massive sulfide deposits in the rocks of the Talkeetna Formation, such as the Johnson River deposit in the Iliamna quadrangle. We found little evidence for undiscovered copper-rich iron-skarn deposits, such as the Crevice Creek occurrence in the Iliamna quadrangle or the Kasna Creek deposit in the Lake Clark quadrangle; however, the Granite Creek site warrants further evaluation. We found only sparse evidence of mineralization associated with the Jurassic intrusive rocks of the Alaska–Aleutian Range batholith in the Katmai study area.

Geologic and geochemical data for the Buttress Range define a small, poorly exposed porphyry Cu-Mo occurrence in the Margot Creek drainage that is associated with a Tertiary(?) pluton. Geologic and geochemical data outline additional areas that have potential for concealed, undiscovered porphyry Cu deposits in the area south of Fourpeaked Mountain and north of the Big River, and in the Ikagluik Creek drainage basin. Geologic and geochemical data also define areas that have potential for undiscovered porphyry Cu deposits in the Kejulik Mountains and the Kulik Lake area. Geologic and geochemical data for the Barrier Range area have been interpreted to suggest that the area has potential for concealed, undiscovered low-fluorine porphyry Mo deposits. Finally, the geochemical data for the Sugarloaf Mountain area is very similar to that reported for the Pebble Beach porphyry Cu-Au deposit (Danielson, 1991) and suggest that this area may have potential for undiscovered porphyry Cu-Au deposits. In all cases, the areal extent of the geochemical expression of these exploration targets is smaller than that associated with undiscovered porphyry deposits sited farther south on the Alaska Peninsula, which suggests that they are either smaller in size or are more deeply buried.

Geologic and geochemical data define areas favorable for undiscovered base- and precious-metal-bearing polymetallic-vein deposits throughout much of the Katmai study area. Polymetallic veins have been noted in the Kulik Lake area, the Ikagluik Creek drainage basin, the Fourpeaked Mountain area, and the Barrier Range area. In addition, areas having favorable geologic and geochemical characteristics for undiscovered polymetallic-vein deposits are found in the Kukak Bay area, the Kejulik Mountains, and the Ninagiak River area.

Geologic and geochemical data also define several areas favorable for undiscovered epithermal quartz-vein deposits. Gold-bearing, pyritic quartz veins were found at Hagelbargers Pass in the Barrier Range. Additional exploration targets for gold-bearing quartz vein deposits may be present in the Katmai Lakes–Hagelbargers Pass–Dakavak Lake area and in the Sugarloaf Mountain area. Many of the Quaternary volcanic centers are also favorable for undiscovered gold-bearing quartz veins deposited by hot springs as evidenced by limited work near Mount Mageik. Geochemical data for the rootless fumaroles within the Valley of Ten Thousand Smokes and at Novarupta (Keith, 1984, 1991) also have an epithermal-quartz-vein signature similar to that associated with dacitic domes that crop out elsewhere in calc-alkaline volcanic arcs (Cunningham and Ericksen, 1991). However, the short duration of the eruption and the hydrothermal activity at Novarupta suggest that it is unlikely that a hydrothermal deposit formed as a result.

REFERENCES CITED

Andreasen, G.E., Dempsey, W.J., Vargo, J.L., and others, 1963, Aeromagnetic map of part of the Naknek quadrangle, Alaska: Geophysical Investigations Map GP–353, scale 1:125,000.

Atwood, W.W., 1911, Geology and mineral resources of parts of the Alaska Peninsula: U.S. Geological Survey Bulletin 467, 137 p.

Bailey, E.A., Sutley, S.J., Arbogast, B.F., Willson, W.R., and Church, S.E., 1986, Analytical results and sample locality map of stream-sediment and heavy-mineral-concentrate samples from the Mt. Katmai quadrangle, and portions of the Naknek, Afognak, and Iliamna quadrangles, Alaska: U.S. Geological Survey Open-File Report 86–586, 126 p., scale 1:250,000.

Bennett, G.J., and Church, S.E., 1987, Mineralogy and sample locality map of the nonmagnetic heavy-mineral-concentrate samples from the Mt. Katmai quadrangle, and portions of the Naknek, Afognak, and Iliamna quadrangles, Alaska: U.S. Geological Survey Open-File Report 87–615, 39 p., scale 1:250,000.

Berger, B.R., 1986, Descriptive model of epithermal quartz-alunite Au, *in* Cox, D.P., and Singer, D.A., eds., Mineral deposit models: U.S. Geological Survey Bulletin 1693, p. 158.

Bowers, T.S., Jackson, K.J., and Helgeson, H.C., 1984, Equilibrium activity diagrams for coexisting minerals and aqueous solutions at pressures and temperatures to 5 kb and 600° C: Springer-Verlag, New York, 397 p.

Burk, C.A., 1965, Geology of the Alaska Peninsula—Island arc and continental margin: Geological Society of America Memoir 99, 250 p., 3 pls.

Calderwood, K.W., and Fackler, W.C., 1972, Proposed stratigraphic nomenclature for Kenai Group, Cook Inlet Basin, Alaska: American Association of Petroleum Geologists Bulletin, v. 56, p. 739–754.

Case, J.E., Detterman, R.L., Wilson, F.H., Chuchel, B.A., and Yount, M.E., 1988, Maps showing aeromagnetic survey and geologic interpretation of the Ugashik and part of the Karluk quadrangles, Alaska: U.S. Geological Survey Miscellaneous Field Studies Map MF–1539–D, scale 1:250,000.

Church, S.E., 1981, Multiple element determinations in geological reference samples—An evaluation of the inductively coupled plasma-atomic emission spectroscopy method for geochemical applications, *in* Barnes, R.M., ed., Developments in atomic plasma spectrochemical analysis: Philadelphia, Hayden and Sons, p. 410–434.

Church, S.E., and Arbogast, B.F., 1989, Geochemical maps showing the distribution of selected elements determined in nonmagnetic heavy-mineral concentrates from the Mount Katmai and parts of the Afognak and Naknek quadrangles, Alaska: U.S. Geological Survey Miscellaneous Field Studies Map MF–2021–C, scale 1:250,000.

Church, S.E., Bailey, E.A., and Riehle, J.R., 1989, Geochemical map showing the distribution of selected elements determined in stream sediments from the Mount Katmai and parts of the Afognak and Naknek quadrangles, Alaska: U.S. Geological Survey Miscellaneous Field Studies Map MF–2021–A, scale 1:250,000.

Church, S.E., and Bennett, G.J., 1989, Mineralogical maps showing the distribution of selected minerals identified in nonmagnetic heavy-mineral concentrates from the Mount Katmai and parts of the Afognak and Naknek quadrangles, Alaska: U.S. Geological Survey Miscellaneous Field Studies Map MF–2021–D, scale 1:250,000.

Church, S.E., Detterman, R.L., and Wilson, F.H., 1989, Mineral and energy resource assessment maps of the Ugashik, Bristol Bay, and western Karluk quadrangles, Alaska: U.S. Geological Survey Miscellaneous Field Studies Map MF–1539–I, scale 1:250,000.

Church, S.E., Ford, A.B., Flanagan, V.J., and Stotelmeyer, R.B., 1984, Mineral resource potential map of the Glacier Peak Wilderness and adjacent areas, Chelan, Skagit, and Snohomish Counties, Washington: U.S. Geological Survey Miscellaneous Field Studies Map MF–1652–A, scale 1:250,000.

Church, S.E., Frisken, J.G., Detra, D.E., and Willson, W.R., 1988, Geochemical map showing the distribution of selected elements determined in stream sediments from the Ugashik, Bristol Bay, and western Karluk quadrangles, Alaska: U.S. Geological Survey Miscellaneous Field Studies Map MF–1539–F, scale 1:250,000.

Church S.E., Frisken, J.G., and Wilson, F.H., 1989, Interpretation of exploration geochemical data from the Ugashik, Bristol Bay, and western Karluk quadrangles, Alaska: U.S. Geological Survey Bulletin 1858, 45 p.

Church, S.E., Mosier, E.L., and Motooka, J.M., 1987, Mineralogical basis for the interpretation of multi-element (ICP-AES), oxalic acid, and aqua regia digestion of stream sediments for reconnaissance exploration geochemistry: Journal of Exploration Geochemistry, v. 29, p. 207–233.

Church, S.E., and Motooka, J.M., 1989, Geochemical maps showing the distribution of selected leachable metals determined by ICP in stream sediments from the Mount Katmai and parts of the Afognak and Naknek quadrangles, Alaska: U.S. Geological Survey Miscellaneous Field Studies Map MF–2021–B, scale 1:250,000.

Church, S.E., Motooka, J.M., Werschky, R.S., Bigelow, R.C., and VanTrump, George, Jr., 1983, Contour maps, statistical summaries, and analytical data from stream-sediment samples collected from the Glacier Peak study area and analyzed using an aqua regia leach/inductively coupled plasma method: U.S. Geological Survey Open-File Report 83–366, 116 p.

Church, S.E., Riehle, R.J., Magoon, L.B., and Campbell, D.L., 1992, Mineral and energy resource assessment maps of the Mount Katmai, Naknek, and western Afognak quadrangles, Alaska: U.S. Geological Survey Miscellaneous Field Studies Map MF–2021–F, scale 1:250,000.

Cobb, E.H., 1972, Metallic mineral resources map of the Mount Katmai quadrangle, Alaska: U.S. Geological Survey Miscellaneous Field Studies Map MF–461, scale 1:250,000.

Conklin, N.M., and Slack, J.F., 1983, Trace element analyses of tourmalines from Appalachian-Caldonian massive sulfide deposits: U.S. Geological Survey Open-File Report 83–890, 5 p.

Cox, D.P., 1986a, Descriptive model of Fe skarn deposits, *in* Cox, D.P., and Singer, D.A., eds., Mineral deposit models: U.S. Geological Survey Bulletin 1693, p. 94.

———1986b, Descriptive model of Zn-Pb skarn deposits, *in* Cox, D.P., and Singer, D.A., eds., Mineral deposit models: U.S. Geological Survey Bulletin 1693, p. 90.

———1986c, Descriptive model of porphyry Cu, *in* Cox, D.P., and Singer, D.A., eds., Mineral deposit models: U.S. Geological Survey Bulletin 1693, p. 76.

———1986d, Descriptive model of porphyry Cu-Au, *in* Cox, D.P., and Singer, D.A., eds., Mineral deposit models: U.S. Geological Survey Bulletin 1693, p. 110.

———1986e, Descriptive model of porphyry Cu-Mo, *in* Cox, D.P., and Singer, D.A., eds., Mineral deposit models: U.S. Geological Survey Bulletin 1693, p. 115.

———1986f, Descriptive model of polymetallic veins, *in* Cox, D.P., and Singer, D.A., eds., Mineral deposit models: U.S. Geological Survey Bulletin 1693, p. 125.

Cox, D.P., Detra, D.E., and Detterman, R.L., 1981, Mineral resource maps of the Chignik and Sutwik Island quadrangles, Alaska: U.S. Geological Survey Miscellaneous Field Studies Map MF–1053–K, scale 1:250,000.

Cox, D.P., and Singer, D.A., editors, 1986, Mineral deposit models, U.S. Geological Survey Bulletin 1693, 379 p.

Cunningham, C.G., and Ericksen, G.E., 1991, Exploration guides for precious-metal deposits in volcanic domes, *in* Good, E.E., Slack, J.F., and Kotra, R.K, eds., USGS research on mineral resources—1991; Program and abstracts, seventh annual V.E. McKelvey forum on mineral and energy resources: U.S. Geological Survey Circular 1062, p. 15–16.

Curtis, G.H., 1968, The stratigraphy of the ejecta from the 1912 eruption of Mount Katmai and Novarupta, Alaska: Geological Society of America, Memoir 16, p. 153–210.

Danielson, Vivian, 1991, Cominco discovers large copper-gold porphyry in Alaska: Northern Miner, v. 76, No. 47, p. 1 and 19.

Davis, J.C., 1973, Statistics and data analysis in geology: New York, John Wiley and Sons, 550 p.

Detterman, R.L., Case, J.E., and Wilson, F.L., 1979, Paleozoic rocks on the Alaska Peninsula, *in* Johnson, K.M., and Williams, J.R., eds., The United States Geological Survey in Alaska—Accomplishments during 1978: U.S. Geological Survey Circular 804–B, p. 85–86.

Detterman, R.L., Case, J.E., Wilson, F.L., and Yount, M.E., 1987, Geologic map of the Ugashik, Bristol Bay, and part of the Karluk quadrangles, Alaska: U.S. Geological Survey Miscellaneous Investigations Series Map I–1685, scale 1:250,000.

Detterman, R.L., Hudson, Travis, Plafker, George, Tysdal, R.G., and Hoare, J.M., 1976, Reconnaissance geologic map along the Bruin Bay and Lake Clark faults in the Kenai and Tyonek quadrangles, Alaska: U.S. Geological Survey Open-File Report 76–477, 2 pl., scale 1:250,000.

Detterman, R.L., and Miller, J.W., 1985, Kaguyak Formation—An Upper Cretaceous flysch deposit, *in* Bartsch-Winkler, Susan, and Reed, K.M., eds., The United States Geological Survey in Alaska—Accomplishments during 1983: U.S. Geological Survey Circular 945, p. 49–51.

Detterman, R.L., Miller, J.W., Case, J.E., Wilson, F.H., and Yount, M.E., in press, Stratigraphic framework of the Alaska Peninsula: U.S. Geological Survey Bulletin 1969–A.

Detterman, R.L., and Reed, B.L., 1980, Stratigraphy, structure, and economic geology of the Iliamna quadrangle, Alaska: U.S. Geological Survey Bulletin 1368–B, 86 p.

Egbert, R.M., and Magoon, L.B., 1981, Petrography, provenance, and tectonic significance of Middle and Upper Jurassic sandstone from Tuxedni Bay, Cook Inlet, Alaska, *in* Albert, N.R.D., and Hudson, T., eds., The United States Geological Survey in Alaska—Accomplishments during 1979: U.S. Geological Survey Circular 823–B, p. 86–88.

Erlich, Olga, Motooka, J.M., VanTrump, George, Jr., and Church, S.E., 1988, Analytical data and sample locality map for aqua-regia leachates of stream sediments analyzed by ICP from the Mt. Katmai quadrangle, and portions of the Naknek, Afognak, and Iliamna quadrangles, Alaska: U.S. Geological Survey Open-File Report 88–422, 74 p., scale 1:250,000.

Fenner, C.N., 1920, The Katmai region, Alaska, and the great eruption of 1912: Journal of Geology, v. 28, p. 569–606.

Fisher, M.A., Bruns, T.R., and von Huene, Roland, 1981, Transverse tectonic boundaries near Kodiak Island, Alaska: Geological Society of America Bulletin, v. 92, p. 10–18.

Fisher, R.A., 1970, Statistical methods for research workers (14th ed.): New York, Hafner Press, 362 p.

Frisken, J.F., and Arbogast, B.F., 1992, Map showing the distribution of anomalous concentrations of selected elements determined in stream sediments from the Port Moller, Stepovak Bay, and Simenof Islands quadrangles, Alaska Peninsula, Alaska: U.S. Geological Survey Miscellaneous Field Studies Map MF–2155–B, scale 1:250,000.

Frisken, J.G., Church, S.E., Detra, D.E., and Willson, W.R., 1988, Geochemical map showing the distribution of selected elements determined in nonmagnetic heavy-mineral concentrates from the Ugashik, Bristol Bay, and western Karluk quadrangles, Alaska: U.S. Geological Survey Miscellaneous Field Studies Map MF–1539–G, scale 1:250,000.

Frisken, J.G., Church, S.E., and Willson, W.R., 1988, Mineralogical map showing the distribution of selected ore-related minerals identified in nonmagnetic heavy-mineral concentrates from the Ugashik, Bristol Bay, and western Karluk quadrangles, Alaska: U.S. Geological Survey Miscellaneous Field Studies Map MF–1539–H, scale 1:250,000.

Goldfarb, R.J., Gray, J.E., and Tripp, R.B., 1988, Geochemical anomalies in the eastern Katmai region of the Alaskan Peninsula, *in* Galloway, J.P., and Hamilton, T.D., eds. Geologic studies in Alaska by the U.S. Geological Survey during 1987: U.S. Geological Survey Circular 1016, p. 132–135.

Green, C.B., Bundtzen, T.K., Peterson, R.J., Seward, A.F., Deagen, J.R., and Butron, J.E., 1989, Alaska's mineral industry, 1988: Alaska Division of Geological and Geophysical Surveys Special Report 43, 79 p.

Grimes, D.J., and Marranzino, A.P., 1968, Direct-current arc and alternating-current spark emission spectrographic field methods for the semiquantitative analysis of geologic materials: U.S. Geological Survey Circular 591, 6 p.

Heald, Pamela, Foley, N.K., and Hayba, D.O., 1987, Comparative anatomy of volcanic-hosted epithermal deposits: acid-sulfate and adularia-sericite types: Economic Geology, v. 82, p. 1–26.

Hildreth, Wes, 1983, The compositionally zoned eruption of 1912 in the Valley of Ten Thousand Smokes, Katmai National Park, Alaska: Journal of Volcanology and Geothermal Research, v. 18, p. 1–56.

———1987, New perspectives on the eruption of 1912 in the Valley of Ten Thousand Smokes, Katmai National Park, Alaska: Bulletin of Volcanology, v. 49, p. 680–693.

Hollister, V.F., 1978, Geology of the porphyry copper deposits of the Western Hemisphere: American Institute of Mining Engineers, New York, p. 55–88.

Jacob, K.H., Nakamura, Kazuaki, and Davies, J.N., 1977, Trench-volcano gap along the Alaska–Aleutian Arc—Facts, and speculations on the role of terrigenous sediments for subduction, *in* Talwani, Mark, and Pitman, W.C., III, eds., Island arcs, deep sea trenches, and back-arc basins: Washington, American Geophysical Union, p. 243–258.

Jensen, M.L., and Bateman, A.M., 1981, Economic mineral deposits (3rd ed.): New York, John Wiley and Sons, 593 p.

Johnston, R.J., 1980, Multivariant statistical analysis in geography: London, Lorgman, 280 p.

Jones, D.L., Siberling, N.J., Coney, P.J., and Plafker, George, 1987, Lithotectonic terrane map of Alaska (west of the 141st meridian): U.S. Geological Survey Miscellaneous Field Studies Map MF–1874–A, scale 1:2,500,000.

Keith, T.E.C., 1984, Preliminary observations on fumarole distribution and alteration, Valley of 10,000 Smokes, Alaska, *in* Reed, K.M., and Bartsch-Winkler, Susan, eds., The United States Geological Survey in Alaska—Accomplishments during 1982: U.S. Geological Survey Circular 939, p. 82–85.

———1991, Fossil and active fumaroles in the 1912 eruptive deposits, Valley of Ten Thousand Smokes, Alaska: Journal of Volcanology and Geothermal Research, v. 45, p. 227–254.

Keller, A.S., and Reiser, H.N., 1959, Geology of the Mount Katmai area, Alaska: U.S. Geological Survey Bulletin 1058–G, p. 261–298.

Kimura, E.T., Bysouth, G.D., and Drummond, A.D., 1976, Endako, *in* Brown, A.S., ed., Porphyry copper deposits of the Canadian Cordillera: Canadian Institute of Mining and Metallurgy Special Volume 15, p. 444–454.

King, H.D., Tripp, R.B., Cooley, E.F., and Crim, W.D., 1985, Maps showing the distribution and abundance of selected elements in two geochemical sampling media, Lake Clark quadrangle, Alaska: U.S. Geological Survey Miscellaneous Field Studies Map MF–1114–C, scale 1:250,000.

MacKevett, E.M., Jr., and Holloway, C.D., 1977, Map showing metalliferous mineral deposits in the western part of southern Alaska: U.S. Geological Survey Open-File Report 77–169 F, 39 p.

Martin, G.C., 1920, The Alaskan mining industry in 1918: U.S. Geological Survey Bulletin 712, p. 11–52.

———1926, The Mesozoic stratigraphy of Alaska: U.S. Geological Survey Bulletin 776, 493 p.

Martin, G.C., and Katz, F.J., 1912, A geologic reconnaissance of the Iliamna region, Alaska: U.S. Geological Survey Bulletin 485, 138 p.

Mosier, D.L., Sato, Takeo, Page, N.J., Singer, D.A., and Berger, B.R., 1986, Descriptive model of Creede epithermal veins, *in* Cox, D.P., and Singer, D.A., eds., Mineral deposit models: U.S. Geological Survey Bulletin 1693, p. 145.

Mullen, M.W., 1987, Petrology and provenance of sandstones of the Naknek Formation, Alaska Peninsula, *in* Hamilton, T.D., and Galloway, J.P., eds., Geologic studies in Alaska by the U.S. Geological Survey during 1986: U.S. Geological Survey Circular 998, p. 86–90.

Nelson, W.H., King, H.D., Case, J.E., Tripp, R.B., Crim, W.D., and Cooley, E.F., 1985, Mineral resource map of the Lake Clark quadrangle, Alaska: U.S. Geological Survey Miscellaneous Field Studies Map MF–1114–B, scale 1:250,000.

Newberry, R.J., 1986, Mineral resources of the northcentral Chugach Mountains, Alaska: Alaska Division of Geological and Geophysical Surveys Report of Investigations 86–23, 44 p.

Newberry, R.J., Burns, L.E., and Pessel, G.H., 1986, Volcanogenic massive sulfide deposits and the missing complement to the calc-alkaline trend—Evidence from the Jurassic Talkeetna island arc of southern Alaska: Economic Geology, v. 81, p. 951–960.

O'Leary, R.M., and Meier, A.L., 1986, Analytical methods used in geochemical exploration in 1984: U.S. Geological Survey Circular 948, 47 p.

Page, N.J, 1986, Descriptive model of Bushveld Fe-Ti-V, *in* Cox, D.P., and Singer, D.A., eds., Mineral deposit models: U.S. Geological Survey Bulletin 1693, p. 15.

Reed, B.L., 1967, Results of stream sediment sampling and bedrock analyses in the eastern part of the Iliamna quadrangle, and at Kasna Creek, Lake Clark quadrangle, Alaska: U.S. Geological Survey Open-File Report 897, 18 p.

Reed, B.L., and Detterman, R.L., 1965, A preliminary report on some magnetite-bearing rocks near Frying Pan Lake, Iliamna D–7 quadrangle, Alaska: U.S. Geological Survey Open-File Report 817, 2 p.

Reed, B.L., and Lanphere, M.A., 1969, Age and chemistry of Mesozoic and Tertiary plutonic rocks in south-central Alaska: Geological Society of America Bulletin, v. 80, p. 23–44.

———1972, Generalized geologic map of the Alaska–Aleutian Range batholith showing potassium-argon ages of the plutonic rocks: U.S. Geological Survey Miscellaneous Field Studies Map MF–372, scale 1:1,000,000.

———1973, Alaska–Aleutian Range batholith—Geochronology, chemistry, and relation to circum-Pacific plutonism: Geological Society of America Bulletin, v. 84, p. 2583–2610.

Richter, D.H., and Herreid, G., 1965, Geology of the Paint River area, Iliamna quadrangle, Alaska: Alaska Division of Mines and Minerals Geologic Report no. 8, 18 p.

Riehle, J.R., Bailey, E.A., Church, S.E., and Yount, M.E., 1989, Sample locality maps, analytical data, and statistical summary of analyses of rock samples from the Mount Katmai quadrangle and adjacent portions of the Naknek and Afognak quadrangles, Alaska: U.S. Geological Survey Open-File Report 89–570, 136 p., scale 1:250,000.

Riehle, J.R., and Detterman, R.L., 1993, Quaternary geologic map of the Mount Katmai quadrangle and adjacent parts of the Naknek and Afognak quadrangles, Alaska: U.S. Geological Survey Miscellaneous Investigations Map I–2032, scale 1:250,000.

Riehle, J.R., Detterman, R.L., Yount, M.E., and Miller, J.W., in press, Geologic map of the Mount Katmai quadrangle and adjacent parts of the Naknek and Afognak quadrangles, Alaska: U.S. Geological Survey Miscellaneous Investigations Map I–2204, scale 1:250,000.

Rummel, R.J., 1970, Applied Factor Analysis: Evanston, Ill., Northwestern University Press, 617 p.

Shew, Nora, and Lanphere, M.A., 1992, Sample localities and potassium-argon ages of igneous rocks from the Mount Katmai quadrangle and adjacent parts of the Naknek and Afognak quadrangles, Alaska: U.S. Geological Survey Miscellaneous Field Investigations Map MF 2021–E, scale 1:250,000.

Sinclair, A.J., 1976, Applications of probability graphs in mineral exploration: Association of Exploration Geochemistry Special Volume 4, 95 p.

Singer, D.A., 1986a, Descriptive model of Kuroko massive sulfide, *in* Cox, D.P., and Singer, D.A., eds., Mineral deposit models: U.S. Geological Survey Bulletin 1693, p. 189.

———1986b, Descriptive model of Cyprus massive sulfide, *in* Cox, D.P., and Singer, D.A., eds., Mineral deposit models: U.S. Geological Survey Bulletin 1693, p. 131.

Smith, S.M., Closs, L.G., and Theobald, P.K., 1987, Trace-element variation in hydrothermal tourmalines associated with mineralization—El Correo, Sonora, Mexico, *in* Elliott, I.L., and Smee, B.W., eds., GEOEXPO/87; Exploration in the North American Cordillera: Association of Exploration Geochemists, p. 109–125.

Smith, W.R., 1925, The Cold Bay–Katmai district [Alaska]: U.S. Geological Survey Bulletin 773, p. 183–207.

Steefel, C.I., 1987, The Johnson River prospect, Alaska—Gold-rich sea-floor mineralization from the Jurassic: Economic Geology, v. 82, p. 894–914.

Streckeisen, A.L., 1973, Plutonic rocks—Classification and nomenclature recommended by the IUGS subcommittee on the systematics of igneous rocks: Geotimes, p. 26–30.

Theodore, T.G., 1986, Descriptive model of porphyry Mo, low-F, *in* Cox, D.P., and Singer, D.A., eds., Mineral deposit models: U.S. Geological Survey Bulletin 1693, p. 120.

Tukey, J.W., 1977, Exploration data analysis: New York, Addison-Wesley, 250 p.

VanTrump, George, Jr., and Miesch, A.L., 1977, The U.S. Geological Survey RASS-STATPAC system for management and statistical reduction of geochemical data: Computers and Geosciences, v. 3, p. 475–488.

von Huene, Roland, Fisher, M.A., McClellan, P.H., Box, Stephen, and Ryan, Holly, 1985, Centennial Continent/Ocean Transect A–2, North Pacific Ocean Basin to Kuskokwim Mountains: Geological Society of America Map and Chart Series, scale 1:500,000.

Wahraftig, Clyde, 1965, Physiographic divisions of Alaska: U.S. Geological Survey Professional Paper 482, 52 p.

Warfield, R.S., and Rutledge, F.A., 1951, Investigations of Kasna Creek copper prospect, Lake Kontrashibuna, Lake Clark region, Alaska: U.S. Bureau of Mines Report of Investigations 4828, 10 p.

Welch, E.P., 1983, A rapid geochemical spectrophotometric determination of tungsten with dithiol: Talanta, v. 30, p. 876–878.

Westra, Gerhard, and Keith, S.B., 1981, Classification and genesis of stockwork molybdenum deposits: Economic Geology, v. 76, p. 844–873.

White, W.H., and Queen, L.D., 1989, Preliminary geologic and rock-chip geochemical data from drill core and trenches at the Shumagin gold deposit, Unga Island, Alaska: U.S. Geological Survey Open-File Report 89–361, 36 p.

Wilson, F.H., and Cox, D.P., 1983, Geochronology, geochemistry, and tectonic environment of porphyry mineralization in the central Alaska Peninsula: U. S. Geological Survey Open-File Report 83–783, 24 p.

Wilson, F.H., and O'Leary, R.M., 1986, Maps and tables showing data and analyses of semiquantitative emission spectrometry and atomic-absorption spectrometry of rock samples, Ugashik and western Karluk quadrangles, Alaska: U.S. Geological Survey Miscellaneous Field Studies Map MF–1539–C, 2 sheets, scale 1:250,000.

———1987, Tables showing analyses of semiquantitative emission spectrometry and atomic-absorption spectro-photometry of rock samples collected in the Ugashik, Bristol Bay, and western part of the Karluk quadrangles, Alaska: U.S. Geological Survey Open-File Report 87–419, 35 p.

Wilson, F.H., and Shew, Nora, 1988, Map and tables showing geochronology and whole-rock geochemistry of selected samples from the Ugashik, Bristol Bay, and part of Karluk quadrangles, Alaska: U.S. Geological Survey Miscellaneous Field Studies Map MF–1539–E, scale 1:250,000.

Wilson, F.H., White, W.H., and DuBois, G.D., 1988, Brief descriptions of mines, prospects, and occurrences in the Port Moller and Stepovak Bay quadrangles, Alaska Peninsula: U.S. Geological Survey Open-File Report 88–666, 128 p.

Published in the Central Region, Denver, Colorado
Manuscript approved for publication December 29, 1992
Edited by Diane E. Lane
Illustrations prepared by Norma Maes
Photocomposition by Shelly Fields

☆ U.S. GOVERNMENT PRINTING OFFICE: 1994-573-038/86040